2008

Aquaporin 3 Water Channel Protein Gene Expression in Squalis Acanthias Dogfish Shark

Debra Lee Murray

AQUAPORIN 3 WATER CHANNEL PROTEIN GENE EXPRESSION IN SQUALUS ACANTHIAS DOGFISH SHARK

by

DEBRA LEE MURRAY

(Under the Direction of Christopher P. Cutler)

ABSTRACT

Aquaporins are a family of membrane proteins that provide channels for the rapid movement of water molecules and some small solutes across the cellular membrane. Since the discovery of the first water channel protein, hundreds of homologous proteins have been found in all forms of life and much has been learned about their complex role in body water homeostasis. This is the first study to use molecular and immunological techniques to demonstrate that an orthologue of mammalian AQP3 is present in the epithelial cells of *Squalus acanthias* dogfish shark kidney, gills, rectal gland, esophagus, stomach, eye and brain. The full-length *Squalus acanthias* sequence has 73.8% amino acid identity to human AQP3. Quantitative PCR experiments suggest that constitutive AQP3 expression in the esophagus and kidney may be regulated by external salinity, but the role of AQP3 in water homeostasis of marine elasmobranchs such as *Squalus acanthias* is yet to be described.

INDEX WORDS: Aquaporin, Aquaglyceroporin, Osmoregulation, Water Homeostasis, Elasmobranch, Biological Transport, Molecular Sequence, Sequence Homology, Kidney, Rectal Gland

AQUAPORIN 3 WATER CHANNEL PROTEIN GENE EXPRESSION IN SQUALUS ACANTHIAS DOGFISH SHARK

by

DEBRA LEE MURRAY

B.S., Seton Hall University, 1974

A Thesis Submitted to the Graduate Faculty of Georgia Southern University in Partial Fulfillment of the Requirements for the Degree

MASTER OF SCIENCE

STATESBORO, GEORGIA

2008

AQUAPORIN 3 WATER CHANNEL PROTEIN GENE EXPRESSION IN SQUALUS ACANTHIAS DOGFISH SHARK

by

DEBRA LEE MURRAY

Major Professor: Christopher P. Cutler

Committee: James B. Claiborne
Daniel F. Gleason

Electronic Version Approved:
December 2008

DEDICATION

For Noel, and for John.

“Live as if you will die tomorrow. Learn as if you were to live forever”

- Mahatma Gandhi

ACKNOWLEDGMENTS

I would like to thank everyone who helped me to complete this project, firstly, my major professor, Dr. Christopher P. Cutler for his direction and enduring support. I would also like to thank my committee members for their enormous support and patience, Dr. James B. Claiborne and Dr. Daniel F. Gleason. Also, I am very grateful for the support of the Biology Faculty, especially Dr. Dana Nayduch, Dr. Lorenza Beati, Dr. Lance A. Durden, and Dr. Quentin Fang, who opened up the world of biology again for me as I begin my encore career in this second half of my life.

Without the unconditional guidance from my friend, Andrew Diamanduros, the art of molecular biology would still be a mystery to me. And many other friends and fellow students have inspired me to continue my pursuit of this degree when quitting would have been an easier option and I thank them all from the bottom of my heart. Many thanks to all the graduate students who welcomed me into their group and have always been there for me in the toughest of times. Also, I would especially like to thank Wanda Hodgson, Jake Wysowski, Hana Kratochvilova, Linsey Cozzie, Dr. Kelly Hyndman, Dr. David Evans and many other friends at the Mount Desert Island Biological Laboratory in Maine, to name a few, for all their help and encouragement these past two and a half years. Also, I would like to thank my two counselors, Otha L. Everett and Fran Fowler, for obtaining the funding for my educational endeavors. And, of course, I want to thank my son, Noel Sean Murray, my husband, John Murray, and my parents, Frank and Florence Skye, for their extreme patience and support to the end.

TABLE OF CONTENTS

Page

LIST OF TABLES

Page

LIST OF FIGURES

Page

CHAPTER 1

INTRODUCTION

There are fundamental differences between life on land and life in water, and an aquatic environment presents special problems and challenges to which animals must adapt. Throughout the evolution of aquatic vertebrates, strategies have developed in order to counter the net movement of water and solutes across permeable body surfaces so that extracellular fluid volume, and salt and water content of their internal tissues, could be maintained at a constant level. These homeostatic processes concerning regulation of salt and water concentrations are known as osmoregulation, and involve various organs and cellular membrane transport mechanisms (Evans, 2002).

Water and salt tend to move down their individual concentration gradients through the membranes of cells by the processes of osmosis and diffusion. All animals must balance their rate of water uptake and loss to preserve the integrity of their cells. Too much water intake will cause a cell to swell and burst and too much water loss will cause a cell to shrivel and die (Campbell and Reece, 2005). Animals living in freshwater environments must cope with a constant influx of water and must actively import ions from the water and/or their diet. Animals in marine environments must cope with high ion concentrations and potentially much water loss. Fish are classified as stenohaline if they can only tolerate a narrow range of salt concentration and euryhaline if they can tolerate freshwater, seawater, as well as the brackish water found in estuaries (Moyes and Schulte, 2006).

The following figures illustrate the movement of water and solutes in teleost freshwater and marine fish, and in marine elasmobranchs, such as the spiny dogfish

shark. In freshwater teleost fish (Figure 1), there is a net osmotic gain of water and a diffusional loss of salt across the gills. This is balanced by the excretion of relatively dilute urine and active uptake of salt across the gills and perhaps some ingestion of salt in the food (Evans, 2002).

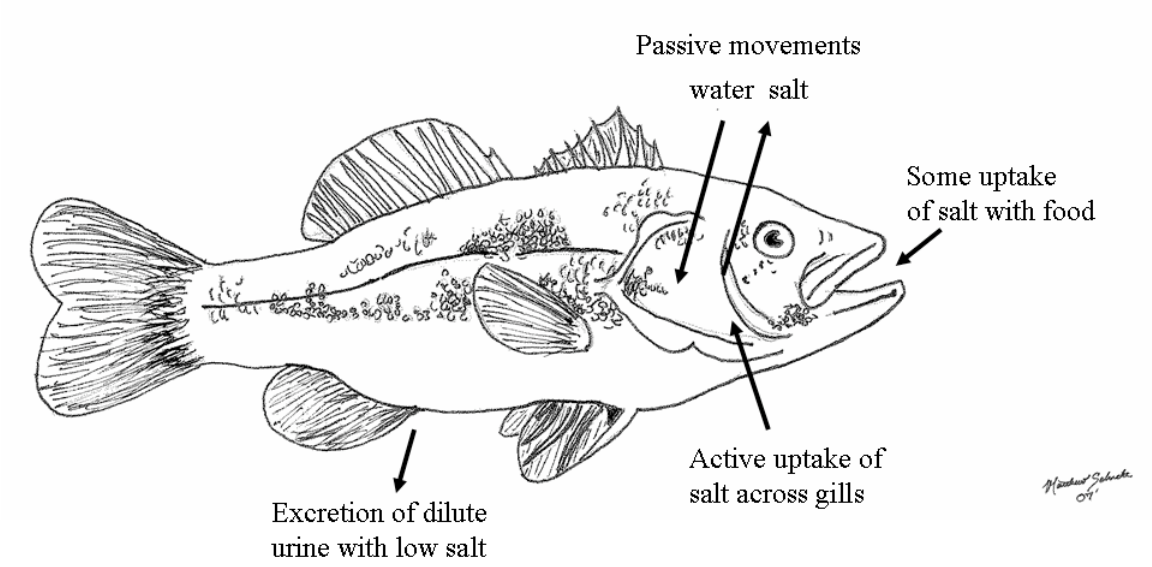

Figure 1. Schematic presentation of osmoregulation in a freshwater fish.

In teleost marine fish (Figure 2), the osmotic situation is reversed. There is a net osmotic loss of water across the gill epithelium and a diffusional gain of salt. The marine teleost copes with this by ingesting seawater and producing small volumes of urine that contains some salt and by active extrusion of salt across the gill. These fish achieve a net salt secretion by use of a set of transport proteins in the gill tissue, which are similar to those found in human kidney tubules. A favorable electrochemical gradient for Na^+ drives it into the gill cell from the blood, co-transported with K^+ and Cl^-. Cl^- exits the apical portion of the cell through the cystic fibrosis transmembrane regulator channel (CFTR). A homologous channel produces cystic fibrosis in humans. The sodium pump,

Na^+- K^+-activated ATP-ase, transports Na^+ back across the basolateral membrane into the blood. Then it diffuses out into the seawater by leaking through paracellular pathways between adjacent gill cells which is driven by a favorable electrochemical gradient (Evans, 2002). The same transport mechanism is also found in the shark rectal gland to be described in paragraphs to follow.

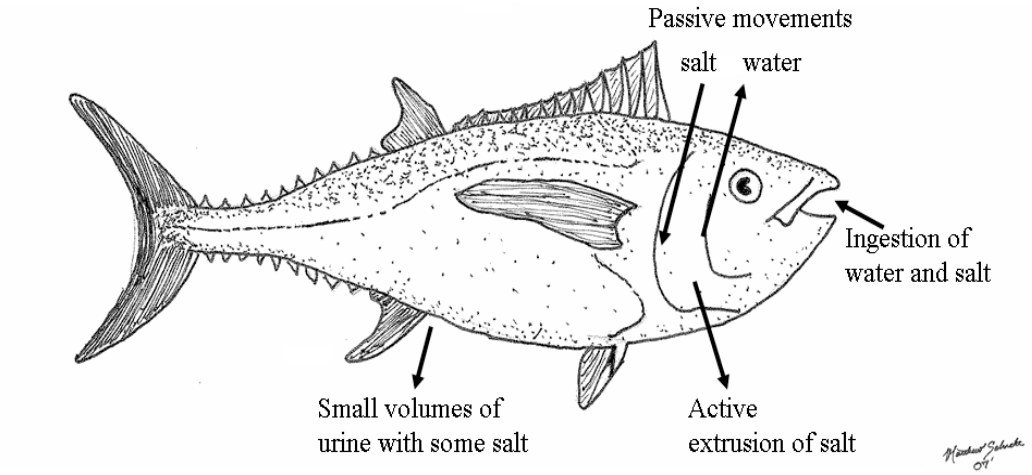

Figure 2. Schematic presentation of osmoregulation in a marine teleost fish.

Marine and euryhaline elasmobranchs (sharks, skates and rays) have developed an unusual strategy for osmoregulation (Figure 3). Many of them are known to avoid the osmotic loss of water by maintaining a total solute concentration in their blood slightly higher than that of the surrounding seawater. They actively produce and retain urea (an end product of nitrogen metabolism) in the blood as an organic osmolyte by reabsorbing it in the kidney. It is also retained because the gills have a low permeability to urea (Marshall and Grosell, 2005). This osmotic gradient favors the uptake of water across the

gills and provides water for the relatively large urine flow demonstrated in marine elasmobranchs (Hazon et al., 2003; Evans, 2002; Piermarini and Evans, 2000). Marine elasmobranchs retain urea by reabsorbing it in the kidney. But, on its own as a counteracting solute, urea disrupts hydrophobic actions, particularly of proteins, and must be counteracted with another solute. In sharks, trimethylamine oxide (TMAO) is employed to negate the effects of urea.by strengthening hydrophobic actions, hence, each solute negates the effect of the other (Moyes and Schulte, 2006).

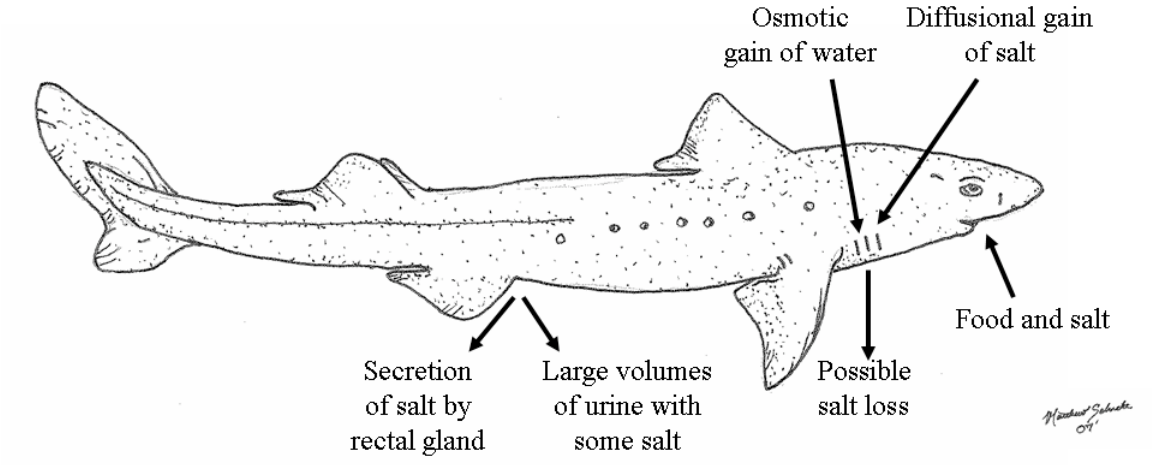

Figure 3. Schematic presentation of osmoregulation in a shark.

As in teleosts, marine elasmobranchs must cope with a diffusional gain of salt from the seawater and their diet, as well as changes in the acid-base chemistry of environmental water (e.g., temperature change, hypercapnia and low pH). The excess of salt is balanced by the salt excretory mechanisms of the rectal gland and possibly the acid-base extrusion mechanism of the gills, although this is largely unstudied (Evans et al. 2004; Piermarini and Evans, 2000). The rectal gland is a digiform extension of the terminal intestine tract. Its secretory fluid contains high concentrations of NaCl, higher

even than the concentrations of NaCl in blood, which are more or less iso-osmotic with seawater. The columnar epithelial cells of the secretory tubules in the rectal gland form a large surface area for the ion transport proteins to facilitate NaCl secretion. Also, the active NaCl secretion transport proteins occur in the subapical cytoplasm where membranous vesicles contain a chloride channel similar to the one found in teleost marine fish, the CFTR (Evans et al., 2004).

The net secretion of sodium chloride by the secretory tubules in the rectal gland occurs through the combined activity of four transport pathways that allow transcellular chloride transport as well as paracellular sodium chloride secretion: the Na^+- K^+ -ATPase pump, the Na^+- K^+ -$2Cl^-$ co-transporter, potassium channels and chloride channels. Figure 4 diagrams these pathways in a rectal gland epithelial cell.

The basolateral Na^+- K^+ -ATPase actively transports K^+ into the cell in exchange for Na^+- (Figure 4). Na^+ is transported out of the cell into the paracellular space on the blood side of the epithelium and creates a steep electrochemical gradient for the passive re-entry of Na^+ into the cell. In doing so, energy is provided to simultaneously drive the uphill translocation of K^+ and two $2Cl^-$ by the Na^+- K^+ -$2Cl^-$ symporter. Na^+ entering the cell is pumped out of the cell again by the Na^+ - K^+ -ATPase and excess K^+ within the cell does not accumulate because of passive diffusion through a potassium channel which raises the membrane potential by leaving more negative ions inside the cell (Olson, 1999). The greater membrane potential drives Cl^- out into the lumen through the CFTR-like channel. The decrease in intracellular Cl^- stimulates the Na^+- K^+ -$2Cl^-$ co-transporter to bring in more Cl^- into the cell, along with Na^+ . The build up of Na^+ in the paracellular space and Cl^- outside leads to a net movement of Na^+ via a paracellular path through the

tight junctions into the lumen thereby overall causing the net secretion of NaCl through the lumen of the intestine and back into the seawater (Hazon et al., 1997).

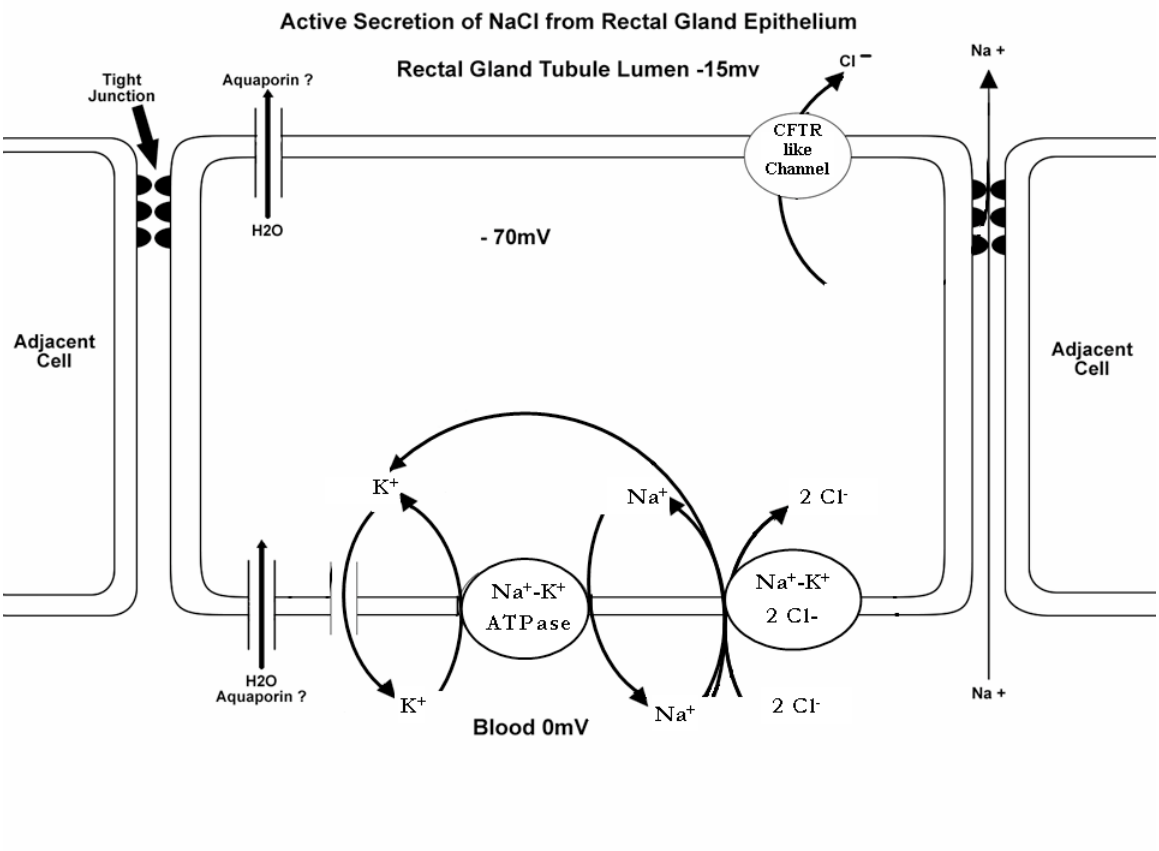

Figure 4. Schematic presentation of rectal gland transport. The activity of the basolateral Na^+, K^+-ATPase maintains Na^+ well below equilibrium within the cell. This allows for entry of not only Na^+ but also Cl- and K^+ via the NKCC which is also located in the basolateral membrane. K^+ recycles across the basolateral membrane via K^+ channels, while Cl- exits the cell across the apical membrane through CFTR-like channels down the electrochemical Cl- gradient. Na^+ is extruded across the basolateral membrane by the Na^+, K^+-ATPase and follows its electrochemical gradient. Na^+ is excreted through the tight junctions of the paracellular pathway and accompanies the secondary active transcellular Cl- secretion (Marshall and Grosell 2005). Theoretical locations of aquaporins are also shown in the diagram.

Although the rectal gland of marine elasmobranchs is highly involved in regulating extracellular Na^+, Cl^- ions and water, the kidney clearly plays an important role in the regulation of urea, as well as Na^+, Cl^- ions and water. The anatomy of the nephron in shark kidneys is more complex than that of mammalian kidney. This is most

likely because of the additional function concerning the reabsorption of the urea and TMAO. Much of the data for shark kidney physiology is decades old, but it has been shown that urea and TMAO are absorbed against a concentration gradient from the renal tubule lumen because the concentration of these molecules in the final urine is much below their levels in plasma. But more molecular characterization studies are needed to identify and localize all the urea and TMAO transport mechanisms and transporter proteins in the shark kidney (Evans et al., 2004).

Elasmobranch kidneys are long and narrow paired organs found along the dorsal wall of the abdominal cavity. In cross section, they appear to have distinct "bundle zones" in the dorsal and lateral part of the kidney and "sinus zones" found in the ventral and medial regions. These different zones are due to the elaborate system of the nephrons and vasculature (Evans et al., 2004).

The arterial blood is supplied to the kidney through intercostal arteries branching from the dorsal aorta. These arteries branch into renal arteries that become the arterioles of the glomeruli and bundle arteries providing the blood to the interstitial capillaries of the bundle zones. Blood is drained from the glomeruli into the sinus zones that bathe certain segments of the nephron . The sinus zones also receive blood from the renal portal veins and the efferent blood from the bundle interstitial capillaries. The blood from the sinus zones is returned to the systemic venous circulation through an efferent renal vein (Evans et al., 2004).

The marine elasmobranch nephron is composed of five distinct tubule segments termed: neck, proximal, intermediate, distal, and collecting duct (Lacy and Reale, 1999). The nephrons begin at the renal corpuscles that lie in the sinus zone, near the interface

with the bundle zone (Figure 5). The renal corpuscle is composed of a glomerulus, which is surrounded by an epithelial Bowman's capsule and is responsible for urine formation by ultrafiltration. The first nephron segment (neck) arises from the distal end of Bowman's capsule and enters the bundle zone. Here the tubule begins the first of four loops through the bundle and sinus zones. The first and third loops of the nephron are contained in the bundle zone, and the second and fourth loops are contained in the sinus zone.

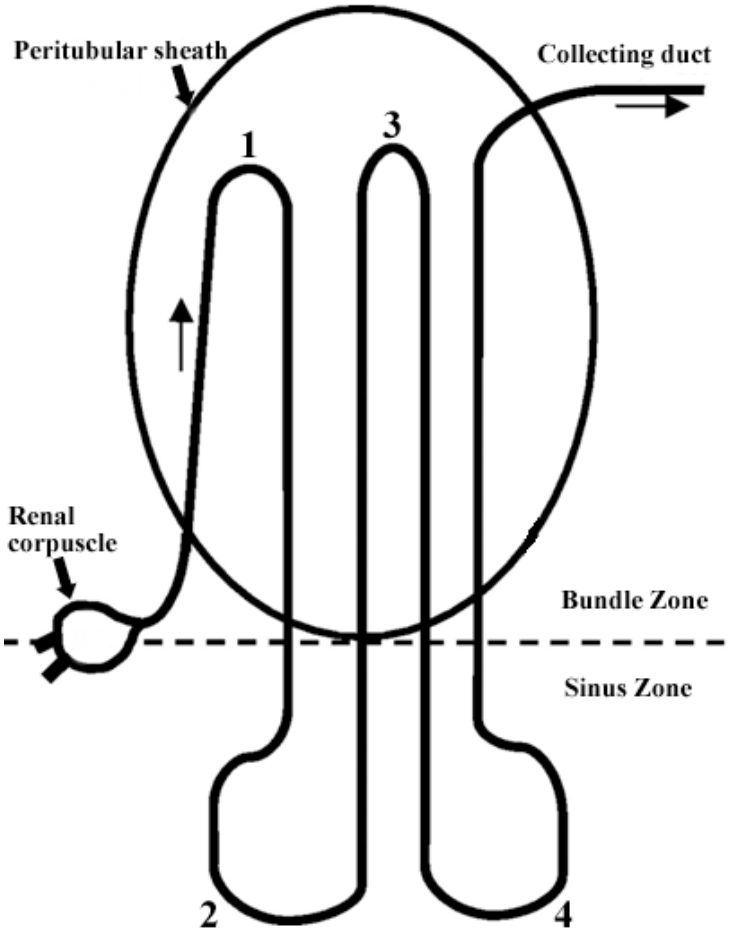

Figure 5. Simplified drawing of an elasmobranch nephron, adapted from Morgan, et al., 2003.

The tubules in the bundle zone are highly organized and run countercurrent to one another. They are packed tightly together by a peritubular sheath that surrounds the

tubules and isolates them from blood in the sinus zone. It has been suggested that this arrangement of tubules in the bundle zone functions as a countercurrent multiplier for urea and plays a role in urea reabsorption (Lacy et al., 1985). The tubules in the sinus zone are not packed tightly and are loosely organized. It has been inferred that this arrangement maximizes the surface area for diffusion between the urine in the tubules and the blood in the sinus and that this allows for the osmotic equilibrium between the two fluids (Friedman and Hebert, 1990).

Although secretion can occur in the proximal tubules of elasmobranchs, the kidney's main function is filtration and tubular reabsorption. The fraction of filtered fluid that is reabsorbed is variable but is thought to be approximately 60% to 85% and is related to the reabsorption of urea and TMAO, as they are the most abundant solutes found in the absorbed fluid. The marine elasmobranch nephron can reabsorb more than 90% of the filtered load of urea and TMAO. This could be due to simple solvent drag, i.e. when solvents in the ultrafiltrate are transported back by the flow of water. But since urine urea concentrations are much lower than plasma urea concentrations, excess urea and TMAO transport probably occurs. Although these mechanisms are still unresolved, it is clear that the majority of the reabsorption of urea occurs between the end of the proximal tubule and the beginning of the collecting ducts or perhaps within the collecting ducts (Marshall and Grosell, 2005).

The complex countercurrent arrangement in the elasmobranch nephron has led investigators to suggest passive, rather than active movement of urea along a favorable concentration gradient created by the absorption of Na^+, Cl^-, and water. According to this suggestion, the absorption of water causes low urea concentrations in the environment

surrounding the distal segments of the nephron and so provides a gradient for urea diffusion. Other lines of thought suggest the selective permeability for water and urea which, together with the countercurrent arrangement of the nephron, might concentrate urea within the tubules to encourage passive diffusion out of the terminal nephron segments. Both these ideas for the mechanisms of passive urea absorption would depend upon Na^+, Cl^-, and water absorption and so are in accord with original observations that link Na^+ with urea reabsorption (Marshall and Grosell, 2005).

Carrier-mediated urea transport has been demonstrated in the spiny dogfish shark (shark urea transporter, ShUT) and has shown high expression in the kidney (Marshall and Grosell, 2005). Two different apical urea transport pathways have also been characterized recently in elasmobranch kidneys (Morgan et al., 2003). A Na^+-urea co-transporter driven by Na^+- K^+ -ATPase activity in the basolateral membrane may perform secondary active urea transport. Further research is needed to determine the handling of tubular TMAO, as well as urea transport (Marshall and Grosell, 2005).

After taking this brief look at water homeostasis in marine elasmobranchs, the question could be asked, what about the transport of water itself through the plasma membranes of the cells in shark osmoregulatory organs? Is the transport of water due to simple osmosis through the plasma membrane lipids themselves? Or is there channel-mediated water movement? The answer is that both are likely to exist (Agre et al., 2002).

In 1991 Peter Agre discovered the function of a family of cell membrane proteins called aquaporins and later received a Nobel prize for the discovery (Preston et al., 1992). Aquaporins provide channels for the rapid movement of water molecules across the lipid bilayer of the plasma membrane along osmotic gradients and are vital to the regulation of

body water homeostasis. The aquaporin water channel proteins give cell membranes a 10- to 20-fold higher water permeability (Agre et al., 2002). Since the discovery of the first water channel protein, hundreds of homologous proteins have been found in all forms of life (Fujiyoshi et al., 2002). To date, 13 members of the aquaporin family have been identified in mammals where they have been studied most extensively and much has been learned about their complex role in body water homeostasis (Cutler et al., 2007; Evans et al., 2006; Rai et al., 2006).

The family of aquaporins is generally divided into the two groups: aquaporins 0,1, 2, 4, 5, 6, and 8, which are water-selective, and aquaglyceroporins 3, 7, 9, and 10, which are also able to transport glycerol, urea and other small solutes as well, the physiological significance of which is not completely understood (Hara-Chikuma, 2006; Nejsum, 2005). More recently, a new AQP subfamily has been discovered called superaquaporins, AQP11 and AQP12, so far present in multicellular organisms including plants, insects, nematodes, and vertebrates. Some superaquaporins are localized intracellularly at the membranes of organelles, but their role has not yet been established (Nozaki et al., 2008).

Peter Agre and his collaborators discovered how the aquaporin protein molecule is able to allow water molecules to pass through its pore without allowing protons to follow along. Through X-ray diffraction analysis, they saw that AQP1 has four monomers associated in a tetramer (Fu et al., 2000). Each monomer forms its own transmembrane pore with a diameter (2 to 3 angstroms) midway between the leaflets of the bilayer sufficient to allow the passage of water molecules in single file. Each monomer consists of six membrane-spanning helical segments and two shorter helices,

each of which contains the sequence of asparagine, proline, and alanine, known as "NPA" (Figure 6). These short helices containing NPA extend toward the middle of the membrane bilayer NPA regions overlapping in the middle of the bilayer thereby forming part of the specificity filter, or wall, which is the structure that allows only water to pass through (Fujiyoshi et al., 2002).

Figure 6 is a representation of an aquaporin showing the single water molecules in the very center of the pore of the cross-section. The adjacent charged residues, arginine and histidine, provide fixed positive charges to repel the passage of protons. A single molecule of water forms hydrogen bonds with the side chains of asparagine, which is highly conserved in aquaporins. A well-conserved residue, a cysteine, is also along the wall, which is the site of mercurial inhibition. There are also partial positive charges provided by the orientation of two α helices that enter, but do not actually span the bilayer (Agre et al., 2002).

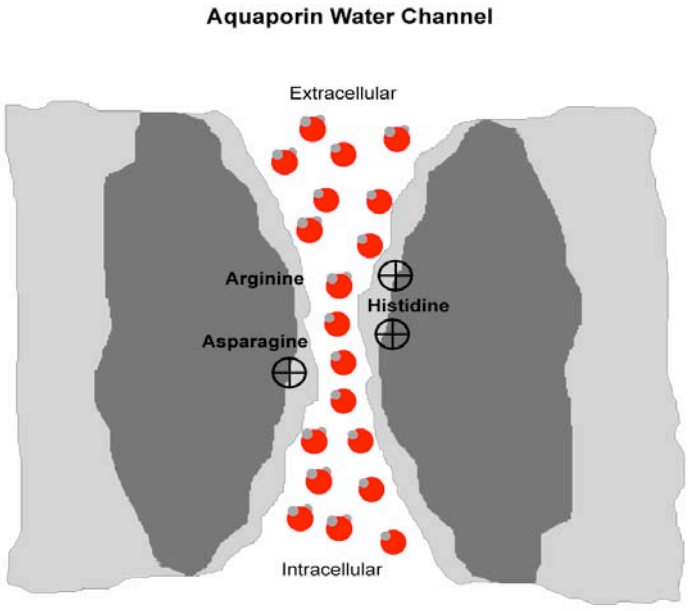

Figure 6. Schematic presentation of an aquaporin molecule in a plasma membrane.

Why do water molecules pass through these pores, but protons fail to be carried through them? The answer lies in the unique properties of water. In solution, hydrogen bonds between water molecules cause water to be a liquid. In bulk solution, water molecules are close together and hydrogen bonding occurs. This allows free movement of protons hopping between the molecules. Water exists in bulk solution in the extracellular and intracellular areas surrounding the aquaporin. But at the center of the aquaporin, water transits the pore in single file. A fixed positive charge on the adjacent side chain of arginine will repel the protons. Then the water molecules are spaced within the pore at intervals so that hydrogen bonding cannot occur between them. There is a second barrier existing in the center of the pore where an isolated water molecule will form transient hydrogen bonds to the side chains of the highly conserved asparagine

residues. This arrangement provides a mechanism for water to move with no resistance (Agre et al., 2002).

Approximately 3×10^9 water molecules per monomer per second can pass through the pore of an aquaporin. Studies of *Escherichia coli* glycerol factor (GlpF) have shown that the pore region of aquaglyceroporins is slightly larger than those of aquaporins, allowing the passage of the larger glycerol molecules to pass through (Fu et al., 2000).

Aquaporins are expressed in humans in multiple tissues and are essential for the regulation of body water homeostasis. At least seven aquaporins have been expressed in distinct sites in the human kidney and correlate with observed water permeability of each nephron segment. The proximal tubule and descending thin limb of Henle have shown high water permeability due to the expression of AQP1. The collecting duct water permeability is tightly regulated by the antidiuretic hormone vasopressin and the regulation of AQP3 seems to occur with AQP2 (Nejsum, 2005). AQP3 has been shown to be localized in the basolateral plasma membranes of collecting duct principal cells as well as the connecting tubule located before the duct (Ma et al., 2000). AQP3 is also distributed in the human lung, skin, and eye. Functional relationships between the cystic fibrosis transmembrane regulator (CFTR) and AQP3 suggest that the regulatory defect in cystic fibrosis may involve both these proteins (Agre et al., 2002).

Aquaporins are represented in nearly all life forms, including higher mammals, other vertebrates, invertebrates such as in the digestive tract and brain of insects; eubacteria, archebacteria and other microbials, and perhaps the largest collection of homologues are being identified in plants (Agre et al., 2002). In teleost fish, AQP3 has

been shown to occur in at least four species including the European eel, Osorezan dace, Mozambique tilapia and Japanese eel (Cutler et al., 2007).

The subject of this study is to demonstrate that at least one aquaporin homologue, AQP3, exists in sharks and to demonstrate that aquaporins play a role in water homeostasis. Aquaporin 3 is an aquaglyceroporin that allows the permeation of water molecules as well as glycerol and urea, yet the physiological significance of this glycerol and urea permeation is not well understood (Hamann et al., 1998). One possible role of Aquaporin 3 in teleost fish suggests that it plays a role in the prevention of dehydration in epithelial cells as has been shown previously in mammals (Matsuzaki et al., 1999). In one study, mice that are deficient in AQP3 had dry skin with reduced elasticity and epidermal biosynthesis was impaired (Hara-Chikuma and Verkman, 2006). A Japanese study showed that rat AQP3 was localized in many epithelial cells in the urinary, digestive and respiratory tracts, as well as the skin, and it was specifically expressed in the principal cells of the renal collecting duct on the basolateral membrane (Matsuzaki et al., 1999). There have been no studies that have shown the existence of aquaporins and aquaglyceroporins in sharks, but there is the strongest likelihood of their presence in abundance in shark kidney, as well as some potential presence in the gills, intestines, stomach, esophagus, rectal gland, and, possibly the brain, because of the research studies in teleost fish and mammals. It is hypothesized in this project that their function may vary according to the salinity of the shark's water environment.

It is the purpose of this study to a.) characterize the expression of the AQP3 water channel gene in tissues collected from the organs involved with water homeostasis in dogfish sharks (*Squalus acanthias*). And b.) attempt to manipulate the expression of

the AQ3 gene in sharks that have been acclimated to varying water salinities, namely 100% sea water, i.e. 30 parts per thousand, 75% SW, i.e. 22.5 ppt, and 12% SW, i.e. 36 ppt. These data will in turn, provide new evidence for the presence of AQP3 in dogfish sharks. The data may also suggest important roles of AQP3 in osmoregulation, nitrogenous waste metabolism and fatty acid metabolism as suggested in the literature, But more studies are needed to fully understand the role of AQP3 in sharks.

CHAPTER 2

MATERIALS AND METHODS

Animal Holding Conditions and Dissection

Dogfish sharks (*Squalus acanthias*) were collected by commercial fishermen from Mount Desert Island Frenchman Bay, Maine, and maintained in aquariums with running seawater at 12 - 16°C until needed. Individual sharks were removed from the tank and immediately sacrificed with a sharp knife by cutting behind the gills and a subsequent pithing method which quickly destroyed the spinal cord and brain area of the fish. Various shark tissue samples were dissected for experiments. Gill tissue was scraped off the cartilage using a single-sided razor blade. Likewise, the intestinal and esophageal epithelia was removed and scraped with a glass slide. Rectal gland and kidney tissue were removed and homogenized using a polytron homogenizer (Model 3100 Kinematica).

Dogfish sharks were acclimated to 75% SW and 120% SW in three steps. The 75% group was allowed to acclimate to 85% SW for 3 days, then for 2 days in 75% SW. The 120% group acclimated for 3 days in 110% SW and then for 2 days in 120% SW. The salinity of 100% SW was measured at 29.8 parts per thousand, 120% SW was 35.8 ppt and 75% was 22.4 ppt.

The protocols were approved by the Institutional Animal Care and Use Committee in a memo from the Georgia Southern University Office of Research Services & Sponsored Programs. The research protocols were approved through November 21, 2008, for both GSU and Mount Desert Island Biological Laboratory, Salisbury Cove, Maine.

Total RNA Isolation from Tissues: Extraction of Total RNA Using Modified Chomczynski Method

Fresh tissue samples from dogfish sharks were collected at the Mount Desert Island Biological Laboratory (MDIBL), specifically from the esophagus, stomach, intestine, rectal gland, kidney, gills, brain, and liver. Because these tissues produce RNase enzymes, the tissue was transferred to polypropylene centrifuge tubes or snap top tubes depending on tissue weight, containing Solution D (Appendix A), a chaotropic solution that would inhibit RNase enzymes, 10 ml per gram of tissue, and homogenized as soon as possible.

Then kidney or rectal gland tissues were homogenized for 15-30 seconds at room temperature with a polytron homogenizer at maximum speed (27,000 rpm). Epithelial gill tissue was scraped from the gill using a razor blade and homogenized using a 2 ml syringe and 16-gauge needle. Esophageal and intestinal epithelial samples were scraped off using a glass microscope slide and homogenized as for gill tissue. Samples were subsequently stored at -80°C until the RNA extraction process could be completed. Total RNA was extracted using a modified version of the Chomczynski method described in Chomczynski and Mackey (1995). The modified Chomczynski method uses Solution D and BCP (1-Bromo 3-chloropropane) is used to denature the protein. The original Chomczynski used chloroform instead of the BCP. Ten ml of Solution D were used per gram of tissue. To begin the protocol, Solution D was used to homogenize the sample. Then, sequentially, 2M Na acetate, pH 4 was added, water-saturated phenol, then finally the BCP. The hydrophobic BCP separates the mixture into two phases.

Next, the mixture was centrifuged at 7,500 rpm for 20 minutes at 4°C. Then the upper aqueous phase containing the RNA was transferred to a fresh tube. This was repeated, but only the BCP was added. The RNA from the aqueous phase was precipitated using 0.2 volumes of propanol and high salt buffer (Chomczynski and Mackey, 1995). The precipitate was mixed and stored at room temperature for 10 minutes.

Next, the precipitated RNA was centrifuged at 7,500 rpm at 4°C for 10 minutes. The pellet was washed twice with 70% ethanol and centrifuged again.
Any remaining ethanol was removed with a disposable pipette tip. The pellets were dried partially to allow evaporation of any residual ethanol. Last, the final RNA pellets were dissolved in distilled H_20.

The recipe used a ratio of initial ingredients: 1:0.1:1:0.2., i.e. the first attempt used the ratio of the following amounts:

1.0 ml Solution D

0.1 ml 0.2 M Na Acetate

0.5 ml phenol

0.266 ml BCP

Because the BCP may have caused some tubes to break during centrifugation, another recipe was also used on samples lost, with more phenol but less BCP, as BCP was thought to be responsible for the tube breakage.

1.0 ml Solution D

0.1 ml 0.2 M Na Acetate

0.7 ml phenol

0.225 ml BCP

The protocol proceeded as described in the basic steps above with satisfactory results.

Agarose Gel Electrophoresis

PCR products were visualized using agarose gel electrophoresis. Agarose gels (1.5%) were prepared as follows.

For 135 ml agarose gel:
- 2.025 g agarose
- 2.7 ml 50X TAE buffer (Tris-acetate and EDTA) to a final working concentration of 1X.
- 132.3 ml H_20
- 6.75 μl of 10 mg/ml ethidium bromide to a final working concentration of 0.5 μl/ml

The first three reagents were mixed together and the solution was placed in a microwave oven at full power for 1 minute 40 seconds, then swirled carefully. The gel was heated for another minute at 30% power, swirled, and this was repeated until there were no visible flecks in the solution. The flask was placed in a 45°C water bath to cool down before pouring the agarose solution into the gel tray to harden. The ethidium bromide was added after the solution cooled slightly. The gel was poured into the gel tray before it set completely, then the combs were placed into the gel. 1X TAE was used as the gel electrophoresis running buffer. A gel loading dye made of bromophenol blue and xylene cyanol FF was added to the PCR samples to enable to visualization of the distance traveled by DNA macromolecules in the gel. Once the gel was set completely, the combs were carefully removed and the gel was mounted in the electrophoresis tank.

Just enough buffer was added to cover the gel to a depth of about 1mm. Samples were loaded into the submerged gel using a micropipettor.

The lid of the gel tank was closed and the electrical leads were attached. The negatively charged DNA was run towards the positive electrode. A constant current initially of 500 mA was used to run samples into the gel. Subsequently, the gel was run at approximately 250 mA for 20 minutes until the bromophenol dye had migrated halfway. Once the marker dye had traveled halfway, the electrical current was turned off and the leads and lid were removed from the gel tank. The gel was examined using an UV light transilluminator and photographed. The rate of double-stranded DNA molecule migration are inversely proportional to the $\log_{10}$ of the number of base pairs (Helling et al., 1974) and so it is possible to calculate the molecular mass for each band in a lane of a gel by reference to the distance run by molecules of a known size.

Electrophoresis of RNA through Agarose Gel with Formaldehyde

The first stage in Northern hybridization is to separate RNAs according to size by electrophoresis through denaturing agarose gels. Agarose electrophoresis of RNA has much in common with DNA agarose electrophoresis but with some important differences. Samples of RNA may be denatured by treatment with formamide and formaldehyde and separated by electrophoresis through agarose gels made with formaldehyde (Sambrook and Russell, 2001). Agarose gels containing formaldehyde are more fragile than non-denaturing agarose gels, therefore need greater care in their handling. Unfortunately, formaldehyde gels have high background due to the formaldehyde and so bands produced never appear as crisp as the bands in DNA agarose

gels. Another disadvantage is that formaldehyde gels are less safe as formaldehyde is highly toxic by inhalation as well as contact with the skin and needs to be handled with great care using a chemical fume hood.

A 1.75% gel was prepared as follows:

2.361 g agarose was dissolved into 97.875 ml distilled H_2O by boiling in a microwave oven. The solution was cooled, then 13.5 ml 10X MOPS electrophoresis buffer (3-{N-morpholino} propanesulfonic acid and 10 mM EDTA) and 23.625 ml 17.5% formaldehyde was added carefully under a chemical fume hood.

A 1.5% gel was prepared similarly, but with 2.025 g agarose, 23.625 ml 17.5% formaldehyde, 13.5 ml 10X MOPS, and 97.875 ml H_2O.

The gel was cast under the fume hood using 2-mm comb and allowed to set for one hour at room temperature.

RNA samples were prepared by setting up the denaturation reaction in microfuge tubes. The amount of RNA was determined on an initial agarose gel, using one sample as a standard, and recorded for subsequent use. A master mix for RNA denaturation was then prepared (Appendix A). A total of 23.875 µl master mix was placed into each tube. RNA sample amounts were added according to their normalized concentrations.

RNA samples were incubated for 10 minutes at 65°C, then chilled on ice. They were centrifuged briefly to deposit all the fluid in the bottom of the tubes. The 1X MOPS electrophoresis buffer was added to the electrophoresis box to cover the gel to a depth of ~1 mm. The RNA and marker samples were loaded into the wells of the gel and allowed to run until the bromophenol blue dye in the sample ran near to the bottom of the gel.

Synthesis of cDNA Catalyzed by Reverse Transcriptase

The first stage in molecular cloning is to synthesize complementary DNA (cDNA) from messenger RNA (mRNA). cDNA was also synthesized in order to perform RT-PCR.

First, RNA samples were heated to 65°C for 5 minutes, placed on ice, and vortexed briefly. The RNA samples were prepared by adding H_20 to them, up to a total amount of 10.5 μl, according to the calculation of the amounts of RNA used.

Reagents were mixed together in a microfuge tube and referred to as the Reverse Transcriptase Master Mix (Appendix A). The master mix (8.5 μl) was added to each sample tube and the tube was placed in a thermocycler for 10 minutes at 65°C. The temperature was changed to 50°C before 1 μl Superscript III (Invitrogen) reverse transcriptase enzyme was added to each tube bringing the total reaction volume to 20 μl in each tube. Each sample was mixed by pipetting up and down 5 times gently and placed into the thermocycler to incubate for up to 2 hours so that the reverse transcriptase reaction would occur. When used for quantitative RT-PCR, the samples were made up to 100 μl by adding 80 μl H_20, and then frozen until needed to set up the quantitative RT-PCR test reactions.

Polymerase Chain Reaction

Polymerase chain reaction (PCR) is an invaluable technique where specific segments of DNA are amplified over a millionfold. To begin the amplification, two synthetic oligonucleotide primers are prepared that are complementary to sequences on opposite strands of the target DNA at positions just beyond the segment of interest to be

amplified. The oligonucleotides are replication primers that can be extended by DNA polymerases. The 3' ends of the hybridized probes are oriented toward each other and are positioned to prime the synthesis of DNA across the target segment. Isolated DNA that contains the target segment for amplification is heated briefly to denature it, then cooled in the presence of the synthesized primers. The four deoxynucleoside triphosphates (dNTP's) are added and the primed DNA segment is selectively replicated. The DNA segment is amplified essentially exponentially by a cycle of heating, cooling, and replication which is repeated for 25 or 30 cycles in a few hours in an automated process using a thermocycler resulting in an amplified product that can be used for analysis and cloning.

PCR uses a heat-stable DNA polymerase, such as the *Taq* polymerase enzyme which is derived from bacteria that inhabit very high temperature environments. It loses very little activity after each heating step and does not have to be replenished. The amplifications in this project were performed using either Phusion or *Taq* DNA polymerase enzymes from New England BioLabs and an Eppendorf Master Cycler PCR machine using a 20 μl reaction volume. The components of the reaction were prepared as follows.

To begin a general PCR reaction, 1 μl of each 4 μM DNA primer stock (sense and antisense) was added to a 200 μl PCR tube, placing each droplet on the side wall of the tube, to be pushed down when the Master Mix was added. Then, 0.5 μl of the DNA template (cDNA) was added to the side wall of the tube in a separate place. At this time, the thermocycler was started and paused in its cycling at an initial denaturation temperature of 92°C.

The Master Mix was prepared, adding the least expensive ingredients first (Appendix A). The buffer was provided by the manufacturer (Appendix A).

Alternatively, for rapid amplification of cDNA ends (RACE) PCR, Phusion DNA polymerase (Finnzymes, Inc.) was used instead of *Taq* polymerase because the size of the AQP3 RACE products was unclear and *Taq* polymerase is unable to make products beyond a certain size. Reactions were created as follows:

2.5 μl 4 μM sense primer

2.5 μl 4 μM antisense primer

0.5 μl cDNA

In a separate tube:

4 μl 5X Buffer

0.4 μl dNTP's

9.9 μl H_20

0.2 μl Phusion enzyme

The components were mixed by pipetting.

Once the thermocycler was at its target temperature, 17.5 μl of Master Mix was added to each tube, taking care that there were no air bubbles at the bottom of the tube. As quickly as possible, each tube was placed individually into the thermocycler and the lid of the PCR machine was shut each time. The standard PCR cycle performed used an initial denaturation at 92°C for 2 minutes, followed by 40 cycles denaturing at 96°C for 1 second, annealing of 55°C for 30 seconds, elongation at 72°C for 1 minute, and with a final one step elongation at 72°C for 10 minutes. After completion of PCR, the products were mixed with 1.0 μl of gel loading buffer containing bromophenol blue and xylene

cyanol FF dyes. Electrophoresis was performed on a 1.5% agarose gel for most reactions.

Rapid Amplification of cDNA Ends (RACE) and Primer Design

The initial cDNA fragment, from the central part of AQP3, was cloned and sequenced from *S. acanthias* kidney by Dr. Cutler prior to the onset of this project. But in order to determine the full-length nucleotide sequence of AQP3 in *Squalus acanthias* kidney and rectal gland, a method known as "Rapid Amplification of cDNA Ends" or "RACE" was employed. This is a polymerase chain reaction method used to generate double-stranded cDNA from the 3' end (3' RACE) or the 5' end (5' RACE) of a specific mRNA. A software algorithm (Finnzymes.com) was used to develop 5' and 3' RACE forward and reverse primers. These primers were based on the previously available *Squalus acanthias* AQP3 cDNA sequence with a high enough T_m to anneal to target DNA binding sites at 63°C during PCR (to match the primer T_m's of the AP1 and AP2 primers from the Marathon cDNA synthesis kit). To generate sufficient AQP3 DNA product and to increase the specificity of PCR amplification, a second round of "nested" reactions (a second set of primers located within the DNA fragment generated with the first set of primers) were also performed.

To begin the design of these gene specific primers (GSP's), sequences were located in from the end by at least 50 bp's to allow an overlap with the previous sequence so that the correct sequences from the AQP3 gene could be identified. Areas that contained no runs of G or C nucleotides longer than 3 were selected to prevent non-specific binding of the primer to G-C rich DNA. The primers were designed with 23-26

base pairs in length and were ordered from Integrated DNA Technologies, Inc. (See Table 1).

The nested antisense primers for 5' RACE (for the 5' end of the cDNA) were called 5R1 and 5R2 and the nested sense primers for 3' RACE (for the 3' end of the cDNA) were called 3R1 and 3R2. Nested amplifications are performed one after the other, the second one, using the first as its template. The RACE RT-PCR was performed utilizing pre-existing cDNA template libraries from *Squalus acanthias* kidney and rectal gland tissues, made using a Marathon cDNA Amplification Kit (Clontech). The Marathon Kit incorporates an adaptor ligated on to the end of all cDNA's produced from total RNA from the tissue used. The kit includes two primers located within the adaptors that are present on both ends of all cDNA's. The adaptor primers are called AP1 and AP2 (adaptor primers 1 & 2; AP1 & AP2). (See Figure 7.) The GSP's were used in conjunction with the adaptor primers from the Marathon kit to amplify the 5' and 3' ends of the *Squalus acanthias* AQP3 cDNA.

Initial PCR reactions were performed using the AQP3 GSP (5R1) or AQP3 GSP (3R1) and the adaptor primer (AP1). The specificity of 3' RACE was increased by using a primer made incorporating part of the sequence of the kit's cDNA synthesis primer (an extended oligo dT primer) and partly using the sequence of the end of the marathon adaptor. This primer was called MCDS and was used in conjunction with the AQP3 GSP (3R2) primer. Subsequent nested reactions to amplify the 5' end of AQP3 were performed with AQP3 GSP (5R2) and AP2.

Name	Nucleotide Sequence (5' to 3')	Orientation
Squalus AQP3 5R1	CAGGATTCAAGTGCGCTCCTG with AP1	Antisense
Squalus AQP3 5R2	AGGAGTACACCGAGCATCACTGC with AP2	
Squalus AQP3 3R1	TGCCATGTGGGACTTTAGTGGTC with AP1	Sense
Squalus AQP3 3R2	CCCATCTGTGCCACTTAACTCCACTCA with MCDS primer	
Marathon cDNA Adaptor	CTAATACGACTCACTATAGGGCTCGAGCG GCCGCCCGGGCAGGT	Either
Adaptor Primer 1 (AP1)	CCATCCTAATACGACTCACTATAGGGC	
Nested Adaptor Primer 2 (AP2)	ACTCACTATAGGGCTCGAGCGGC	
MCDS Primer	GGGCAGGT*TTCTAGAATTCAGCGG* Marathon cDNA synthesis primer adaptor	Antisense

Table 1. Gene specific primers (GSP's) for RACE RT-PCR and Marathon adaptor sequences.

```
                                                MCDS Primer
Marathon cDNA Adaptor                           5'-GGGCAGGTTTCTAGAATTCAGCGG-3'
        5'-CTAATACGACTCACTATAGGGCTCGAGCGGCCGCCCGGGCAGGT-3'
AP1 5'-CCATCCTAATACGACTCACTATAGGGC-3'
AP2              5'-ACTCACTATAGGGCTCGAGCGGC-3'
```

Figure 7. Alignment of Marathon adaptor primers.

Cloning of PCR Product

PCR products of the appropriate size (as predicted from other species' AQP3 sequence coding regions) were purified from the gel electrophoresis and inserted into a plasmid for cloning using the Invitrogen TA Cloning Kit for Sequencing, according to a modified version of the manufacturer's instructions.

The TOPO TA Cloning Kit for Sequencing provided a one-step cloning strategy for the direct insertion of *Taq* polymerase-amplified PCR products into a plasmid vector for sequencing. Because the *Taq* polymerase used in the amplification of the PCR product adds deoxyadenosine (A) to the 3' ends, the linearized vector supplied in the kit ligates efficiently because it has a single, overhanging 3' deoxythymidine (T) residues. For RACE products, a Phusion enzyme (Finnzymes, Inc.) was used instead of *Taq* polymerase because the size of the AQP3 RACE products was unclear and *Taq* polymerase is unable to make products beyond a certain size. As this is a proofreading enzyme, additional deoxyadenosine overhangs had to be added separately after gel purification using incubation with *Taq* DNA polymerase and dATP (200 μM) for 10 minutes. The topoisomerase enzyme (TOPO) joins, the DNA to be inserted with the plasmid DNA, together, without the need for a further ligation step.

The basic steps for cloning are as follows:

1. Produce the purified PCR product.
2. Mix the PCR product and pCR4-TOPO together for the ligation reaction.
3. Transform into the TOP10 *E. coli* cells.
4. Plate and pick colonies, then grow in broth.
5. PCR amplify DNA from colonies used, to obtain nucleic acid for sequencing.

Reagents used for each PCR product TOPO cloning reaction are listed in the order in which they were added (Appendix A), for a final volume of 2 μl which was 1/3 of the manufacturer's suggested recipe.

The ligation mixture was incubated at room temperature for 30 minutes. Then, the entire TOPO cloning reaction was added into an aliquot of "One Shot" chemically

competent *E. coli* (the volume of bacteria used varied, depending on the number of samples, but was often 16.67 μl). This was mixed gently, and then placed on ice for 5 minutes. The cells were then heat-shocked in a dry-block heater at 42°C for 30 seconds without shaking, then immediately placed on ice. This sudden change in temperature allows the DNA molecules to enter the bacteria. Next, 83.33 μl of room temperature S.O.C. bacterial medium (supplied with the kit) was added to each tube. The tube was capped tightly and kept on a rotating wheel at 37° C for one hour. Once the incubation was complete, approximately half of each cell culture transformation (50 μl) was spread onto each of two 37 °C prewarmed kanamyacin selective Luria-Bertani (LB) agar plates, which were then incubated overnight at 37 °C. The pCR 4-TOPO plasmid contains a kanamyacin resistance gene that that allows growth of transformed bacteria on antibiotic kanamyacin-treated LB Agar plates. The plasmid's ccdB gene (also known as a "Zero" gene), if disrupted by an insert, is inactive. However, plasmids without inserts produce an active ccdB gene product which kills the bacterial host, reducing the numbers of background colonies not containing an insert.

For each transformation, 10 isolated colonies were selected and the cells were further grown in Terrific Broth (TB) liquid culture containing 50 μg/μl Kanamycin. Individual colonies were picked and placed into approximately 1 ml of broth in 1.5 ml microfuge tubes. The tubes of broth were incubated at 37°C overnight rotation/inversion to ensure adequate mixing of the bacteria, nutrients and oxygen.

On the following day, a 50 μl aliquot of each colonies LB broth was placed in a clean tube, which was spun at 14,000 rpm and the supernatant was discarded. The pellet from each tube was resuspended in 500 μl dH_20. This was used as a DNA template for

colony PCR. PCR was performed using M13 forward and reverse primers, the binding sites for which, were located in the plasmid either side of the PCR fragment insert site. PCR was reduced to 25 cycles to yield products with less non-specific amplification artifacts. PCR reactions were then purified using Edge BioSystems QuickStep 2 PCR Purification Kit as described in the following protocol (PCR Fragment Purification for Sequencing).

Isolation of DNA from Agarose Gels in Preparation for Cloning

Purification and isolation of DNA fragments from the agarose gels was performed using a Qbiogene Geneclean Spin Kit according to manufacturer's instructions with some modifications as per Dr. Cutler as follows. The Geneclean spin kit uses silica in high concentrations of chaotropic salt because DNA generally binds to silica under such conditions and elutes from the silica when the salt concentration is lowered (Melzak et al., 1996).

The initial step of the procedure was to place an agarose gel slice containing the DNA to be purified (up to 300 mg) into a 1.5 ml tube. Glass milk (400 μl), which is a suspension of silica particles in a chaotropic salt solution, was added and the tube was placed into a dry block for a minimum of 3 minutes at 55°C, suspending the glass milk by flicking the tube gently every minute. The gel slice was heated until it was dissolved in the glass milk solution, which usually took about 4 or 5 minutes. During incubation, DNA released from the gel adheres to the glass milk particles due to the high salt conditions. The tube was then spun briefly in a microcentrifuge for 9-12 seconds at maximum speed (14,000 rpm). This step was crucial because the short spin stops the

glass milk from clumping. The liquid was immediately removed from the glass pellet with a 1 ml pipette, as much liquid as possible was removed without taking any of the glass milk. The kit's ethanol wash solution (500 µl) was then added to the glass milk pellet. It was vortexed until the entire pellet had come off the side of the tube and resuspended as single particles in solution. It was then re-spun just up to maximum speed again for 9-12 seconds. As much wash solution as possible was removed with a pipette. These wash steps were repeated with another 500 µl of wash solution.

After the removal of the second wash, the tubes were centrifuged at maximum speed for 1 minute and a P10 pipette tip was used to remove all residual wash buffer. Then, 10 µl of the distilled water (previously heated to 55°C) was added to the tube to elute the DNA and mixed by pipetting up and down until the glass milk was resuspended. The tube was placed in the dry block heater at 55°C and incubated for 3 minutes with occasional mixing by flicking. The tube was spun at full speed for 1 minute, and then the water (and the DNA) was removed from the glass milk pellet . The water containing the DNA was added to a pre-labeled spin column used to catch any residual silica particles. Another 10 µl of water was added to the glass milk in the original tube and this was mixed by pipetting up and down. It was then placed into the dry block heater again at 55°C for 3 minutes. The glass milk tube was spun again at full speed for 1 minute. The water, which contains an additional 10% yield of DNA, was removed and added to the spin column. Finally, the spin column itself was centrifuged at full speed for 1 minute. There was now 15-20 µl of purified DNA solution in the bottom of the spin column catch tube. The column was discarded and the tube containing the DNA was kept and ready to be used in cloning experiments, etc.

PCR Fragment Purification for Sequencing

To purify the cloned products for sequencing, the Edge BioSystems QuickStep 2 PCR Purification Kit was used. The kit contained 2 purification reagents: a solid-phase oligo/protein elimination resin (SOPE) that binds primers, ssDNA, enzymes and other proteins, and the Performa Gel Filtration Cartridge that eliminates up to 99% of salts, dNTPs, buffers, and other small molecules.

First, the SOPE Resin is vortexed briefly to mix. Next, a 1/5 volume of SOPE resin (4 μl) relative to the cloning product volume was added directly to each PCR fragment amplification reaction that had a nominal volume of 20 μl. After thorough mixing, the suspension was allowed to stand at room temperature while the Performa Gel Filtration Cartridge was prepared. The cartridge was first spun for 3 minutes at 850-x g and then transferred to a clean microcentrifuge tube. The SOPE/cloning product mixtures were transferred to the top of the prepared cartridge and centrifuged at 850-x g for 2 minutes and eluates were retained.

The amount of DNA in the purified PCR products was then assessed using gel electrophoresis. Known amounts of DNA marker were run in several lanes of the gel. 2 μl of each purified fragment were run in separate gel lanes. The intensity of each band was measured using a Kodak gel documentation system and compared with the intensity of the DNA marker bands to quantify the amount of DNA in the purified fragments. 20 ng of DNA per 1 Kbp of DNA fragment was used for sequencing.

DNA Sequence Analysis

Once the DNA samples were purified, 4 ρ-moles of sequencing primer (usually a T3 primer based on that region of the plasmid vector) was added and the samples were dried out using an Eppendorf centrifugal evaporator. The samples were then mailed to Clemson University to run on their automated DNA sequencer. Sequences were obtained using the Sanger (or dideoxy) method that makes use of the DNA synthesis by DNA polymerases. Sequence analyses were carried out in a PCR reaction with four different fluorescent dyes, one for each dideoxynucleotide reaction (i.e. an ABI Big dye Sequencing Kit). Chains of every possible length up to 1,000 nucleotides were produced. Each terminated by a dye-labeled dideoxynucleotide. The color of the dye added to each chain was determined by the type of nucleotide present at that location of the sequence (i.e. the end nucleotide of each chain). The samples were separated on a single lane of polyacrylamide gel or polymer-filled capillary tube.

Each fluorescent dye emits a different color of light when it is struck by an argon laser beam. The beam scans each lane of the electrophoretic matrix from the bottom upwards. As each successive labeled fragment passes through the beam, the excitation causes an emission with specific spectral features that are detected by a photomultiplier tube. The emission data are recorded and stored in a computer. The succession of fluorescent signals is then converted to nucleotide sequence information because each dye emits a different wavelength color representing a particular nucleotide on the end of each chain (Nelson and Cox, 2005).

Once these traces were received from Clemson, they were analyzed using 4-Peaks software to remove the various non-AQP3 sequences that were known, e.g., the region

surrounding the insert site of the plasmid vector, Marathon adapters and gene specific primers, and the sequence for each AQP3 fragment was deduced. The manipulation and alignment of the sequences to produce a complete AQP3 cDNA sequence was performed using the Gene Jockey II (Biosoft).

Northern Blotting and Hybridization: Part One – Northern Blotting

Northern blotting and hybridization uses mRNA or total RNA that is extracted from cells and purified. The RNA is loaded onto a formaldehyde gel for electrophoresis with standards made of known sized RNA fragments. The RNA samples for Northern blotting are separated on an RNA agarose electrophoresis gel (see previous section). The transfer can be performed using electro-blotting or by capillary action with a high salt solution. After electrophoresis the RNA samples are transferred to a filter support. A fluorescent or radioactive labeled probe specific for the gene of interest is incubated with the blot. The blot is washed to remove non-specifically bound probe and then a development step allows visualization of the probe that is bound. The binding is specific and requires the base pairs of the probe and the bound mRNA, be complementary (i.e. A to U and C to G, etc.). A wash step removes any probe that is not bound to the mRNA on the membrane. Only probe that forms a double strand with the mRNA for the gene of interest should remain bound.

To begin the Northern hybridization experiment, intact mRNA or total RNA must be isolated and separated according to size through a denaturing formaldehyde gel. This was a difficult procedure to perform because of the varying amounts of RNA in the

Squalus acanthias tissues. Again, RNA formaldehyde gels were prepared as described previously.

Concentrations of RNA samples were normalized after using a series of test gels and resulted in the following dilutions and concentrations of samples. Several samples had been previously split into more than one tube because the volume to dissolve the sample was too great for one tube.

Tissue	Concentration	Amount used in µl
Kidney 3	1.45	6.9
Intestine 1	0.48	20.83
Gill 2	0.50	20.00
Esophagus 2	1.19	8.40
Stomach 1	2.61	3.83
Rectal Gland 2	2.65	3.77
Brain 1	1.56	6.41
Liver	1.51	6.62
Muscle	0.97	10.31
Eye	0.40	25.00

The marker used in the gel showed fragment sizes of the following numbers of kilo bases:
9,000
7,000
5,000
3,000
2,000
1,000
500

After electrophoresis, the RNA was visualized using UV light and bands were approximately even in intensity and deemed suitable for blotting. The gel was soaked for 1 hour in distilled H_20 and then for 1 hour in 1X TAE to remove the gel's formaldehyde by diffusion and replace it with blotting buffer (i.e., 1X TAE). The electroblotter was set up according to manufacturer's directions. Bio-Rad Trans-Blot Paper, 15 x 20 cm, was used. The membrane used was from a 30 cm x 3.3 m roll of Bio-Rad Zeta-Probe GT

genomic tested blotting membrane, using a razor blade to cut it the same size of the gel. The electroblotter was connected to a cooling system, using anti-freeze that was pumped from a reservoir through a cooling coil in the blotting tank. The Fisher Scientific FB200 power pack was set for 1 amp, around 30 to 45 volts, and consequently run for at least three hours of electroblotting. The membrane was carefully removed from the gel and placed in a rectangular plastic bucket and allowed to soak in 1X TAE to keep them wet prior to the hybridization experiment.

Part Two - Northern Hybridization

The Northern hybridization was performed with the following steps:

1. Hybridization of the immobilized RNA to probes complementary to the sequences of interest.
2. Removal of probe molecules that are nonspecifically bound to the solid matrix.
3. Detection, capture, and analysis of an image of the specifically bound probe molecules.

To begin the protocol, the hybridization probes were made as follows.

First add, in order:

31.8 µl H_20

0.77 µl (25 ng) AQP3 DNA probe (32.5 ng/µl of the original central fragment of the cDNA))

10 µl Promega 5X buffer (including random hexanucleotide primers)

2.0 µl 10 mM dNTP (dCTP)

At this point, the reaction was heated to 95°C for 5 minutes (or boil) to denature DNA probe. Snap cool on ice, then add 2.0 μl BSA (1 mg/ml). Next, the solution was brought to the "hot room" to add the radioactive ingredients:

2.5 μl α^{32}P dCTP

1.0 μl (5 units) NEB exo- Klenow DNA polymerase

Mix by pipetting as each item is added and then place in a dry block at 37°C for 1 hour. The probe from the reaction was then purified using a purification column (without SOPE resin) from a Quick Step 2 DNA purification kit.

1. Spin @ 850 x g for 3 minutes.
2. Transfer cartridge to a new1.5 ml microcentrifuge tube.
3. Add the sample "drop-wise", slowly, to the center of the packed column. Be sure fluid runs through the gel.
4. Close the cap and centrifuge. Spin 2 minutes at 3000 rpm (750 x g), retain eluate. Put hole in lid of tubes.
5. Place tubes into dry block at 100°C for 3 minutes to denature probe DNA strands. Snap cool - put on ice immediately.

The hybridization tubes were prepared by cleaning and greasing the O-rings. The blot was placed in a hybridization tube, such that it lined the inside and it was then wetted with 1X TAE buffer solution. After the blot had been brought up to temperature (47°C) in the incubator, the buffer was poured off and replaced with 10 ml of preheated hybridization buffer (Ambion Ultra "ULTRA hyb" Ultrasensitive hybridization buffer). The tube was prehybridized in a rotating oven for 2 hours at 47°C, rotating slowly. The tube was removed from the hybridization oven, and the denatured radioactive AQP3

DNA probe was placed into the bottom and mixed quickly into the hybridization buffer. The tube was then incubated at 47°C while rotating for a minimum of 16 hours.

Part Three - Northern Hybridization: Washing and Detection of Hybridized Probes

After the hybridization incubation was complete, the membrane was washed 4 times to remove nonspecific probe, taking great care not to allow the membrane to dry out. The first step involved two high stringency washes of the membrane in approximately 100 ml pre-warmed 0.23X saline-sodium citrate (SCC), 1% (w/v) SDS at 47° C rotating for 30 minutes in the hybridization oven per wash. Next, the membrane was washed twice more with pre-warmed 0.23X SCC, 0.1% SDS at 47°C and again rotated for 30 minutes. The filter was then removed from the hybridization bottle and sealed in a plastic bag with a heat sealer. To check for successful hybridization of the probe, the membrane was scanned with a Geiger counter. The isotope reading was very intense over areas of the filter where hybridization signals were likely to be found, but there was also radioactivity in the other areas. The bag-sealed membrane was taped into place inside a Biomax X-ray film cassette.

Next, Biomax film was placed into the cassette according to manufacturer's instructions in the dark room, then immediately placed into a -80°C freezer for 90 minutes for the first exposure, then left to expose for 2 ½ hours, trying to adjust for the probe's radioactive intensity. Once exposed, the films were submerged in 500 ml Kodak GBX developer (diluted 1:5 with water) and left to develop for approximately 2 minutes. The developed film was rinsed in 500 ml tap water, then the film was fixed in 500 ml of a 1:5 Kodak GBX fixer and water solution for about 2-3 minutes. Development and

fixation of film was carried out in the dark, but using a "safe red light". The film was then rinsed in 500 ml tap water and air-dried approximately 30 minutes for viewing.

Antibody Production for Detection of AQP3

Once the nucleic acid and, hence, the protein sequence for AQP3 was determined, an affinity-purified polyclonal antibody was ordered from ProSci-Inc. using the C-terminal amino acids of AQP3 linked to KLH carrier protein to use in the Western blotting and immunohistochemistry experiments. The following peptide sequence was sent to ProSci-Inc.

AQP3 Peptide Antigen Sequence (amino acid abbreviations used):

NH_2 – CGGIGEENVKLANVKLRESS – COOH

ProSci-Inc. used an antibody production protocol similar to the following. New Zealand White Rabbits were used to obtain the antibodies produced against the antigen, which was the 17 C-terminal amino acid of AQP3 with CYS-GLY-GLY added as a spacer. The peptide was cross-linked to KLH carrier protein via the N-terminal cysteine. Pre-bleeds of the animals were made to obtain the pre-immune serum. A mixture of adjuvant, saline and the immunogen were used for each injection beneath the skin of the rabbit. An immune response was made by a series of 4 immunizations, usually during an 8-week period. Blood was collected at the 5^{th} and 7^{th} week and at the final bleed from the central ear artery and allowed to clot and retract at 37°C overnight each time. The clotted blood was refrigerated for 24 hours before the serum was decanted and clarified by centrifugation at 2500 RPM for 20 minutes. The serum was then affinity purified according to the manufacturer's standard protocol to remove any non-specific antibodies

that might otherwise give background or erroneous signals in experiments. A goat secondary antibody, Alexa Fluor 488 Goat Anti-Rabbit SFX Kit (Invitrogen), was used for immunohistochemistry and a donkey anti-rabbit alkaline phosphatase secondary antibody was used for Western blotting.

Shark Membrane Protein Extraction

Once the shark had been dissected, the tissues were placed on ice immediately and were then homogenized as soon as possible. Homogenization solutions were prepared in advance as follows.

Homogenization buffer:

25 mM Tris (2.975 g)

0.25 M sucrose (42.75 g)

Both were dissolved in 500 ml H_20 and the pH was adjusted to 7.4. In another tube, 23.4 mg DTT was dissolved in 3 ml H_20 (i.e. 7.8 mg/ml). Homogenization buffer (100 ml) was transferred to a new flask and 1 ml of 100X Protease Inhibitor Cocktail (Research Products International, IL, U.S.A.) and 1 ml of 7.8 mg/ml DTT were added. Then,10 ml of this second homogenization buffer was used for each sample, which was homogenized using a polytron homogenizer, carefully rinsing the nozzle each time in 0.1% SDS, then distilled H_20 between each tissue sample. Homogenized samples were then filtered through 4 layers of muslin into a 50 ml Oak Ridge centrifuge tube, rinsing the first tube out twice with 20 ml homogenization buffer each time and filtering these amounts also through the muslin. The tubes were capped and placed in a pre-cooled centrifuge at 4°C at 20,000 rpm for one hour, approximately 50,000 g max. 5 ml homogenization buffer

was transferred to a new flask and 50 μl of 7.8 mg/ml DTT was added, and the samples were then resuspended in approximately 1 ml of this resuspension buffer. Once the tissue samples were resuspended, a Bradford's protein assay was performed (Bradford, 1976). 150 μl aliquots of the crude membrane preparation obtained were made and frozen at -20°C.

SDS Polyacrylamide Gel Electrophoresis

Polyacrylamide gel electrophoresis is the preferred separation system for proteins. A lattice of cross-linked, linear polyacrylamide strands is formed by the copolymerization of monomeric acrylamide and the cross-linker bisacrylamide (N,N'-methylenebisacrylamide). The porosity of the resulting gel is determined by the length of the chains (concentration of acrylamide) and by the degree of the cross-linking that occurs during the polymerization reaction, which is the ratio of acrylamide to bisacrylamide. Protein samples were treated with the anionic detergent sodium dodecyl sulfate (SDS) before electrophoresis. The SDS binds to proteins, which helps dissociate protein subunits. 2-Mercaptoethanol is a reducing agent that is used to disrupt the disulfide bonds of proteins to ensure that they are fully denatured before they are loaded on the gel, ensuring proteins run uniformly (Nelson and Cox, 2005).

Each SDS-coated protein chain has a similar charge-to-mass ratio, so during electrophoresis, the separation of the SDS-protein chains is based on size and the effect of conformation is eliminated. A tracking dye, usually bromophenol blue, may also be added to the protein solution to track the progress of the protein through the gel during

the electrophoresis run. A 10% polyacrylamide gel was used because it can resolve proteins that range from 20 to 200 kilodaltons (kDa), (Sambrook and Russell, 2001).

Polyacrylamide gels were made for use in Western blotting experiments to determine the presence of AQP3 in 8 different tissues of *Squalus acanthias.* Two different gels were required for electrophoresis. A 5% acrylamide "stacking" gel of high porosity was used so that proteins were stacked together in a very thin zone on the surface of a "resolving" gel. This gel, also known as a running gel, was made of 10% acrylamide. A discontinuous buffer system was used; meaning the buffer in the reservoirs had a different pH and ionic strength from that used to cast the gel. The SDS-polypeptide complexes in the gel are swept along by the moving boundary created by the electrical current passed between the electrodes.

The gels were prepared in the same manner in all the experiments, adjusting total volumes as needed to fill the gel chambers (Appendix A). The TEMED in the recipe is tetramethylethylenediamine, $(CH_3)_2NCH_2CH_2N(CH_3)_2$ which, along with the ammonium persulfate, catalyzes the polymerization of acrylamide to form the gel.

The TRIS-glycine electrophoresis buffer was prepared as follows:
A 5X stock solution was made by dissolving 15.14 g TRIS base and 93.88 g glycine in 900 ml of deionized H_20. Then 5 ml of 20.0% SDS was added and the volume was adjusted up to 1000 ml with deionized H_20.

The electrophoresis protocol was performed in the following order.

1. Assemble the glass plates for the gel chamber according to the manufacturer's instructions, ensuring they are level and a very tight seal is formed to prevent leakage.

2. Prepare the polyacrylamide solution in the order listed, adding the TEMED and ammonium persulfate last, just before pouring.
3. Overlay the solution with butanol, using a slow, even rate of delivery. (A slim catheter tube was used.)
4. Once the gel has set (> 30 minutes) remove the butanol.
5. Clean the area over the running gel with distilled water and remove as completely as possible (per Bio-Rad instructions, p.10) before pouring the stacking gel.
6. Place the comb in the stacking gel.
7. Assemble the buffer chamber, according to manufacturer's instructions.
8. Once the stacking gel has set and the gel wells have been cleaned with distilled H_20, slot the gel into the gel tank, pour the buffer into both chambers and load the protein sample into the wells.
9. Attach the power pack to the Protean II xi Cell gel tank (Bio-Rad) and begin electrophoresis.

The power was turned off when the bromophenol marker dye reached within two millimeters from the end of the gel. Precision Plus Kaleidoscope multi-colored molecular weight protein standards (Bio-Rad) (10 μl) were run in one lane on either side of the protein samples. The gel was then ready for the Western blotting experiment.

Western Blotting

Western blotting is a technique used in molecular biology to identify and quantitate specific proteins in tissue homogenates. Components are separated electrophoretically on a polyacrylamide gel and then transferred from the gel and

immobilized on a membrane. Then specific antibodies to the target protein are used as probes to detect the protein on the membrane.

The protocol begins with the preparation of a polyacrylamide running gel as described in the previous polyacrylamide gel electrophoresis section.

Tissue homogenates produced in Maine, summer 2007, were shark liver, brain, rectal gland, kidney, gill, stomach, esophagus and intestine. The protein in the samples was assayed using Bradford's method (Bradford, 1976). Tubes were prepared with 20 μl of each sample and a blank with 100 μl water. Using a prepared series of protein standards using 2 mg/ml BSA stock solution, samples were then measured using a spectrophotometer at 595 nm wavelength. Relative absorbance and approximate concentrations of each sample were recorded in the laboratory notebook and used to set up samples for Western blotting experiments.

Equipment was set up for Western blotting according to manufacturer's instructions for Trans-Blot Electrophoretic Transfer Cell (Bio-Rad), using their suggestions for strategies to optimize electro-blotting. PVDF filters (not nitrocellulose) filters were used.

Transfer Buffer for blotting was made as follows:

Glycine	14.64 g
Tris (crystallized free base)	29.07 g
0.037% SDS (electrophoresis grade)	9.25 ml
20.0% methanol	1 Liter
H_20	make up to 5 Liters

Blotting was allowed to run overnight to maximize the transfer of proteins to the filter. Filters were removed carefully, labeled, and cut into strips. Glass baking dishes were used as the incubation apparatus for the immunoblotting.

The goal of the immunoblotting portion of the experiment was to recognize a specific antigen in a preparation by showing its reactivity with an antibody with known specificity (Dunbar, 1994). Successful results depend upon the amount of both antigen and antibody used in the procedure and the extent at which the background reactions caused by binding of non-specific immunoglobulin can be limited. The aim of the protocol was to lower these background reactions. The enzyme-conjugated secondary antibody, alkaline-phosphatase was selected to use in combination with the substrate 4-bromo-3-chloro-indolyl phosphate (BCIP)/ nitro blue tetrazolium (NBT): 1-Step NBT/BCIP plus suppressor reagent (Pierce). The best and least costly blocking reagent was 5% non-fat dried milk because it is easy to use and is compatible with all of the common immunological detection systems, although 1% gelatin was also tried as a blocking agent. The blocking buffer (TNT buffer containing a blocking agent) was prepared for the immunoblotting (Appendix A).

To begin the immunoblotting protocol, 10 ml non-fat dried milk (5%) blocking buffer was added to each glass dish to saturate the blots with protein. The dishes were placed on a rocker to incubate for one hour at room temperature. Then they were washed with the TNT solution (without blocking agent) and rocked for 10 minutes twice.

There were 4 experimental blots used, as follows:

1. Pre-immune serum (taken from the animal before it was immunized against the peptide)

2. Immune serum (the actual antibody)
3. Peptide-blocked antibody (antibody blocked with the peptide antigen)
4. Secondary antibody alone

The 4 dishes were labeled with their contents as follows in Maine, 2007, 10 ml TNT buffer plus:

1. Pre-immune placed on AQP3 (25 μl)
2. AQP3 antibody, 25 μl (i.e. 1 in 400 dilution)
3. Peptide-blocked antibody, 25.5 μl (i.e. 25 μl antibody $^{+}$ 0.5 μl peptide (final peptide concentration 40 μg/ml)
4. Buffer only

The dishes were incubated and rocked for 1 hour at room temperature, then washed 4 times with the blocking buffer. The secondary antibodies were then added (2.5 μl: used at 1 in 4,000 dilution) and incubated and rocked for another hour.

The strips were washed 4 times again, then 5 ml of 1-Step NBT/BCIP reagent was added individually while watching closely for the substrate reaction to take place while rocking the glass dish gently in hand. Blots were generally developed for 10 minutes, which was determined to be an optimal time interval.

The following shark crude membrane tissue samples were used in the experiments at GSU in 2008: stomach, esophagus, intestine, gill, kidney, rectal gland, liver and brain.

Immunohistochemistry

Immunohistochemistry experiments were performed at MDIBL and GSU. In July 2007, a female shark was sacrificed and dissected by Dr. Cutler. Less than 0.5 cm slices

were taken from the following organs: stomach, esophagus, rectal portion of the intestine, rectal gland and kidney. The samples were placed in 50 ml centrifuge tubes containing a paraformaldehyde fixative solution as described below, then placed in a refrigerator at 4°C to fix the tissues overnight.

First, a phosphate buffered saline solution (PBS) (Invitrogen) was prepared by adding 6 PBS tablets into 600 ml H_20 and placing the beaker on a stirrer to dissolve completely. The pH was 7.2-7.4. The solution was kept at 4°C until needed.

To begin the preparation of a 4% paraformaldehyde solution, 400 ml PBS was heated on a hotplate stirrer. Paraformaldehyde powder (16 g) was added to the PBS. It was difficult to dissolve the powder into the PBS, so some drops of 2M NaOH were added. The solution was allowed to cool, and then it was necessary to adjust the pH to 7.4 using 1M HCl (Wilson and Meischke, 2004). The osmolality of the solution had to be considered in order to maintain the tissue osmolality. The osmometer reading was 1219, therefore, as this was already above the osmolality of shark tissues/plasma (approximately 1000 osmolality), nothing further could be done to make the osmolality anymore similar to that of the tissue.

After placing the tissue in cassettes and into the 4% paraformaldehyde fixative for one hour, the tissues were rinsed twice in PBS at 4°C before placing the cassettes into 50% alcohol. The samples were then transferred into a series of alcohols and HistoChoice (Cole-Parmer), a clearing solution (Appendix B). Solutions of 500 ml each were placed into one-quart glass jars and the cassettes were carefully placed into the jars and remained in each solution for one hour.

After the series of alcohols, the samples were placed into a series of 3 wax solutions for one hour each to allow penetration of the wax into the tissues. Then the tissues were placed into metal molds which were filled with the embedding wax. The base of the plastic cassette was placed on top of the mold and this was put to cool on ice to set the wax. Once cooled, the wax blocks/cassettes were taken out of the metal molds and 5 μm thick serial sections were cut on a Leica microtome (model number RN2235). Ribbons of sections were placed in a warm (37°C) float bath and individual sections were separated and floated onto microscope slides to be used for immunolabeling experiments. The slides were dried on a 37°C hot plate, which also increased the adherence of the tissue for the slide surface.

The tissues on the slides were dewaxed and rehydrated through a series of solutions followed by washing in PBS. The slides were placed into a slide holder and lifted in and out of each solution after soaking in them for 5 minutes each (Appendix B).

Once dried, the tissue on the slides was circled using a Pap pen (Fisher), which forms a hydrophobic barrier to keep the solutions directly over the sample and not allow them to run off the sides of the slides.

Three solutions were prepared (A, B, and C) to use in the immunolabeling (Appendix B). To begin, 1g of BSA was added to 100 ml PBS and allowed to dissolve without mixing. Then 1 g gelatin was added and dissolved by heating and stirring and decanted into a bottle (Meischke, 2005).

The rehydrated sections were made ready for the immunolabeling according to the following protocol. First, slides were placed into Solution A for 10 minutes to permeabilize the tissues. Next, they were placed into Solution B for 5 minutes in order to

mask the free aldehyde groups of the fixative. Next, the slides were placed into Image-iT™ FX Signal Enhancer (Invitrogen) for 30 minutes. This is a product used to block background staining that results from nonspecific interactions of fluorescent dyes and tissue constituents. The slides were washed 3 times with PBS. Finally, they were placed into Solution C for 10 minutes to block the non-specific sites.

A wet slide chamber was made by placing wet paper towels in the bottom of a microscope slide box. Each slide was removed carefully from Solution C, then dried without contacting the sections and placed into the wet slide chamber. 90 µl of a 1/100 dilution of primary antibody in PBS were carefully pipetted onto the slide and spread over the section, eliminating bubbles with the pipette tip. Once all the slides were treated in this way, the chamber lid was shut and the box was left to sit for 1 hour.

Next, the primary antibody was washed off the slide with PBS 3 times. Then 100 µl of the secondary antibody, Alexa Fluor 488 Goat Anti-Rabbit SFX Kit (Invitrogen), dilution of 1/200, was placed on the slides in as little light as possible and kept in the box for 1 hour. The slides were washed 3 times in PBS and, once excess wash solution was removed, one or two drops of Prolong Gold mounting medium containing Dapi nuclear counter stain was placed on each slide along with a large coverslip. The slides were then ready to view on the Zeiss LSM510 Meta laser-scanning confocal microscope, or a Zeiss Axiovert inverted fluorescent microscope at MDIBL. For control experiments, serial sections were made where adjacent sections were cut one after the other from the wax tissue block. Serial sections were otherwise processed as above.

Quantitative RT-PCR

Quantitative real-time PCR precisely measures and monitors the amplification of a specific nucleic acid sequence from a mixture of cDNA's prepared from tissue total RNA, and enables an experimenter to quantify the level of mRNA expression of a specific gene. The Mx4000 M Q PCR system used at MDIBL is a fully integrated real-time PCR detection system. The system includes real-time quantitative detection software. The Mx4000 system has an open format that allows researchers to work with many fluorogenic probe systems.

The formation of amplification products is monitored at each cycle in real-time PCR and allows the determination of the threshold cycle (C_t) when the product first begins to be detectable. The target cDNA was amplified in the presence of the dye SYBR Green that, upon binding to double-stranded DNA, produced an intense fluorescent signal. A dilution series was produced to generate a set of standard fluorescent C_t values from each successive dilution. The abundance of cDNA in templates determines the C_t value. With high template availability, a lower C_t is produced as shown by the example in Figure 8. When C_t data are plotted as a function of template availability, a log relationship results as shown in the example in Figure 9.

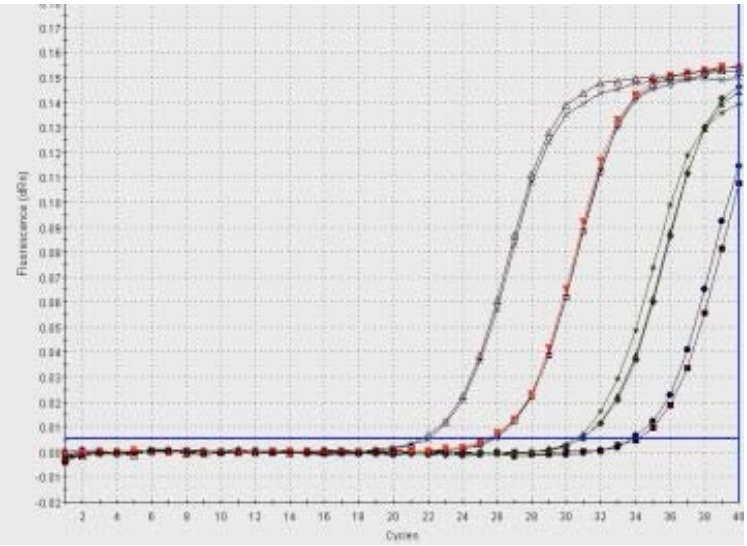

Figure 8. Example of quantitative PCR results with a low C_t.

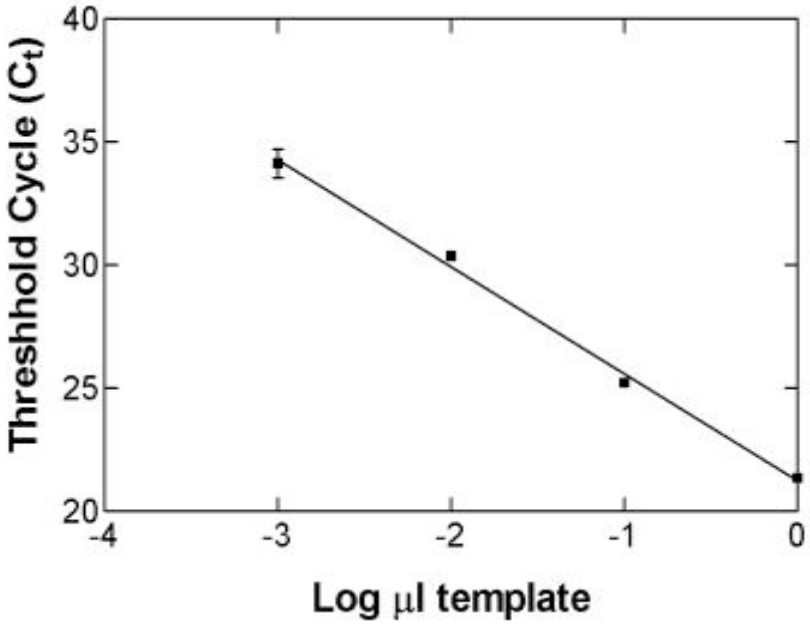

Figure 9. C_t values plotted as a function of template availability.

High quality RNA/cDNA is essential for good results with quantitative PCR. Invitrogen Superscript III reverse transcriptase was used for these experiments (see cDNA synthesis method). It is essential to make the purest possible cDNA for best

results because contamination will adversely affect the experiments. It is equally important to design specific primers to prevent misalignments and reduce primer dimers and other artifacts.

Intercalating fluorescent dyes (e.g. SYBR green) are the simplest and cheapest way to monitor PCR in real-time. These dyes fluoresce only when bound to double-stranded DNA. So as the number of copies of DNA increases during the reaction, the fluorescence increases. The output from a real-time PCR reaction is in the form of a graph showing the number of PCR cycles (1 cycle = 90°C, 50°C, 72°C) against the increasing fluorescence, known as a primer amplification plot. The threshold is set by the user. The horizontal line on the graph represents the point at which the amplification plot crosses this threshold is known as the C_t (cross threshold value). The lower the C_t value for a sample the greater the starting amount of DNA specific to the gene of interest in the sample. So if two amplification plots are compared one can deduce which sample contained the greatest amount of the DNA of interest from the C_t value. The amount of a particular gene's DNA present in a sample is proportional to the amount of that gene's mRNA in the RNA sample used to make the cDNA.

As an example, a series of tenfold dilutions could be prepared containing concentrations of the cDNA template: 1, 1/10, 1/100, 1/1000, i.e. Then, 2.5 μl cDNA and 22.5 μl H_20 are placed in a microfuge tube. 5 μl are taken out and 45 μl H_20 were added to make a 1/10 dilution. The process was repeated to make the 1/100 and 1/1000 dilutions.

Before Q-PCR was performed, normal RT-PCR was used to assess the conditions to be used for PCR (annealing temperature) and the specificity of the Q-PCR primers, to

ensure only one PCR product (AQP3) was generated.

A mixture containing the H_20, sense primer, antisense primer, and ROX was added first to a tube. The lights were kept off for the final addition of the Brilliant II mix. The Brilliant II mix (Stratagene) contained Taq DNA polymerase, dNTP's, SYBR green and PCR buffer. Q-PCR Master mix (20 μl) was placed into each labeled tube (Appendix B). Five μl cDNA were added last to each tube giving a final sample volume of 25 μl. Sample Q-PCR runs were made for esophagus and kidney cDNA samples from 6 fish held in 3 salinities: 75%, 100% and 120% (18 fish).

The amplified products were analyzed by examining the graphs generated by the Mx 4000 software: the dissociation curve and amplification plots. The dissociation curve (melting temperature profile of the PCR product) was checked to make sure only one product was produced during the PCR run (i.e. no primer dimers or other products were made). The threshold was set as low as possible, but above the apparent background level. Then threshold values (C_t) were recorded for each Q-PCR sample in the run. The C_t values of the diluted standard cDNA were plotted to produce a scale to measure the relative level of mRNA expression in the actual samples. This equation for the line was then used to calculate the relative AQP3 expression levels.

CHAPTER 3

RESULTS

Cloning and Sequencing

Dr. Cutler provided the preliminary data necessary for the cloning and sequencing experiments. He had isolated a DNA fragment and determined that it was a homologue of AQP3, by aligning the sequence obtained with AQP sequences from other species. The putative shark AQP3 had significantly higher levels of homology with AQP3 sequences than to other aquaporins. Subsequent cloning experiments were then performed in this project to obtain the 5' and 3' ends of the AQP3 cDNA using a RACE RT-PCR technique.

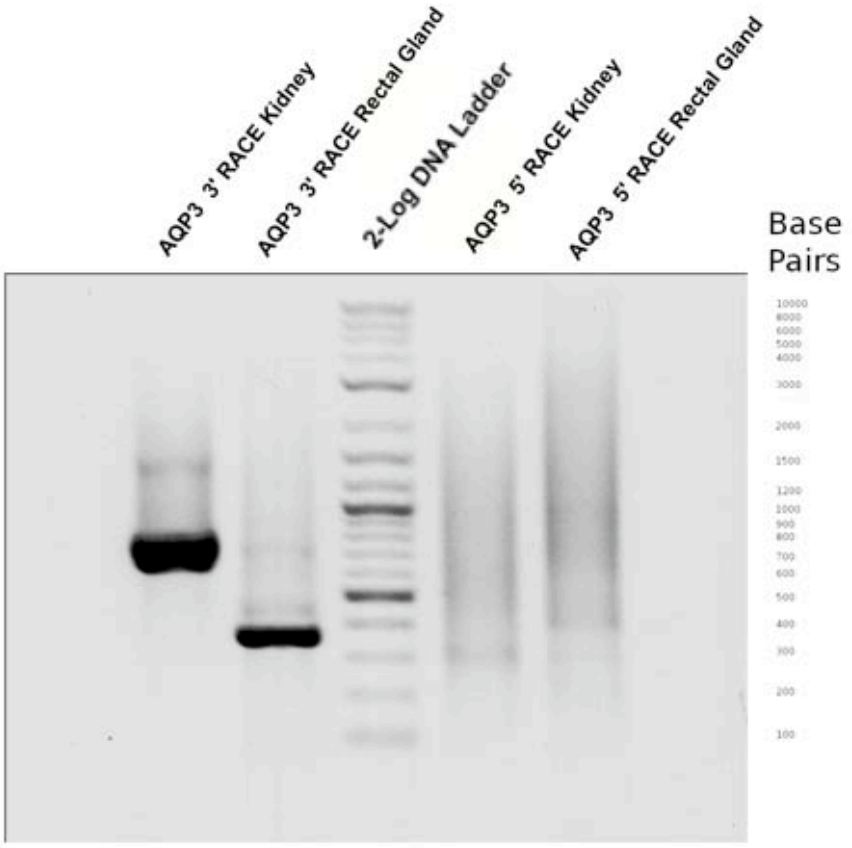

Figure 10. Ethidium bromide stained 1.5% agarose electrophoresis gel of *Squalus acanthias* AQP3 5' and 3' RACE products using rectal gland and kidney cDNA's at an annealing temperature of 62°C. A distinct band of approximately 650 base pairs appears for the 3' RACE kidney and a band of approximately 400 base pairs was produced from the 3' RACE rectal gland. A faint band of approximately 300 base pairs was produced from the 5' RACE kidney and a faint band of approximately 400 base pairs was produced from the 5' RACE rectal gland.

The gel photo in Figure 10 reveals resulting 5' and 3' RACE PCR products produced using kidney and rectal gland Marathon cDNA as described in the legend. Because the rectal gland 5' RACE fragment was approximately 100 base pairs longer than the 5' RACE kidney fragment, testing was needed to determine whether both fragments were part of the AQP3 gene or whether one or the other of the bands represented an artifact. The 3' RACE kidney fragment of approximately 650 base pairs,

the 5' RACE kidney fragment, and the 5' rectal gland fragment were selected for cloning and were cut out and purified. The smaller 3' RACE fragment from rectal gland was too small to represent a complete 3' end of the AQP3 cDNA and so was not investigated further.

Figure 11 shows the results of the PCR analysis of the plasmids produced by the cloning of the RACE cDNA fragments. The colonies with the most intense bands and of the correct size were selected for further sequencing analysis as follows: colonies 1, 2 and 3 for the 5' RACE 300 kidney as their bands were the most intense; colonies 2, 7 and 8 for the 5' RACE 400 rectal gland as they were closest to the expected size of 580 bp's; and colonies 3, 4 and 5 for the 3' RACE 650 kidney as they seemed to have the most intense bands.

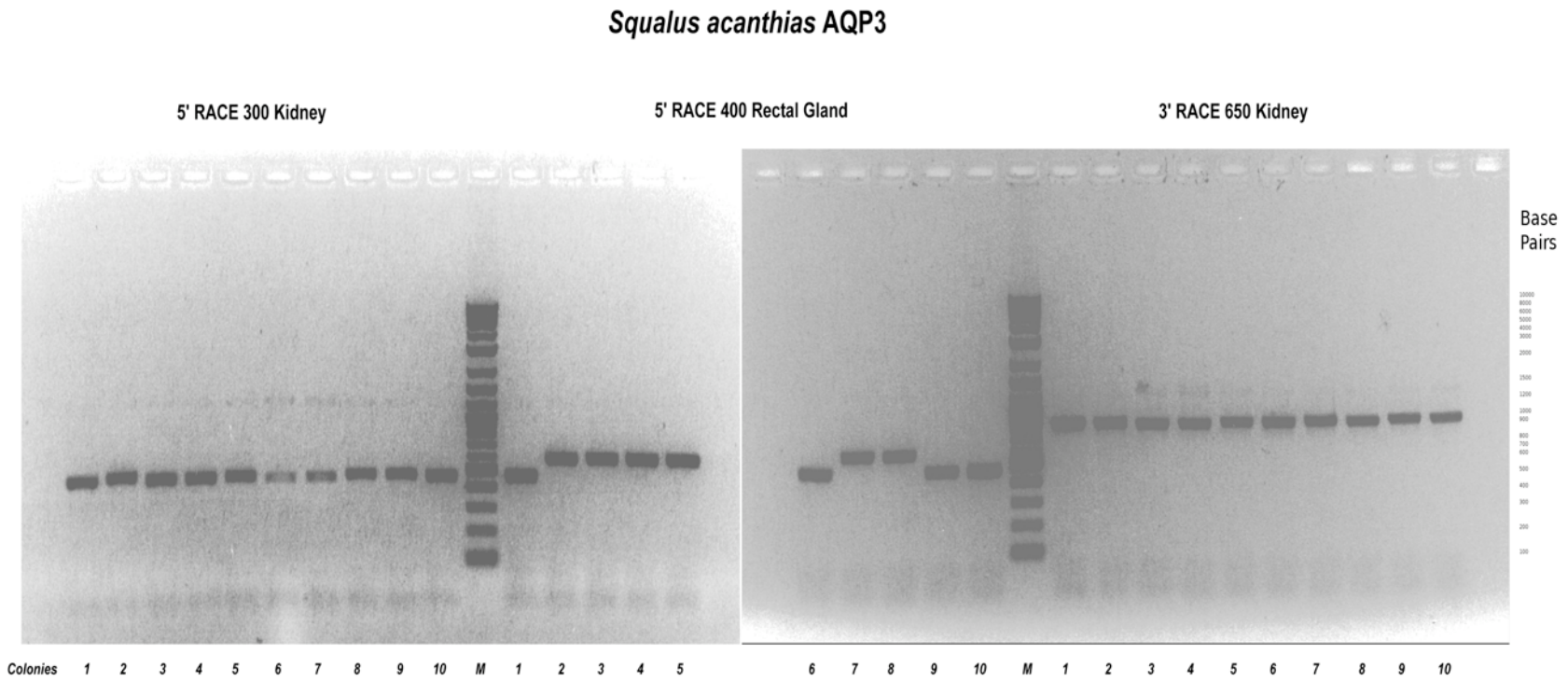

Figure 11. Colony PCR analysis of AQP3 RACE cDNA plasmid bacterial clones shows amplification of an expected size of approximately 480 base pairs for the Kidney 5' RACE, approximately 580 base pairs for the Rectal Gland 5' RACE, and approximately 830 base pairs for the Kidney 3' RACE for most of the colonies. Colonies 1, 2 and 3 (5' RACE 300 kidney); 2, 7 and 8 (5' RACE 400 rectal gland); and 3, 4 and 5 (3' RACE 650 kidney) were selected for sequencing. The cloned plasmid PCR products are larger than the original cDNA fragments due to the presence of some plasmid vector DNA.

Three clones were then picked for each RACE product and re-amplified by PCR to make DNA for sequencing. The amount of DNA obtained was then quantified by agarose gel electrophoresis and using a gel doc system, where the intensity of each band was compared to the bands in the 2-log DNA ladder (NEB) that contain known amounts of DNA (Figure 12). The fact that two 5' RACE products had been obtained led to more PCR experiments to determine whether either or both of these were real 5' ends of the AQP3 cDNA. Another possibility that had occurred previously, was that random pieces of DNA could be ligated (stuck) together during the production of the Marathon cDNA used as DNA template during RACE PCR. A non-AQP3 fragment may therefore have become attached to the AQP3 cDNA during the ligation process.

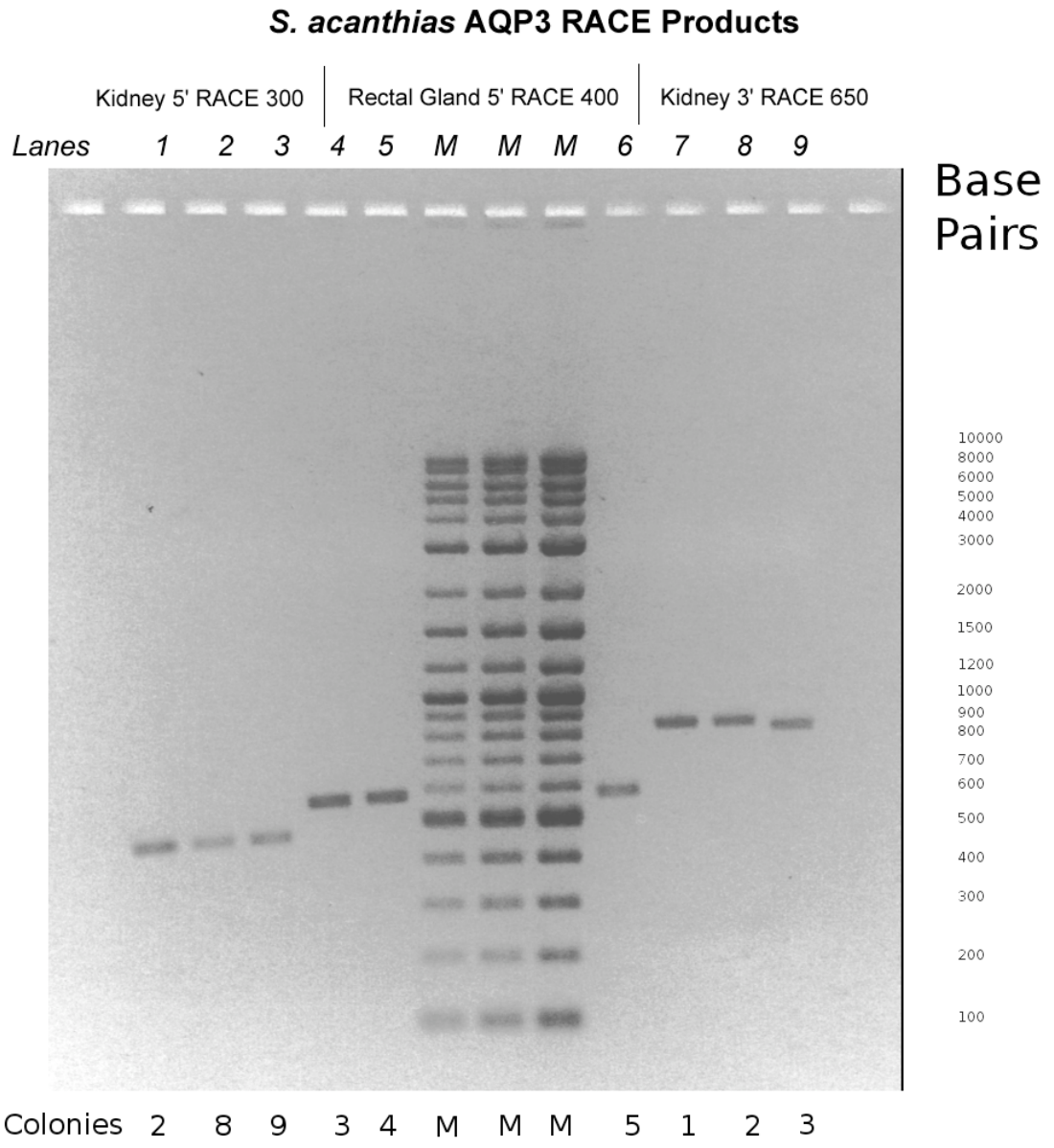

Figure 12. Ethidium bromide stained 1.5% agarose gel of 5' and 3' RACE AQP3 products from *Squalus acanthias* kidney and rectal gland. PCR analysis of RACE PCR cDNA plasmid clones again shows amplification of an expected size of the PCR fragments, i.e. approximately 180 base pairs, plus the size of the RACE PCR product insert. Lanes 1-3 are 5' RACE kidney which produced an appropriate band of approximately 480 base pairs; lanes 4-6 are 5' RACE rectal gland which produced an appropriate band of approximately 580 base pairs; lanes 7-9 are 3' RACE kidney which produced a band of approximately 830 base pairs. Different amounts of 2-log DNA ladder from NEB were used as markers (**M**) with known amounts of DNA in each band to quantify fragment amounts for sequencing using gel doc system.

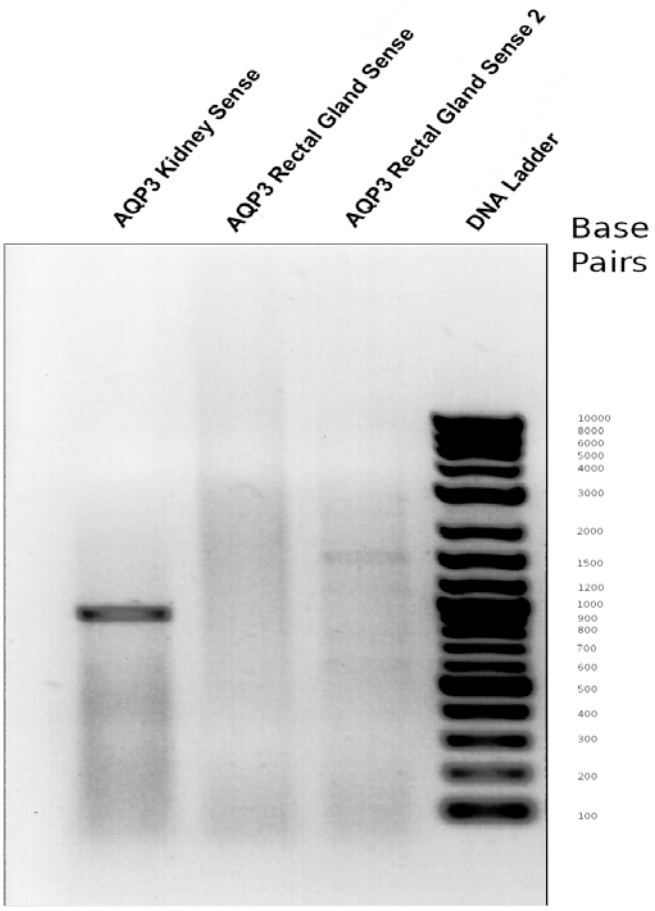

Figure 13. Ethidium bromide stained 1.5% agarose electrophoresis gel of *Xenopus laevis* expression primers specific to each of the two 5' RACE products obtained, at 58°C annealing temperature (see Methods). A band of the correct size (941 nucleotides) is seen for the sense primer in kidney. A faint band was amplified when using the rectal gland sense 2 primer, but not with the sense primer in rectal gland cDNA.

The gel photo in Figure 13 shows the results of PCR analysis to test whether either of the 5' RACE fragments were artifactual. The expected size of the band made with the rectal gland 5' RACE specific sense primer was 995 nucleotides but this was not present on the gel. A band of 1500 nucleotides with the rectal gland 5' RACE specific sense 2 primer did amplify, but this was the wrong size to be the correct piece of DNA,

and a band of the expected size of 941 nucleotides was seen with the kidney 5' RACE specific sense primer.

As Figure 13 showed that the 5' rectal gland sequence did not amplify during PCR using normal (non-Marathon) cDNA, the primers were then tested to ensure that they would amplify a product if such a product existed in the cDNA template, i.e., to ensure the primers themselves were capable of amplifying the correct fragment. A template that contained sequences that the primers should amplify was used (i.e., plasmid containing the 5' rectal gland fragment) as a template (see Figure 14).

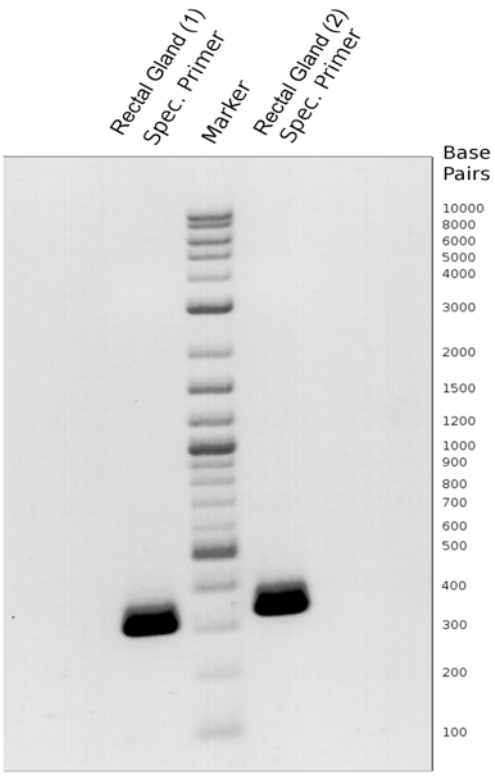

Figure 14. Ethidium bromide stained 1.5% agarose electrophoresis gel of *Squalus acanthias* AQP3 rectal gland 5R clone at 55°C annealing temperature. A distinct band of approximately 300 base pairs is visible for the rectal gland specific primer 1, and a distinct band of approximately 400 base pairs is visible for the rectal gland specific primer 2. These bands were the expected sizes.

The result from Figure 14 (a positive control experiment) showed that if the 5' rectal gland fragment was present in the template DNA, the primers could amplify a PCR product.

RT-PCR was then performed to show the tissue distribution of AQP3 mRNA (Figure 15). The resulting electrophoresis gel indicated the presence of AQP3 mRNA in the gill, kidney, rectal gland, esophagus, stomach, intestine, brain, eye, and to lesser extent in the muscle and liver due to the presence of bands of the expected size. The housekeeping gene, glyceraldehyde-3-phosphate dehydrogenase, was used as a control to show that the RT-PCR was working correctly for each cDNA. The control PCR reaction Lane 13 had no cDNA in it and shows no visible fragment, indicating there was no DNA contamination of the PCR reactions.

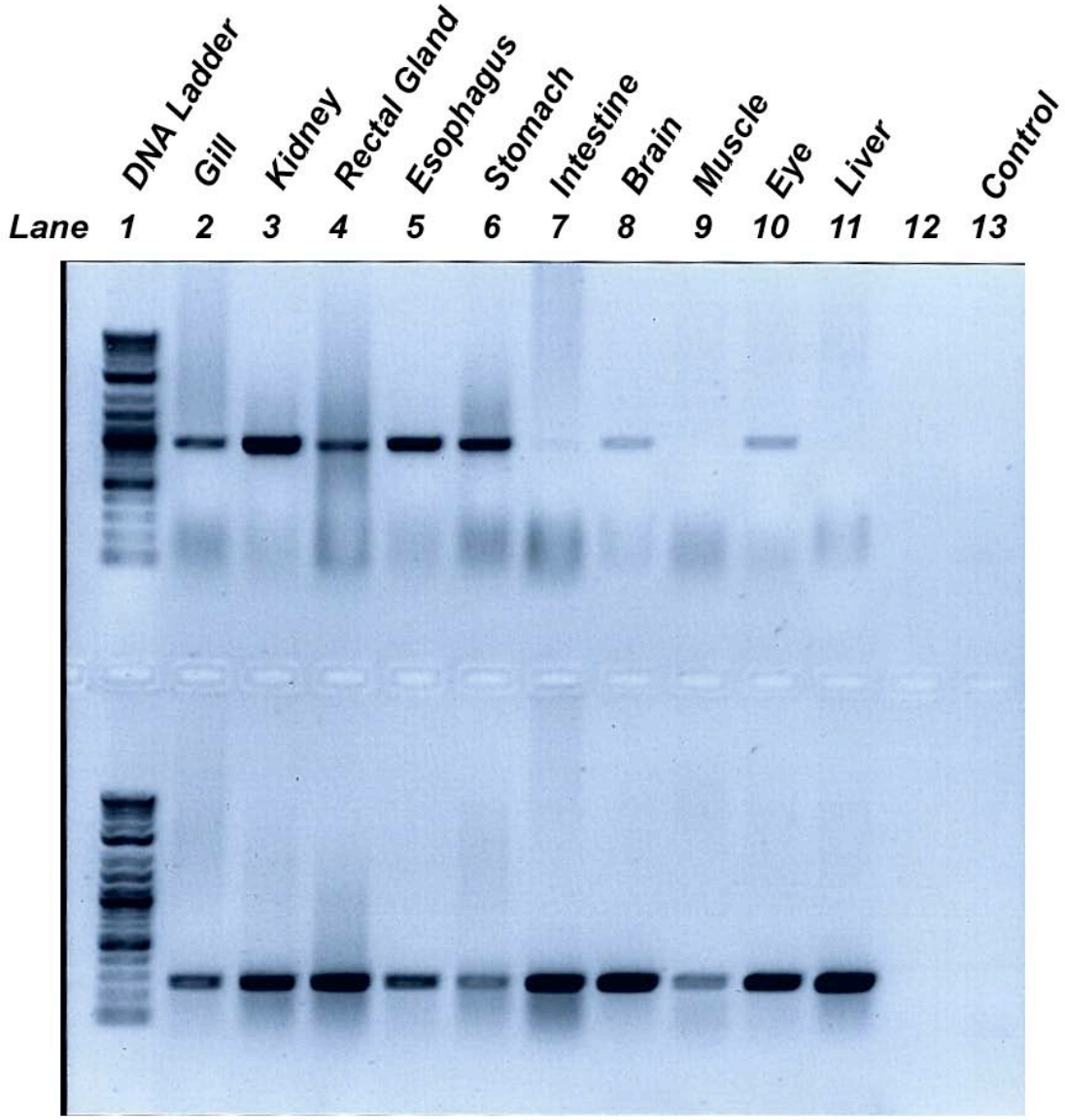

Figure 15. Tissue distribution of *S. acanthias* AQP3 mRNA expression determined using RT-PCR (top row of lanes). In lower lanes, the "housekeeping" gene glyceraldehyde-3-phosphate dehydrogenase was amplified from each cDNA as a control to show that the RT-PCR amplifications were functioning correctly. A 2-log DNA ladder (NEB) was used as the marker. Lane 13 is the negative control sample with no cDNA template indicating there was no contamination of the PCR reactions during amplification.

```
1                                                CATGGAGTCTCCTCCTCCCGTTAGTT
   27 GTTTAATGGTCCACCACGACGGAAAGCAGCAACACTTTGCACCATGAAAGCATCCTGCCAGTAGTAT
      Met Leu Val Ser Lys Ile Lys Pro Cys Met Ser Lys Val Lys Thr Ser Ile     17
   94 ATG CTT GTC TCA AAG ATT AAG CCA TGC ATG TCT AAG GTC AAA ACC TCA ATT
      Leu Gln Phe Lys Met Gly Lys Gln Lys Ala Ile Ile Arg Lys Ile Glu Asp     34
  145 CTA CAA TTC AAA ATG GGA AAA CAA AAA GCA ATA ATC AGA AAA ATT GAA GAT
      Ser Phe Arg Ile Arg Asn Leu Leu Val Arg Gln Cys Leu Ala Glu Cys Leu     51
  196 TCA TTC AGA ATA AGA AAT CTG TTG GTA AGA CAA TGT CTT GCT GAA TGT TTA
      Gly Thr Leu Ile Leu Val Leu Phe Gly Cys Gly Ala Leu Ala Gln Met Thr     68
  247 GGA ACG TTG ATT CTT GTG TTG TTT GGC TGT GGA GCA TTG GCA CAA ATG ACC
      Leu Ser Arg Gly Thr His Gly Gln Phe Leu Thr Val Asn Phe Ala Phe Gly     85
  298 CTC AGT AGG GGT ACA CAC GGA CAG TTT TTG ACT GTT AAT TTT GCC TTC GGA
      Phe Ala Val Met Leu Gly Val Leu Leu Ala Gly Gln Val Ser Gly Ala His    102
  349 TTT GCA GTG ATG CTC GGT GTA CTC CTG GCT GGC CAA GTC TCA GGA GCG CAC
      Leu Asn Pro Ala Val Thr Phe Ala Met Cys Leu Leu Ala Arg Glu Pro Trp    119
  400 TTG AAT CCT GCC GTG ACC TTT GCT ATG TGC TTA CTT GCT CGC GAA CCC TGG
      Leu Lys Phe Pro Leu Tyr Ser Leu Ala Gln Ile Leu Gly Gly Phe Leu Gly    136
  451 TTA AAA TTT CCA CTT TAC TCT TTG GCA CAA ATA CTA GGC GGC TTC CTT GGA
      Ser Gly Ile Ile Phe Gly Leu Tyr Phe Asp Ala Met Trp Asp Phe Ser Gly    153
  502 TCT GGT ATC ATT TTC GGT TTG TAT TTT GAT GCC ATG TGG GAC TTT AGT GGT
      Gln Asn Lys Leu Leu Ile Tyr Gly Pro Asn Ala Thr Ala Gly Ile Phe Ala    170
  553 CAA AAC AAA CTG TTA ATA TAT GGC CCC AAT GCC ACT GCT GGT ATA TTC GCT
      Thr Tyr Pro Ser Val His Leu Thr Pro Leu Asn Gly Phe Phe Asp Gln Leu    187
  604 ACA TAC CCA TCT GTG CAC TTA ACT CCA CTC AAT GGC TTT TTT GAT CAG CTG
      Ile Gly Thr Ala Ala Leu Ile Val Cys Ile Leu Ser Ile Val Asp Lys Phe    204
  655 ATT GGA ACT GCC GCT CTC ATA GTT TGC ATC CTT AGC ATT GTG GAT AAA TTC
      Asn Asn Pro Val Pro Lys Gly Leu Glu Ala Phe Thr Val Gly Phe Thr Val    221
  706 AAT AAC CCG GTG CCA AAG GGA CTG GAG GCA TTT ACT GTT GGC TTT ACC GTC
      Leu Val Ile Gly Leu Ser Met Gly Phe Asn Ser Gly Tyr Ala Val Asn Pro    238
  757 CTG GTA ATT GGC TTG TCT ATG GGT TTC AAC TCT GGG TAT GCC GTG AAC CCT
      Ala Arg Asp Phe Gly Pro Arg Leu Phe Thr Ser Leu Ala Gly Trp Gly Ala    255
  808 GCC AGA GAC TTT GGA CCT CGT TTG TTT ACA TCA TTG GCT GGC TGG GGA GCT
      Glu Val Phe Ile Ala Gly Asn Tyr Trp Phe Trp Ile Pro Ile Phe Ala Pro    272
  859 GAG GTT TTC ATT GCT GGA AAC TAC TGG TTT TGG ATC CCT ATT TTT GCC CCA
      Leu Leu Gly Ser Val Leu Gly Ile Leu Val Tyr Gln Leu Met Ile Gly Ile    289
  910 CTC CTT GGT TCT GTA CTT GGT ATT CTG GTA TAT CAG CTT ATG ATT GGA ATA
      His Leu Glu Pro Glu Asn His Asn Ser Pro Ile Gly Glu Glu Asn Val Lys    306
  961 CAC CTC GAG CCC GAA AAC CAC AAT TCA CCC ATT GGA GAA GAA AAT GTA AAA
      Leu Ala Asn Val Lys Leu Arg Glu Ser Ser Stop                           316
 1012 CTG GCT AAT GTA AAA TTA AGA GAA AGT TCC TGA TATATTAGAGATCATGTGCAGAA
 1068 GATTGCCAATTTAAGATTTGTGATATCCCATGTATTTTCTCATAGCAAATCACAAAATTTGAACCCT
 1135 TTTGAATATTTGATATTTAACTTGATATGCAGAATTTTAATATCTGCTGTAATAAAGTTTCTGTAGG
 1202 TTAAAAAAAAAAAAAAAAAAAAAAA
```

Figure 16. The interleaved complete nucleotide and derived-amino acid sequences of *Squalus acanthias* kidney AQP3 produced from overlapping 5' and 3' RACE sequence and the original AQP3 nucleotide sequence. The amino acid translation is of a large open reading frame (ORF) within the cDNA sequence utilizing three letter amino acid codes. Numbering on the left and right of the sequence indicate positions with the nucleotide and amino acid sequences respectively. The two "NPA" amino acid motifs underlined are highly conserved in all aquaporins and act as their signature sequence.

The 5' and 3' RACE kidney products were aligned with the original AQP3 sequence using GENE JOCKEY II software (Biosoft) and one continuous cDNA sequence was created. The derived amino acid sequence was then determined and an interleaved nucleotide/amino acid sequence produced (see Figure 16).

The nucleotide sequence of AQP3 from *Squalus acanthias* consists of 1,202 nucleotides and has an open reading frame of 316 amino acids. Positive identification of the cDNA as an aquaporin comes from two highly conserved sites present in all aquaporins which form the "NPA" (asparagines, proline, and alanine) amino acid sequence, underlined in Figure 16.

The full-length sequence for *Squalus acanthias* AQP3 was aligned with other AQP3 sequences available in GenBank and the tree in Figure 17 was produced using phylogenetic analysis techniques. The highest degree of homology with Squalus acanthias appears to be with the tetrapods.

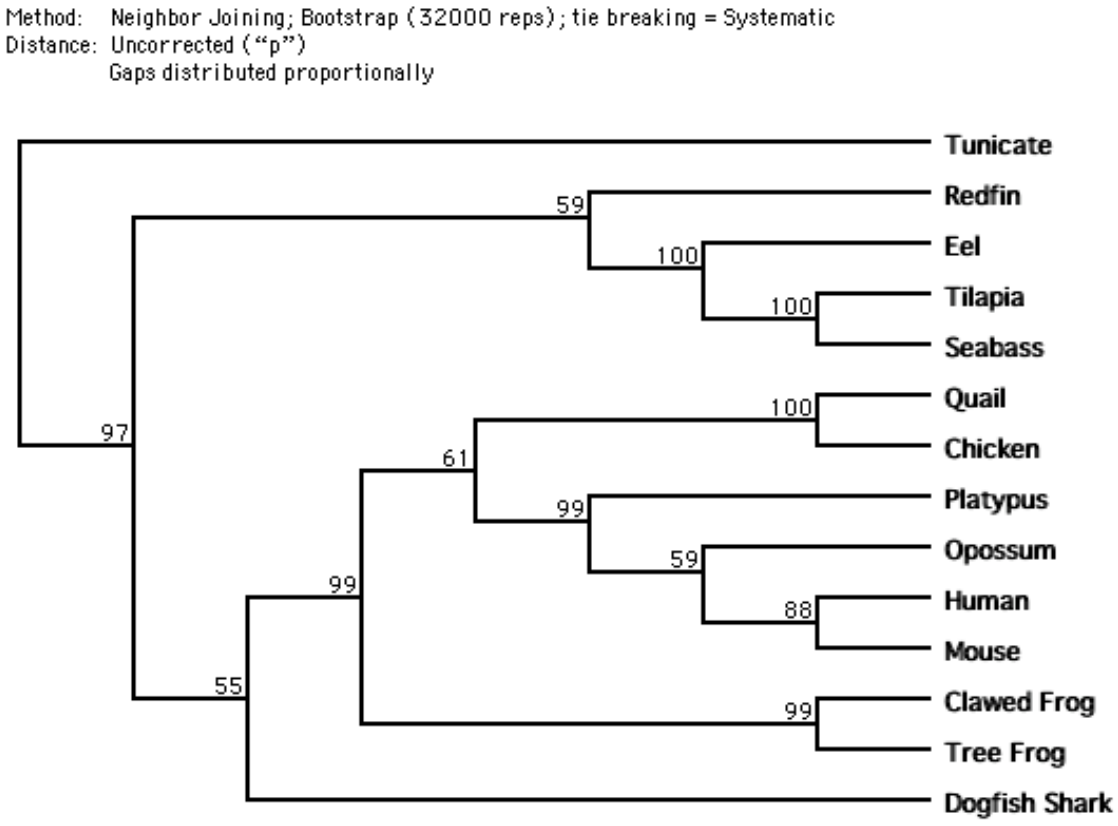

Figure 17. A nearest neighbor gene tree produced using MacVector software. The tree was generated from an alignment of the amino acid sequences of human AQP3 as well as other organisms, using the tunicate as the outgroup. The exact method is shown above the tree. Numbers represent the differences between two sequences.

Figure 18 shows a ClustalW alignment of *Squalus acanthias* AQP3 with the AQP3 sequences used in the tree in Figure 16, using MacVector software Version 10.

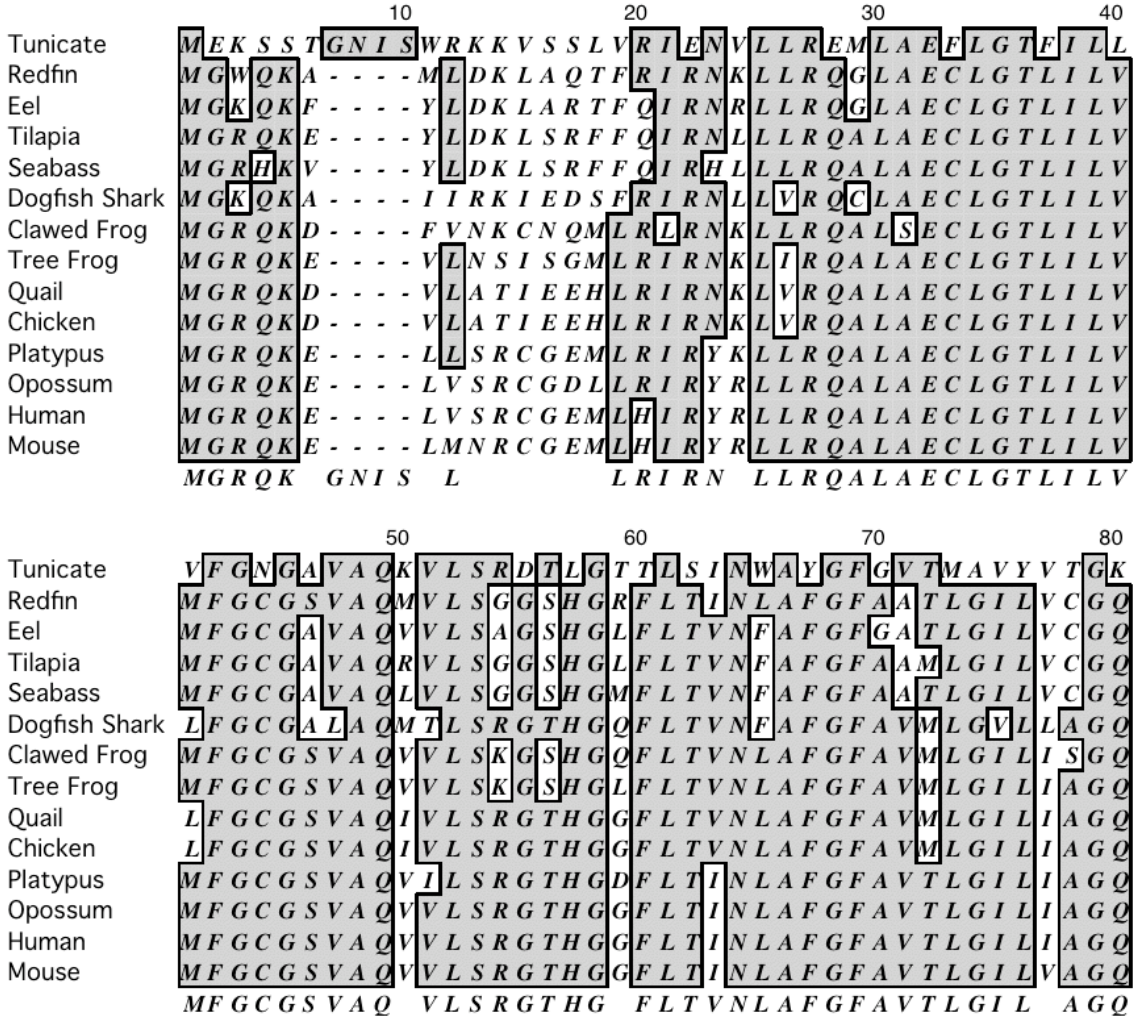

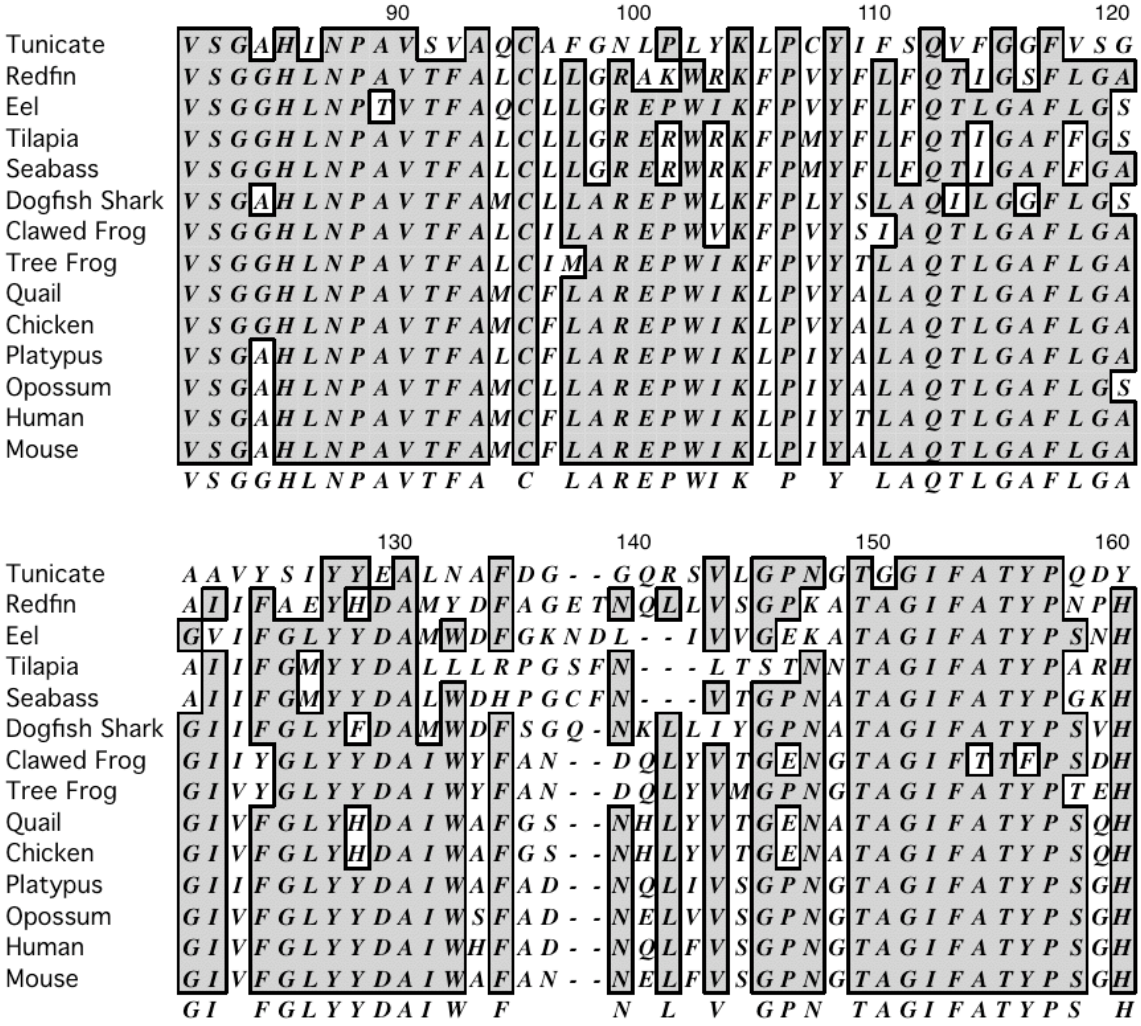
90
100
110
120
Tunicate V S G A H I N P A V S V A Q C A F G N L P L Y K L P C Y I F S Q V F G G F V S G
Redfin V S G G H L N P A V T F A L C L L G R A K W R K F P V Y F L F Q T I G S F L G A
Eel V S G G H L N P T V T F A Q C L L G R E P W I K F P V Y F L F Q T L G A F L G S
Tilapia V S G G H L N P A V T F A L C L L G R E R W R K F P M Y F L F Q T I G A F F G S
Seabass V S G G H L N P A V T F A L C L L G R E R W R K F P M Y F L F Q T I G A F F G A
Dogfish Shark V S G A H L N P A V T F A M C L L A R E P W L K F P L Y S L A Q I L G G F L G S
Clawed Frog V S G G H L N P A V T F A L C I L A R E P W V K F P V Y S I A Q T L G A F L G A
Tree Frog V S G G H L N P A V T F A L C I M A R E P W I K F P V Y T L A Q T L G A F L G A
Quail V S G G H L N P A V T F A M C F L A R E P W I K L P V Y A L A Q T L G A F L G A
Chicken V S G G H L N P A V T F A M C F L A R E P W I K L P V Y A L A Q T L G A F L G A
Platypus V S G A H L N P A V T F A L C F L A R E P W I K L P I Y A L A Q T L G A F L G A
Opossum V S G A H L N P A V T F A M C L L A R E P W I K L P I Y A L A Q T L G A F L G S
Human V S G A H L N P A V T F A M C F L A R E P W I K L P I Y T L A Q T L G A F L G A
Mouse V S G A H L N P A V T F A M C F L A R E P W I K L P I Y A L A Q T L G A F L G A
V S G G H L N P A V T F A C L A R E P W I K P Y L A Q T L G A F L G A
130
140
150
160
Tunicate A A V Y S I Y Y E A L N A F D G - - G Q R S V L G P N G T G G I F A T Y P Q D Y
Redfin A I I F A E Y H D A M Y D F A G E T N Q L L V S G P K A T A G I F A T Y P N P H
Eel G V I F G L Y Y D A M W D F G K N D L - - I V V G E K A T A G I F A T Y P S N H
Tilapia A I I F G M Y Y D A L L L R P G S F N - - - L T S T N N T A G I F A T Y P A R H
Seabass A I I F G M Y Y D A L W D H P G C F N - - - V T G P N A T A G I F A T Y P G K H
Dogfish Shark G I I F G L Y F D A M W D F S G Q - N K L L I Y G P N A T A G I F A T Y P S V H
Clawed Frog G I I Y G L Y Y D A I W Y F A N - - D Q L Y V T G E N G T A G I F T T F P S D H
Tree Frog G I V Y G L Y Y D A I W Y F A N - - D Q L Y V M G P N G T A G I F A T Y P T E H
Quail G I V F G L Y H D A I W A F G S - - N H L Y V T G E N A T A G I F A T Y P S Q H
Chicken G I V F G L Y H D A I W A F G S - - N H L Y V T G E N A T A G I F A T Y P S Q H
Platypus G I I F G L Y Y D A I W A F A D - - N Q L I V S G P N G T A G I F A T Y P S G H
Opossum G I V F G L Y Y D A I W S F A D - - N E L V V S G P N G T A G I F A T Y P S G H
Human G I V F G L Y Y D A I W H F A D - - N Q L F V S G P N G T A G I F A T Y P S G H
Mouse G I V F G L Y Y D A I W A F A N - - N E L F V S G P N G T A G I F A T Y P S G H
G I F G L Y Y D A I W F N L V G P N T A G I F A T Y P S H

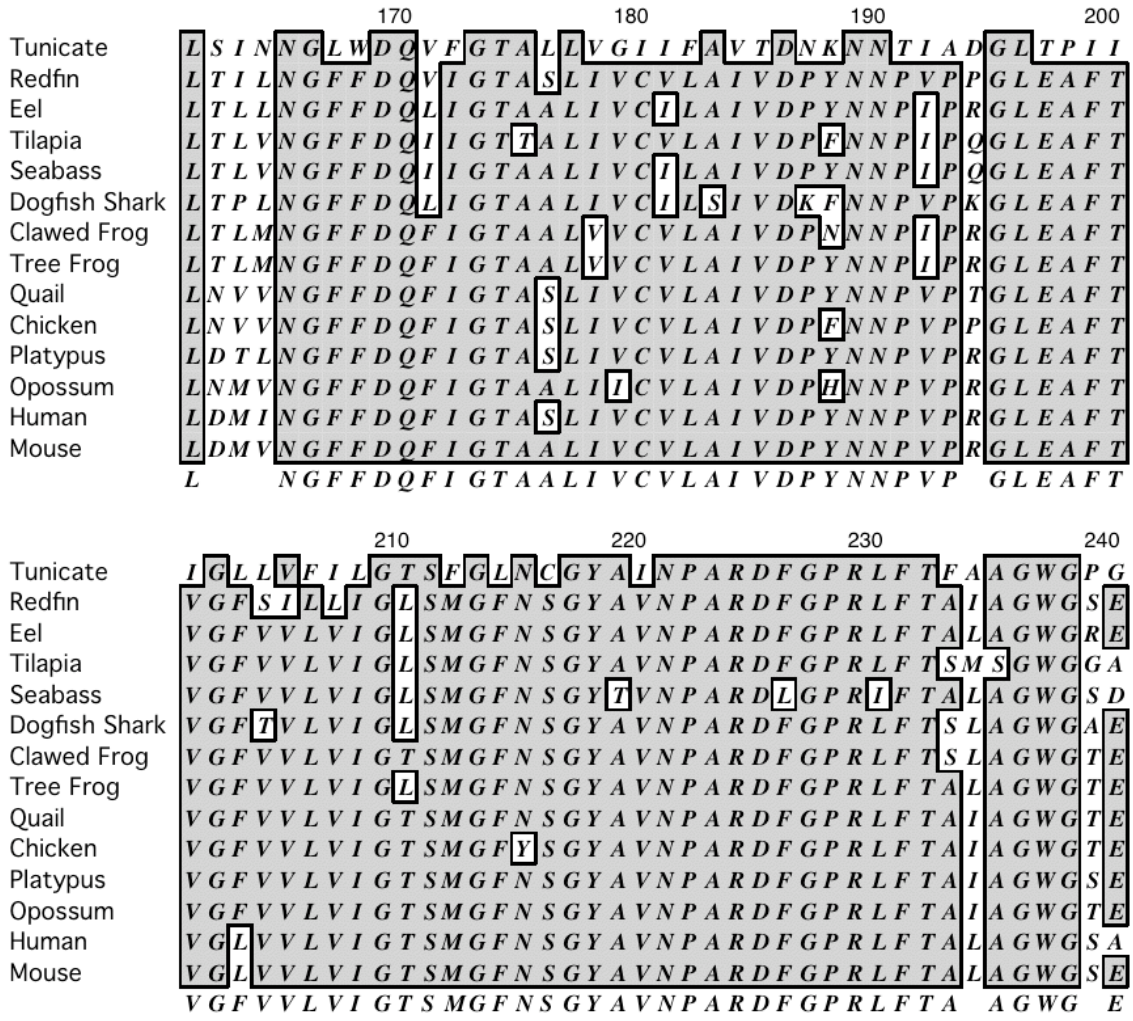
170
180
190
200
Tunicate
Redfin
Eel
Tilapia
Seabass
Dogfish Shark
Clawed Frog
Tree Frog
Quail
Chicken
Platypus
Opossum
Human
Mouse
210
220
230
240

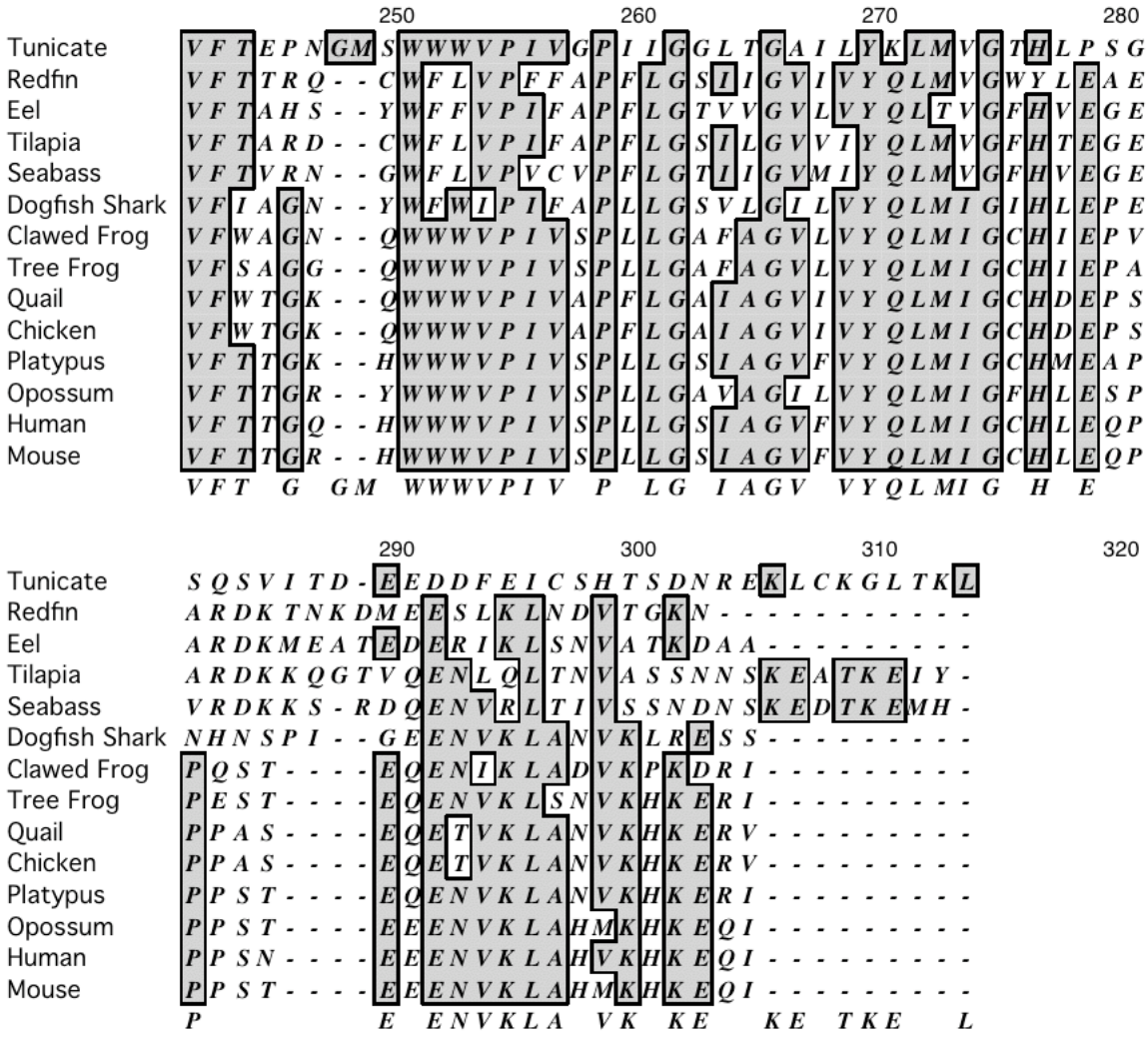

Figure 18. ClustalW alignment of *Squalus acanthias* AQP3 with the AQP3 sequences used in the tree in Figure 17, using MacVector software Version 10. Homologous regions are shaded and boxed.

Information for the phylogenetic tree is listed in Table 2.

ClustalW alignment and Phylogenetic Tree done on MacVector from MacVector Inc.

Scientific Name, Common Name, GenBank or Ensemble # :
Anguilla anguilla, Eel, CAC85286; Dicentrarchus labrax , European seabass, ABG36519; Oreochromis mossambicus, Mozambique tilapia, BAD20708; Tribolodon hakonensis, Redfin fish, BAB83082; Monodelphis domestica, opossum, XP_001362292; Homo sapiens, Human, NP_004916; Mus musculus, Mice, NP_057898; Ornithorhynchus anatinus, platypus, XP_001512694; Gallus gallus, chicken, XP_424500; Coturnix coturnix, quail, ACF19804; Xenopus laevis, clawed frog, NP_001087946; Hyla japonica, Treefrog, BAF63030; Ciona intestinalis, tunicate, ENSCINP00000019491.

Scientific Name	Common Name	GenBank #
Anguilla anguilla	Eel	CAC85286
Dicentrarchus labrax	European seabass	ABG36519
Oreochromis mossambicus	Mozambique tilapia	BAD20708
Tribolodon hakonensis	Redfin fish	BAB83082
Monodelphis domestica	Opossum	XP_001362292
Homo sapiens	Human	NP_004916
Mus musculus	Mice	NP_057898
Ornithorhynchus anatinus	Platypus	XP_001512694
Gallus gallus	Chicken	XP_424500
Coturnix coturnix	Quail	ACF19804
Xenopus laevis	Clawed frog	NP_001087946
Hyla japonica	Treefrog	BAF63030
Ciona intestinalis	Tunicate	ENSCINP00000019491

Table 2. List of scientific and common names with GenBank numbers.

Northern Hybridization

Northern blot analysis was performed to show whether AQP3 mRNA could be detected in a range of tissues of *Squalus acanthias*. Two different exposures of the blot were made (Figures 19 and 20). Previous blots performed by Dr. Cutler revealed two transcript sizes of 1.6 and 1.2 kb. The blots in this study further revealed two bands each at each of these sizes. Higher levels of expression in the intestine, gill, esophagus, stomach, and eye can best be seen in the blot after one and a half hour of exposure (Figure 19). Lower levels of expression are more visible in the kidney, brain, liver, and muscle in the blot after two and a half hours of exposure (Figure 20). Upon closer examination, several bands may have resolved into four bands. A faint band of rectal gland AQP3 mRNA expression is also seen in Figure19, which is a photo adjusted for increased contrast. These Northern blots are not 100% consistent with PCR results that showed distinct bands in the kidney and rectal gland. The less than satisfactory results may be explained by the high background from contamination with genomic DNA as evidenced by the lack of genomic DNA contamination in the rectal gland as this particular RNA sample had previously been treated with a DNAse enzyme prior to cDNA synthesis.

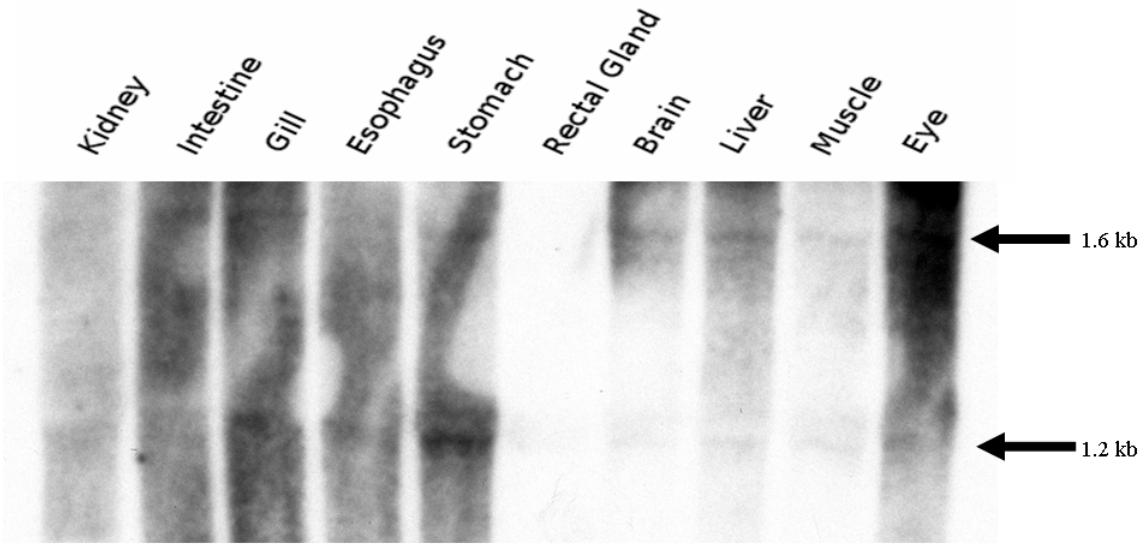

Figure 19. Northern blot analysis of tissue distribution of *Squalus acanthias* AQP3 mRNA expression in approximately 10 μg total RNA in each lane. Filters were probed with α^{32}P radio labeled AQP3 cDNA probe and hybridized at 47°C, developed after one and a half hours of exposure. The sizes of mRNA transcripts are indicated in kb.

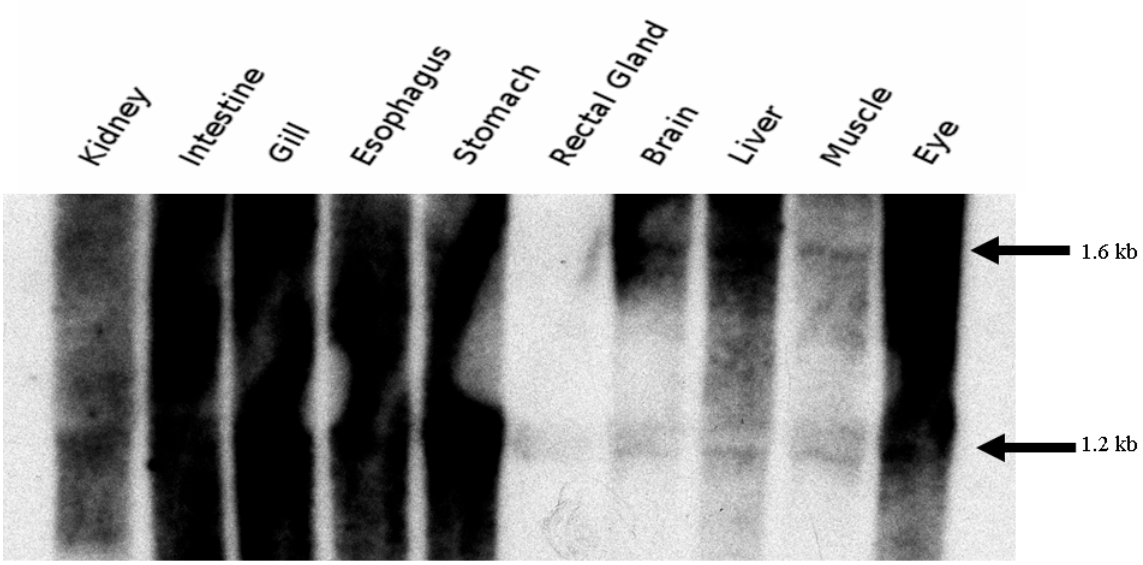

Figure 20. Northern blot analysis of tissue distribution of *Squalus acanthias* AQP3 mRNA expression in approximately 10 μg total RNA in each lane. Filters were probed with α^{32}P radio labeled AQP3 cDNA probe and hybridized at 47°C, developed after two and a half hours of exposure. The sizes of mRNA transcripts are indicated in kb.

Western Blotting

Western blotting experiments were performed using the AQP3-specific antiserum and plasma membrane fractions from the *Squalus acanthias* and controls included the use of pre-immune serum, peptide-negated antiserum and secondary antibodies used without primary AQP3 antisera.

As initial immunohistochemistry experiments showed potential staining in kidney, esophagus, and possibly rectal gland, these tissues were chosen for initial Western blotting experiments. The expected size of the protein molecule was calculated to be 321 kDa molecular weight using the amino acid sequence obtained in this project.

These first blots performed using 1% gelatin or 5% Blotto (skimmed milk powder) in TNT buffer to determine which one gave the best blocking of the filter. The 1% gelatin was unsatisfactory because it gave a large number of, presumably, largely artifactual bands (Figure 21). The kidney sample was defrosted and re-frozen several times and that may have affected the amount of signal. Consequently, only a faint signal was obtained with the Blotto blocking agent and nothing was apparent with the gelatin blocked blots.

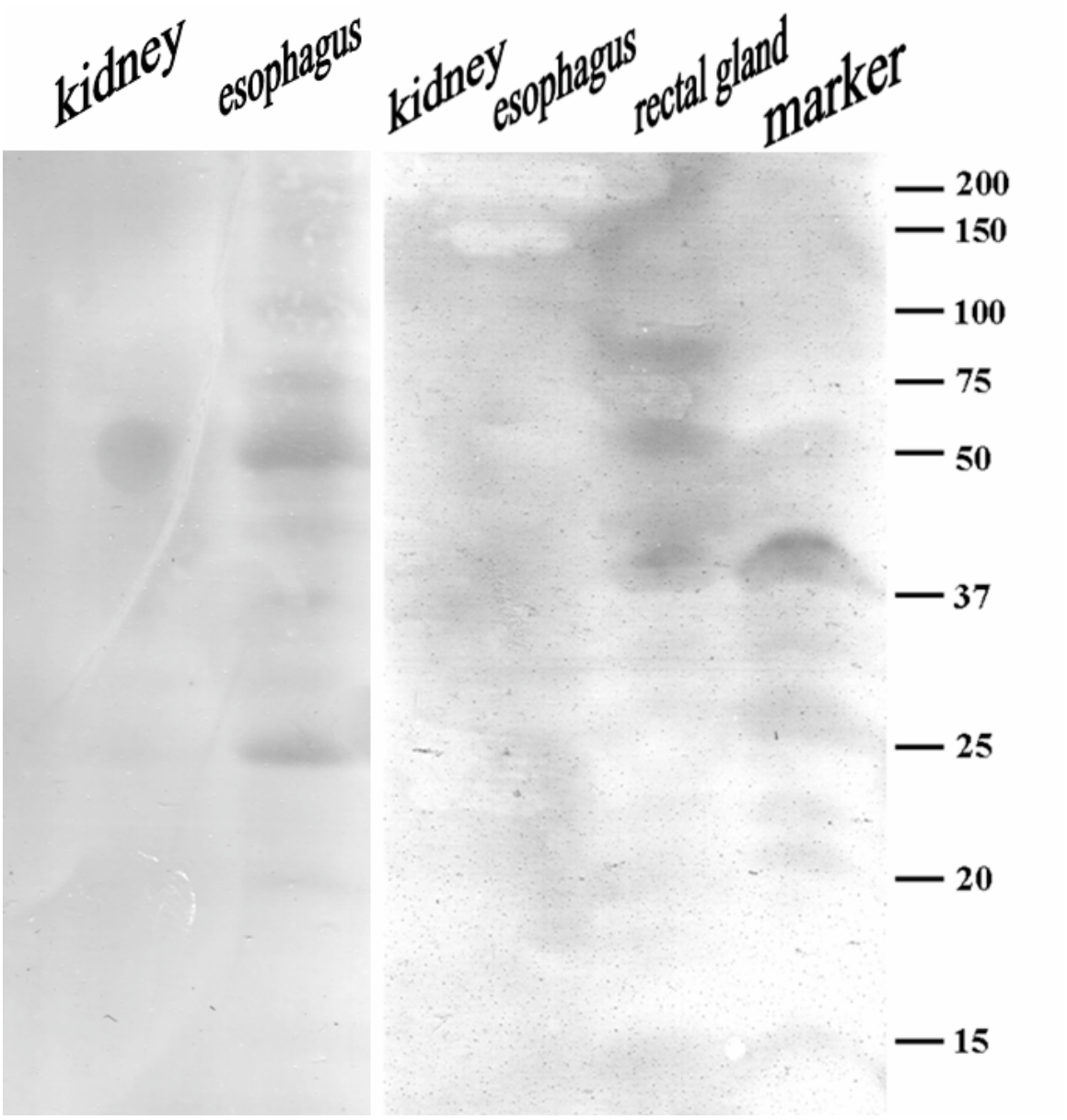

Figure 21. Western blot analysis of AQP3 in kidney, esophagus and rectal gland plasma membrane fractions of *Squalus acanthias*. The two lanes on the left side were blocked with 5% Blotto; the 3rd, 4th, and 5th lanes were blocked with 1% gelatin. Size markers on right are in kDa.

Western blot analysis was secondly performed to show the presence of AQP3 proteins in 8 different *Squalus acanthias* tissues and this resulted in strongly staining bands of AQP3 immunoactivity in the crude membrane fractions from the stomach and brain. These tissues had bands of approximately 24 kDa, but these lanes on the gel

appear to have merged with the marker lanes on the outermost sides of the filter. There was also an appearance of faint bands staining in the gill and kidney at the same size. Another line of faint banding was also seen above 25 kDa in several tissues. The filter was slightly curved during the processing and thus continually raised up out of the solution and this may explain the high background along the edges (Figure 22). There were also other bands of a large molecular weight and these may be tetramers or AQP3.

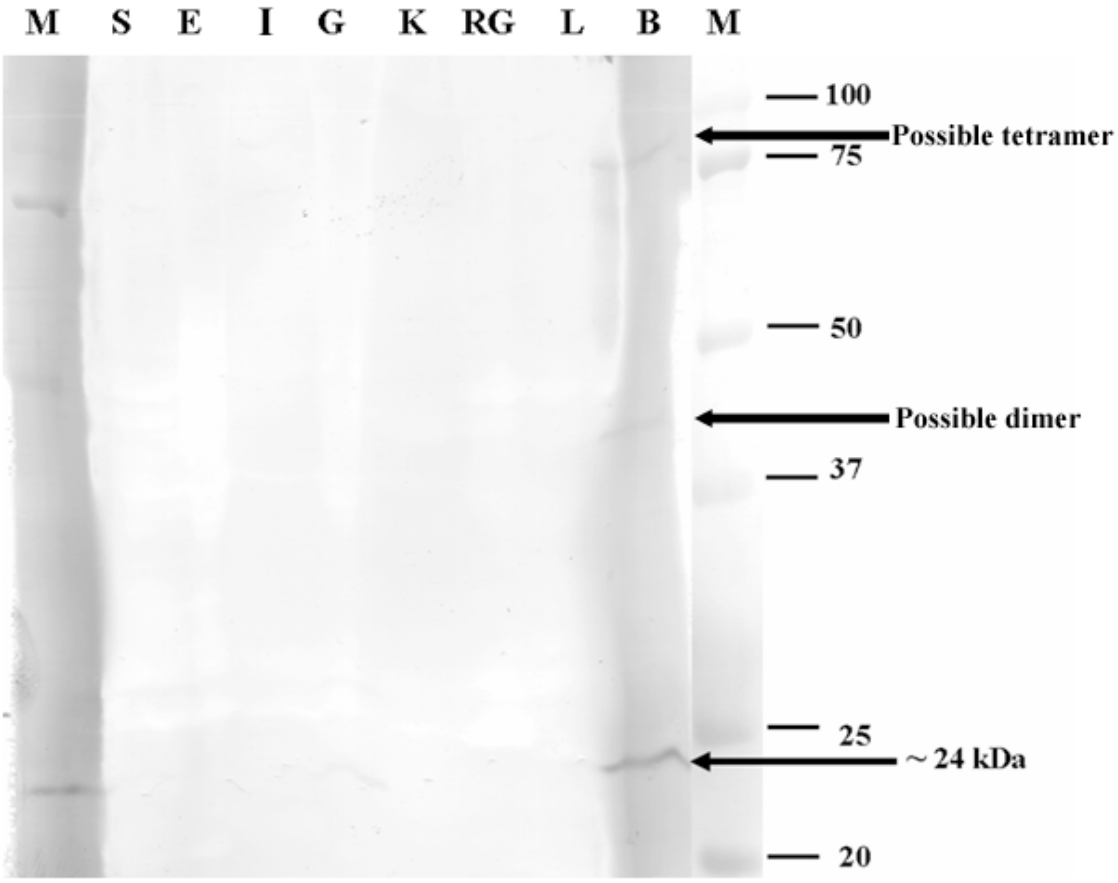

Figure 22. Western blot analysis of AQP3 in tissues of *S. acanthias*. The blot shows immunoreactivity in the 24-25 kDa range in each lane with varying degrees of staining in (S) stomach, (E) esophagus, (I) intestine, (G) gill, (K) kidney, (RG) rectal gland, (L) liver, (B) brain. Size markers (M) are in kDa, scale on right. Possible metamers indicated by arrows.

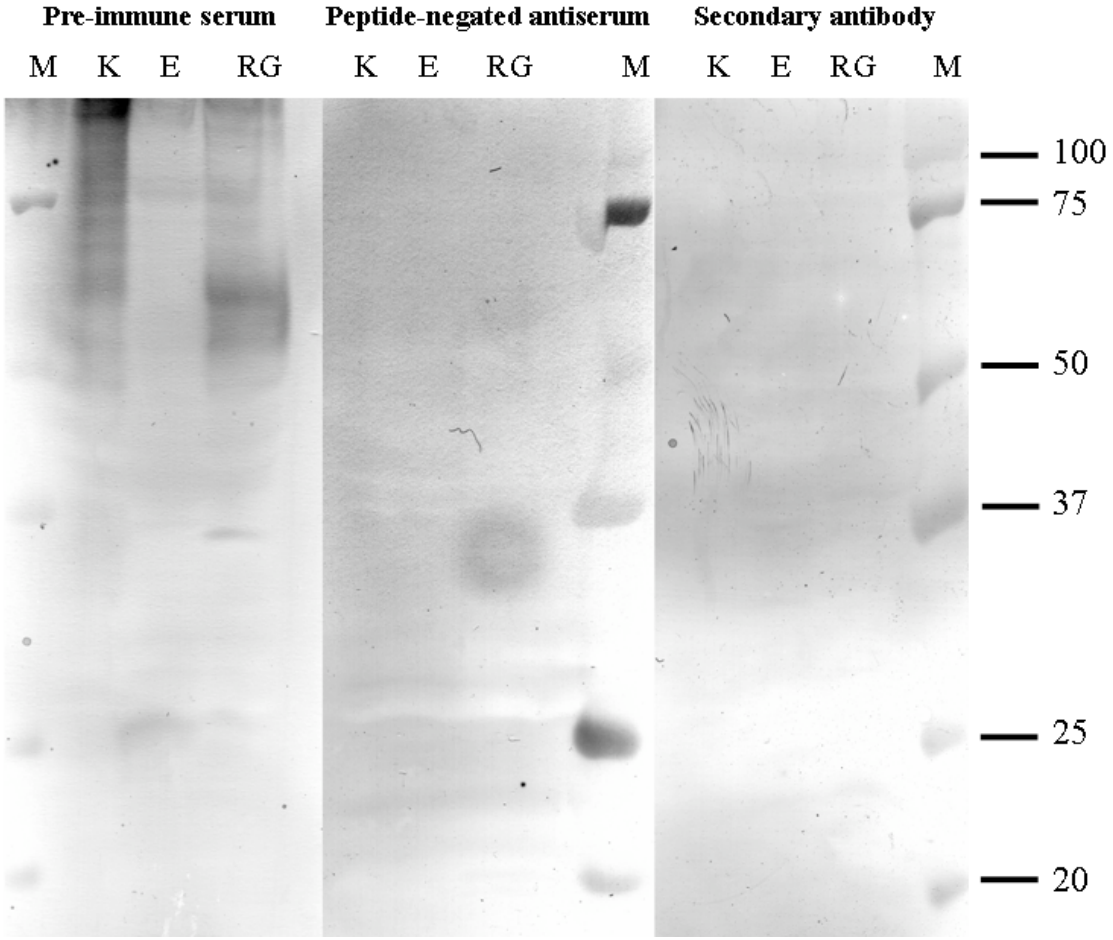

Figure 23. A composite of Western blot analysis of AQP3 controls in kidney (K), esophagus (E), and rectal gland (RG) of *Squalus acanthias* using pre-immune serum, peptide-negated antiserum and secondary antibodies. Size markers (M) are in kDa.

The controls in Figure 23 showed slight immunoreactivity above 25 kDa in the pre-immune serum. However, there are antibodies present in the pre-immune serum that are no longer in the primary AQP3 antisera (as this was affinity purified). These bands may not be present in blots using the AQP3 antisera. The peptide-negated antiserum and

secondary antibody controls showed no similar staining to the AQP3 tissue samples in Figure 21 or 22.

Immunohistochemistry

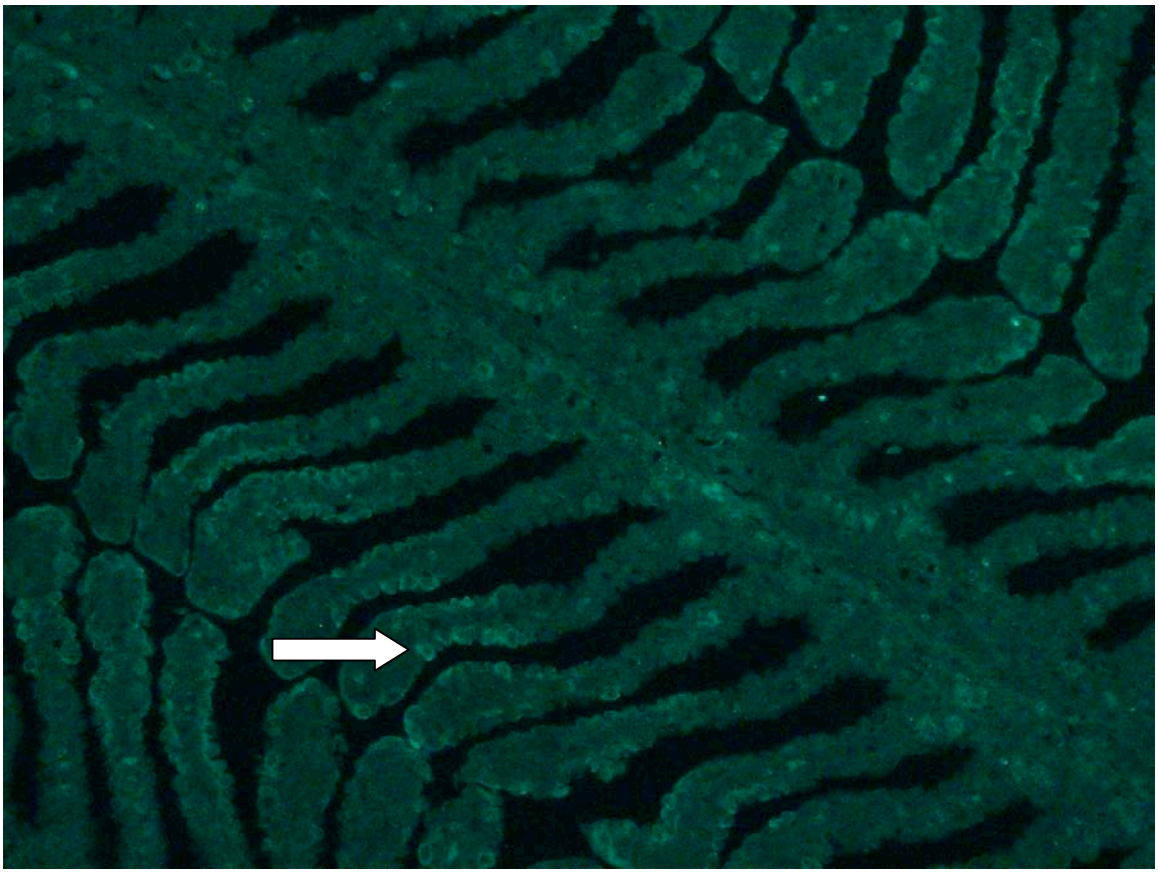

Figure 24. Axiovert inverted fluorescent micrograph of the gill of *Squalus acanthias* after immunohistochemical staining with AQP3 polyclonal antiserum showing cross-section of filament and lamellae (x400 magnification). Arrow indicates example of AQP3 Alexa Fluor 488 immunostaining.

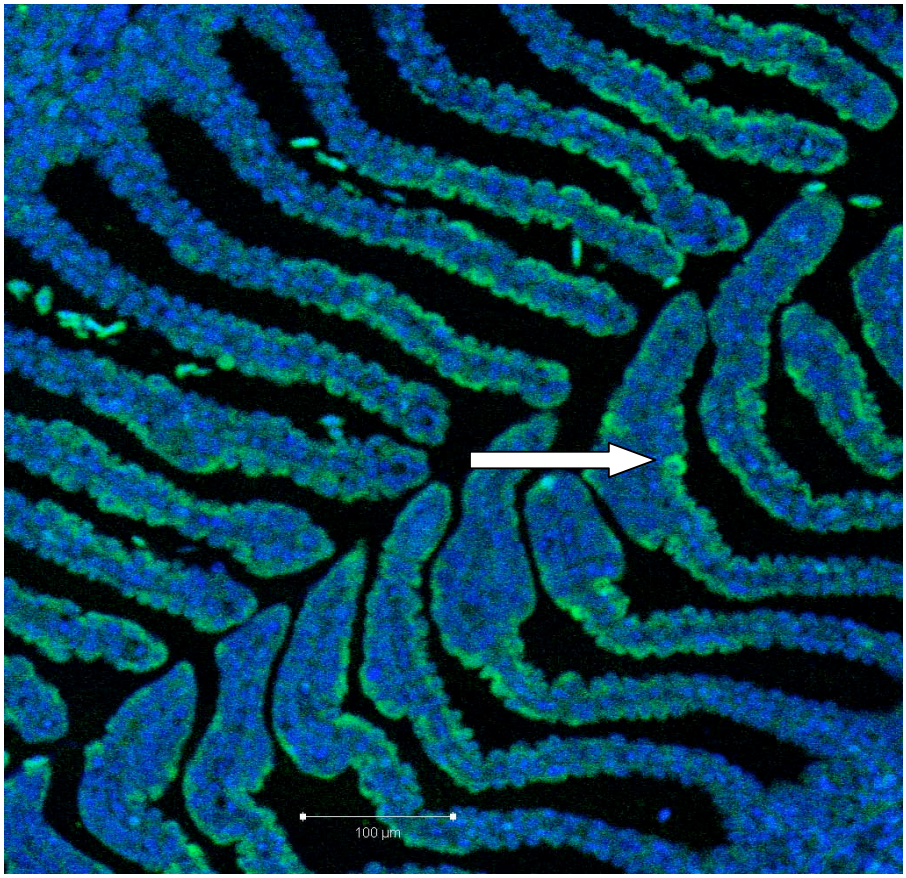

Figure 25. Confocal laser scanning micrograph of the gill of *Squalus acanthias* after immunohistochemical staining with AQP3 polyclonal antiserum showing immunolocalization in the surface epithelial cells of the lamellae. Blue staining is DAPI; green is Alexa Fluor 488. Bar in the bottom of image represents 100 µm.

Immunohistochemistry experiments used the AQP3 polyclonal antiserum on sections made from gill, kidney, and rectal gland. The fixation and paraffin embedding procedures generally yielded good antigenicity and good structural preservation. The intensity of the immunostaining varied between the tissues. There was consistent, but weak, AQP3 immunostaining in the gill as shown in Figure 24.

AQP3-specific staining was localized on surface epithelial cells of the gill lamellae as shown in Figure 25 and 26(A). The immunohistochemical controls used were the peptide-negated antiserum (Figure 26, B) and the secondary antibody (Figure 26, D)

and both showed no similar staining. The pre-immune serum showed some generalized staining (Figure 26, C), as with the Western blotting experiments. There are antibodies present in the pre-immune serum that have been removed from the AQP3 immune serum by affinity purification and therefore the pre-immune serum does not represent a particularly good control.

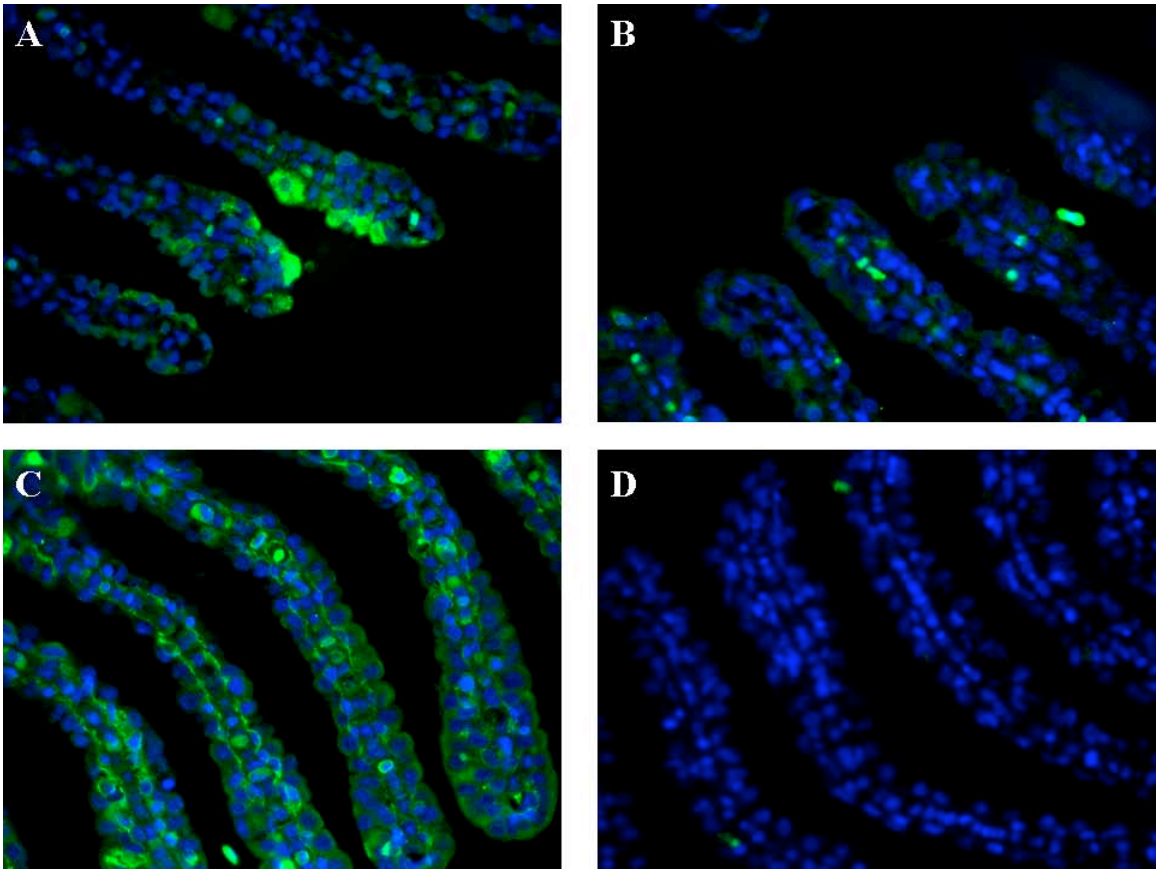

Figure 26. Axiovert inverted fluorescent micrograph of the gill of *Squalus acanthias* after immunohistochemical staining with (A) AQP3 affinity purified polyclonal antiserum, (B) peptide-negated antiserum control, (C) pre-immune serum control and (D) secondary antibody control. Blue staining is DAPI; green is Alexa Fluor 488 (x400 magnification).

The immunohistochemical staining of the *S. acanthias* kidney yielded apparently specific staining. The staining was always located on the basolateral but not on the apical side of renal tubule cells. The staining appeared to be only in specific parts of the nephron tubules, mainly in the thin-walled tubules located within the bundle zone (see Introduction, Figure 5), although no staining was seen in the actual bundles themselves in any of the micrographs (Figure 27).

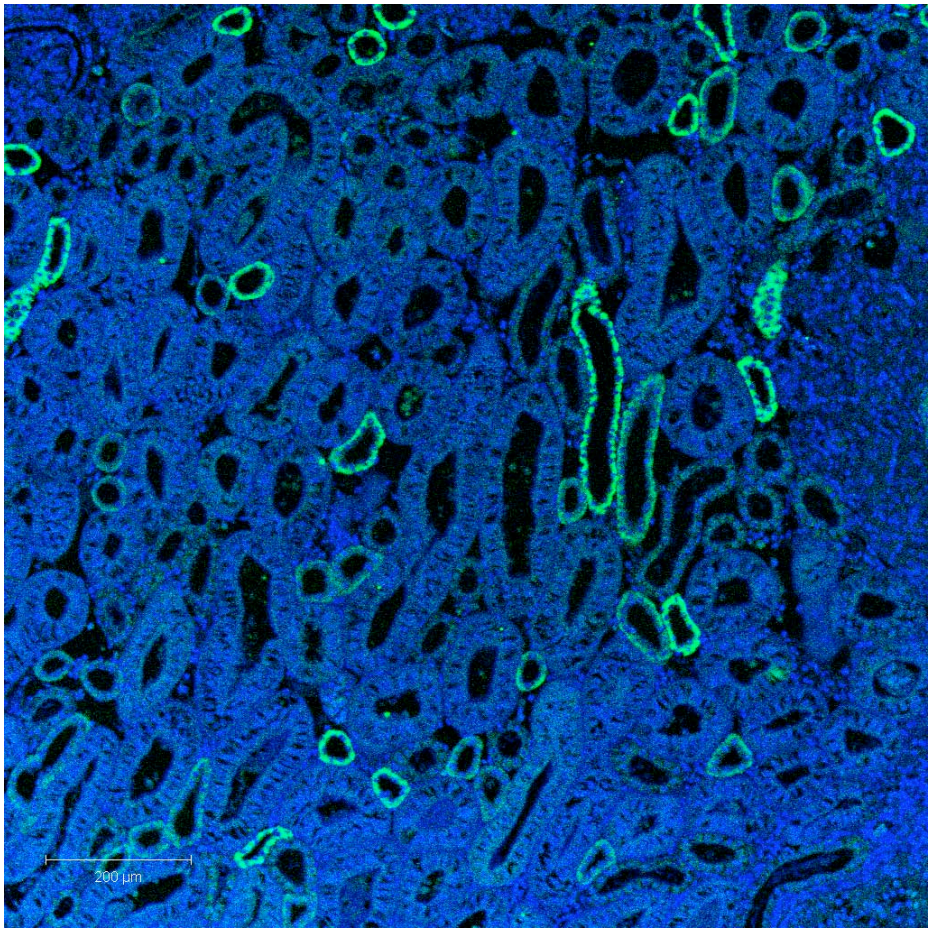

Figure 27. Low power confocal laser scanning micrograph of the kidney of *Squalus acanthias* after immunohistochemical staining with AQP3 polyclonal antiserum showing immunolocalization in the basolateral membranes of kidney tubule cells. Blue staining is DAPI; green is Alexa Fluor 488. Bar in the bottom of image represents 200 µm.

Immunohistochemical staining controls in the kidney were the same as those used in the gill. The peptide-negated antiserum, secondary antibody and pre-immune samples showed no similar staining to the AQP3 stained samples (Figures 28 and 29).

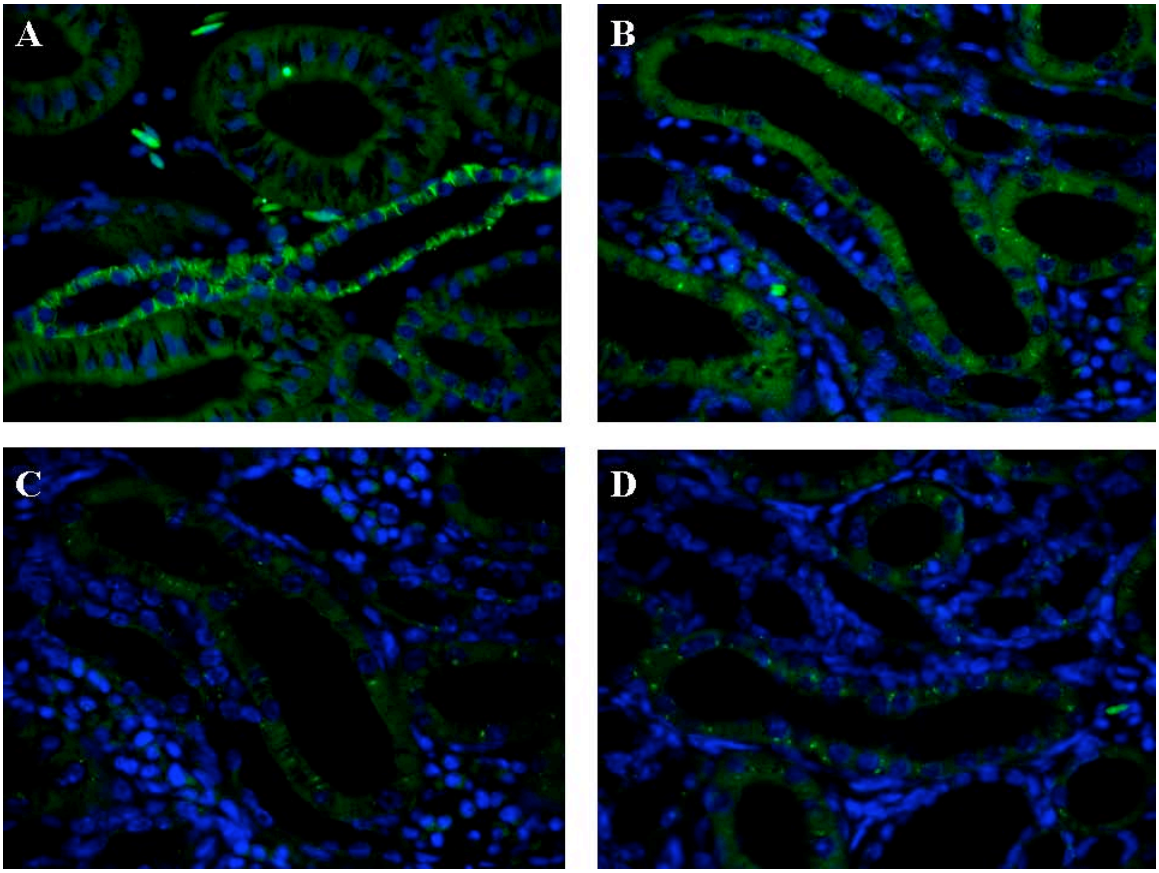

Figure 28. Axiovert inverted fluorescent micrographs of the kidney of *Squalus acanthias* after immunohistochemical staining with AQP3 polyclonal antiserum showing immunolocalization in the basolateral membranes of kidney tubules (A). No similar staining is seen in the secondary antibody (B), pre-immune serum (C), and peptide-negated antiserum samples (D). Blue staining is DAPI; green is Alexa Fluor 488. Slides are in near serial sections. All sections x400 Magnification.

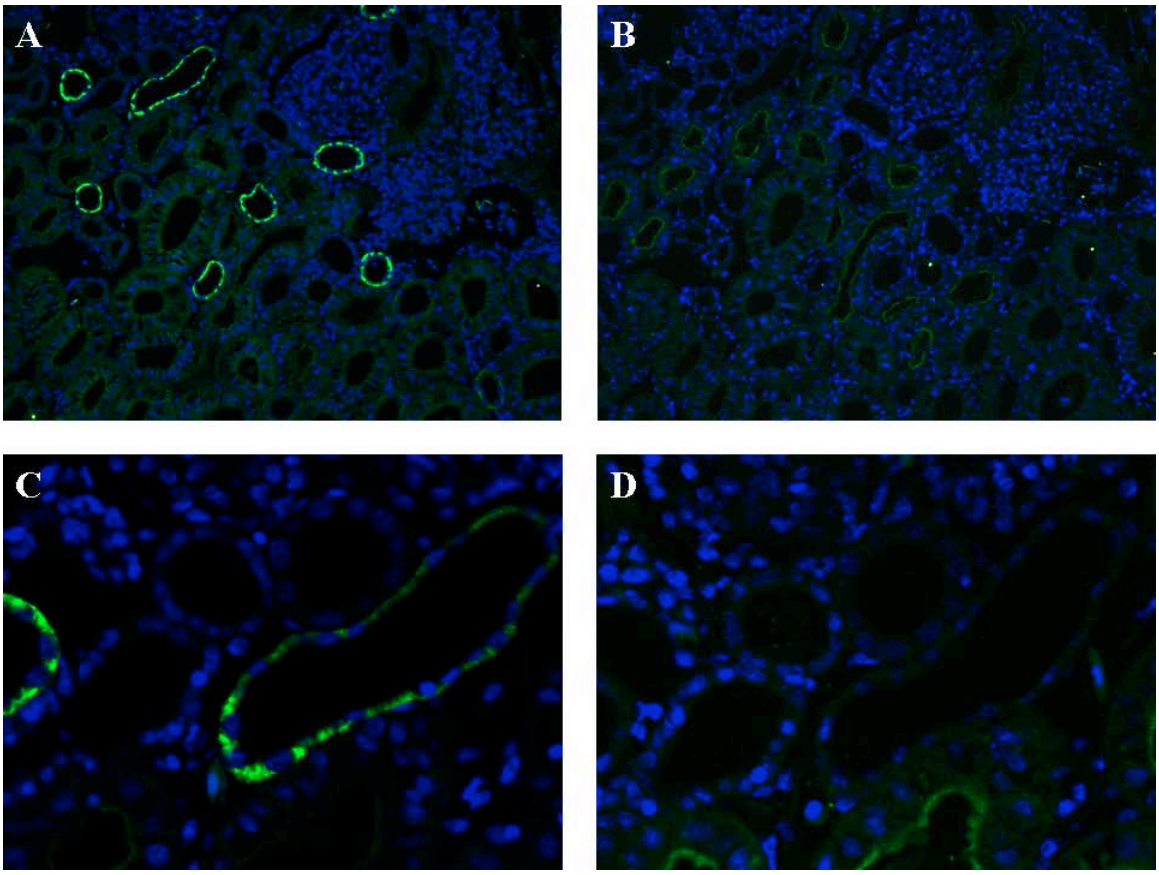

Figure 29. Axiovert inverted fluorescent micrographs of serial sections of the kidney of *Squalus acanthias* after immunohistochemical staining with AQP3 polyclonal antiserum showing immunolocalization in the basolateral membranes of kidney tubules (A and C). No similar staining is seen in the peptide-negated antiserum samples (B and D). A and B low magnification, C and D higher magnification, micrographs of the same region of tissue. Blue staining is DAPI; green is Alexa Fluor 488. A, B x100 magnification. C, D x400 magnification.

Figure 30 shows strong basolateral AQP3 staining in one kidney tubule and the higher magnification of the same tubule shows a triangular shape staining the basolateral corners of two adjacent cells.

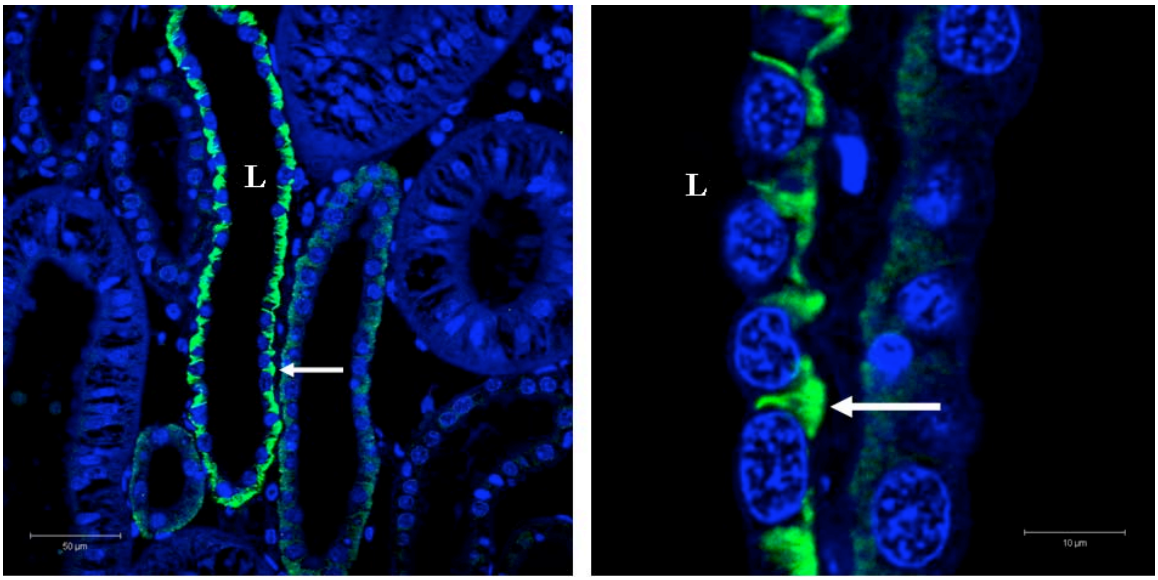

Figure 30. Confocal laser scanning micrographs of the kidney of *Squalus acanthias* after immunohistochemical staining with AQP3 polyclonal antiserum showing immunolocalization in the basolateral membranes of kidney tubules, lumen (L). Blue staining is DAPI; green is Alexa Fluor 488. Bars in the bottom of image represent 50 μm on left and 10 μm on right.

Immunostaining with AQP3 in the rectal gland section yielded poor results, therefore no controls were performed. Although there was some expression in the PCR of rectal gland, there only seems to be low level fluorescence in longitudinal muscle blocks in the capsule that surrounds the rectal gland (Figure 31). This may be the result of tissue auto-fluorescence.

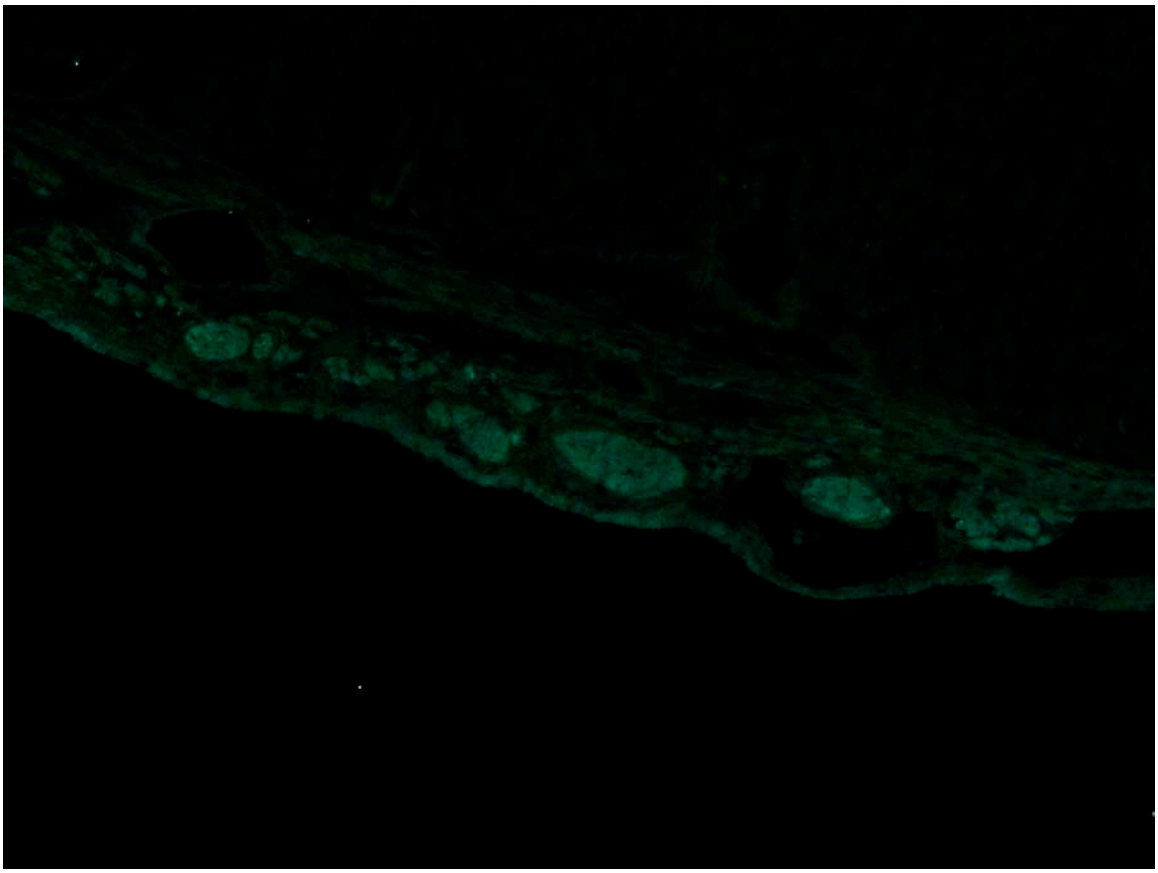

Figure 31. Axiovert inverted fluorescent micrograph of the rectal gland of *Squalus acanthias* after immunohistochemical staining with AQP3 polyclonal antiserum (x400 magnification).

Quantitative PCR (qRT-PCR)

Real-Time PCR (qRT-PCR) with cDNA from esophagus and kidney was conducted to determine the distribution of AQP3 in the tissues of the sharks that were acclimated into the various salinities, 75% SW, 100% SW, and 120% SW. Other tissue samples did not show a sufficient signal to perform the qRT-PCR, i.e., the products were generated very late in the PCR process (>35 cycles) and so primer dimers produced under such circumstances would have interfered with the result.

Standard curves were produced using a series of dilutions made from one of the cDNA's. The resulting cycle number thresholds (C_t) were then plotted against the $\log_{10}$ of the relative cDNA concentration (see an example in Figure 32). There was a negative linear relationship between cDNA concentration and cycle threshold, where samples with higher levels of mRNA/cDNA have lower cycle thresholds. The equation (for the regression fit line generated by Cricket Graph III software; Computer Associates International) was then used to calculate the relative level of AQP3 mRNA in cDNA samples, i.e., the C_t values from these samples was converted to a relative AQP3 mRNA level using the graph equation.

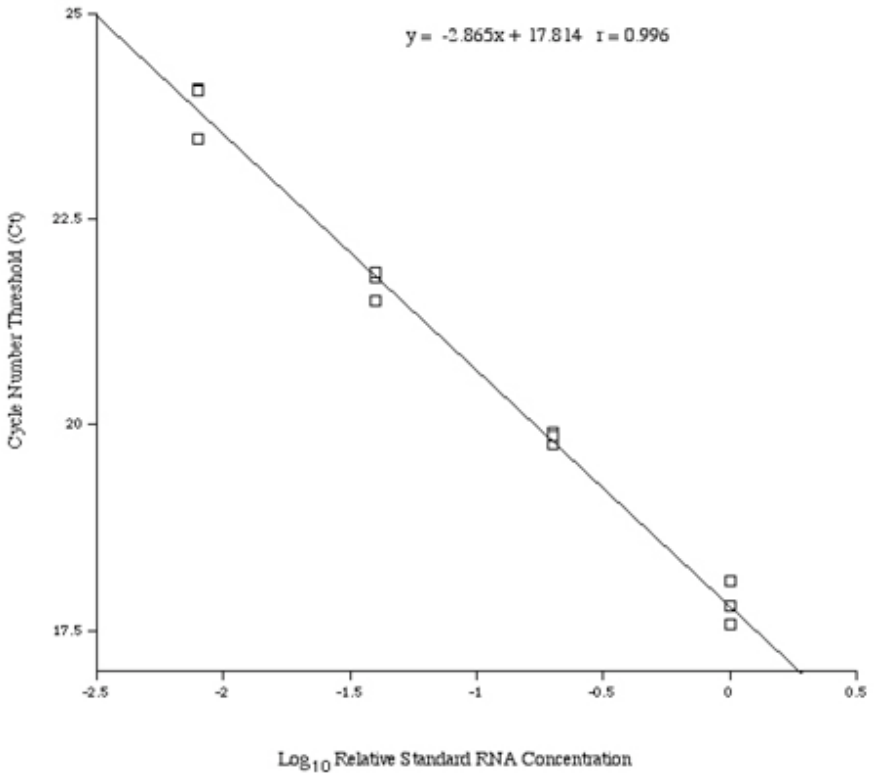

Figure 32. Typical quantitative Real-Time PCR standard curve. cDNA was diluted six-fold and the cycle threshold determined for the PCR amplification of *Squalus acanthias* AQP3 cDNA from a standard RNA sample.

Results showed that the (AQP3) mRNA levels in kidney were similar in the samples from 100% and 120% SW fish and showed the least amount in the 75% SW samples (Figure 33), but there were no statistically significant differences between the three groups as determined by an ANOVA statistical test with a Fisher post hoc test.

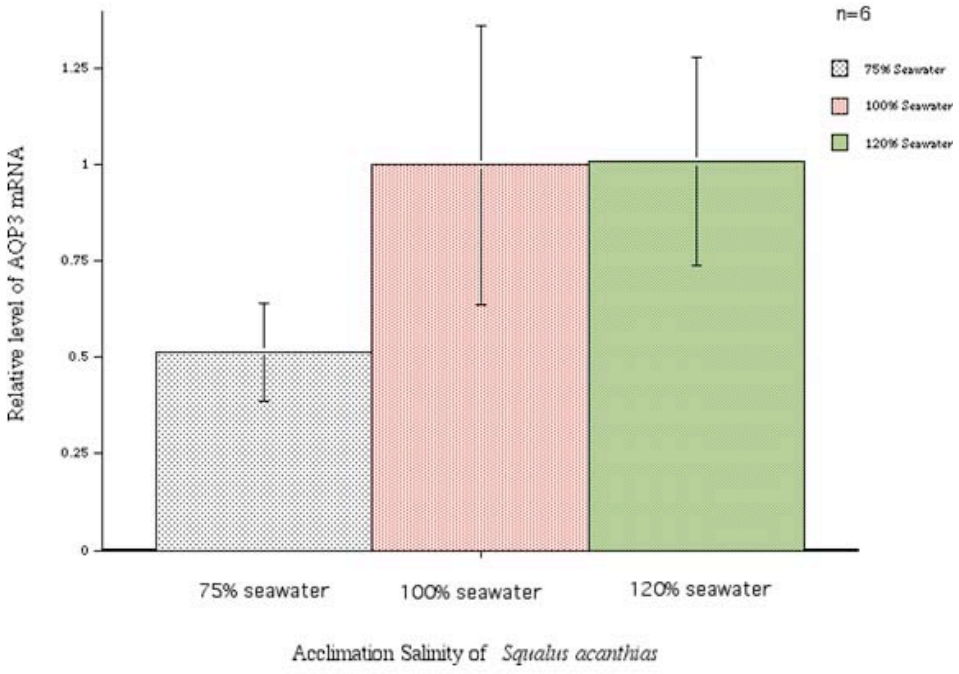

Figure 33. Graph showing the expression of *Squalus acanthias* AQP3 mRNA in kidney after acclimation to 75%, 100%, and 120% seawater salinities, n = 6 for each group, showing standard errors.

Conversely, the mRNA levels of esophagus AQP3 were lowest in the 120% SW and highest in the 75% SW (Figure 34).

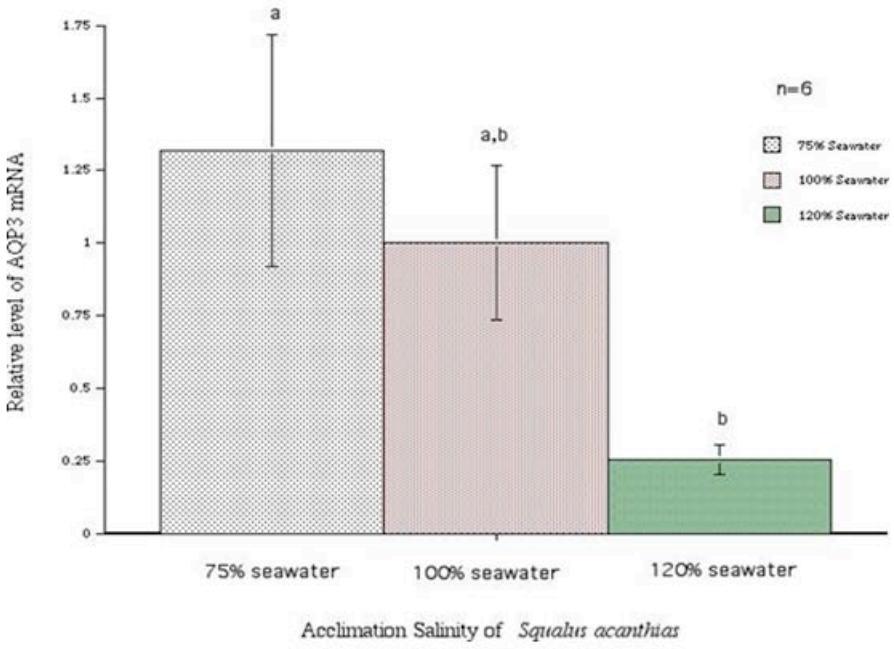

Figure 34. Graph showing the expression of *Squalus acanthias* AQP3 mRNA in esophagus after acclimation to 75%, 100%, and 120% seawater salinities, n = 6 for each group, showing standard errors.

Although this comparison shows a trend, conclusions cannot be drawn from the results because there was no statistically significant difference between either the 75% SW or 120% SW fish and the 100% SW control animals according to an analysis of variance with post ad hoc testing (ANOVA) using Statsview software, Version 4.0. Lower levels of AQP3 mRNA expression in fish held at higher salinities show possible changes in expression as the 75% SW fish and 120% SW fish groups did show statistically different levels of expression ($P<0.05$) compared to each other.

CHAPTER 4

DISCUSSION

This is the first study to use molecular and immunological techniques to demonstrate that an orthologue of mammalian AQP3 is expressed in the tissues of the dogfish shark. Those tissues include kidney tubules, gills, and esophagus, as well as the intestine, stomach, eye, and brain. The phylogenetic analysis of the full-length shark AQP3 cDNA sequence with available AQP3 sequences from other species demonstrates that it is an elasmobranch orthologue of mammalian AQP3. The high homology of the dogfish shark and human AQP3 (73.8%) suggests that AQP3 has changed very little both in the elasmobranch as well as more generally in the tetrapod lineage, (including in mammals), since these two groups separated over 450 million years ago.

Cartilaginous fishes, such as sharks, skates, rays and chimaeras, provide a critical reference for our understanding of vertebrate genome evolution because of their phylogenetic position (Figure 35). In fact, a recent comparative analysis of the elephant shark, the authors found that the degree of conserved synteny (precise order of genes on a chromosome) and conserved sequences between the human and elephant shark genomes are higher than that between human and teleost fish genomes (Venkatesh et al., 2007).

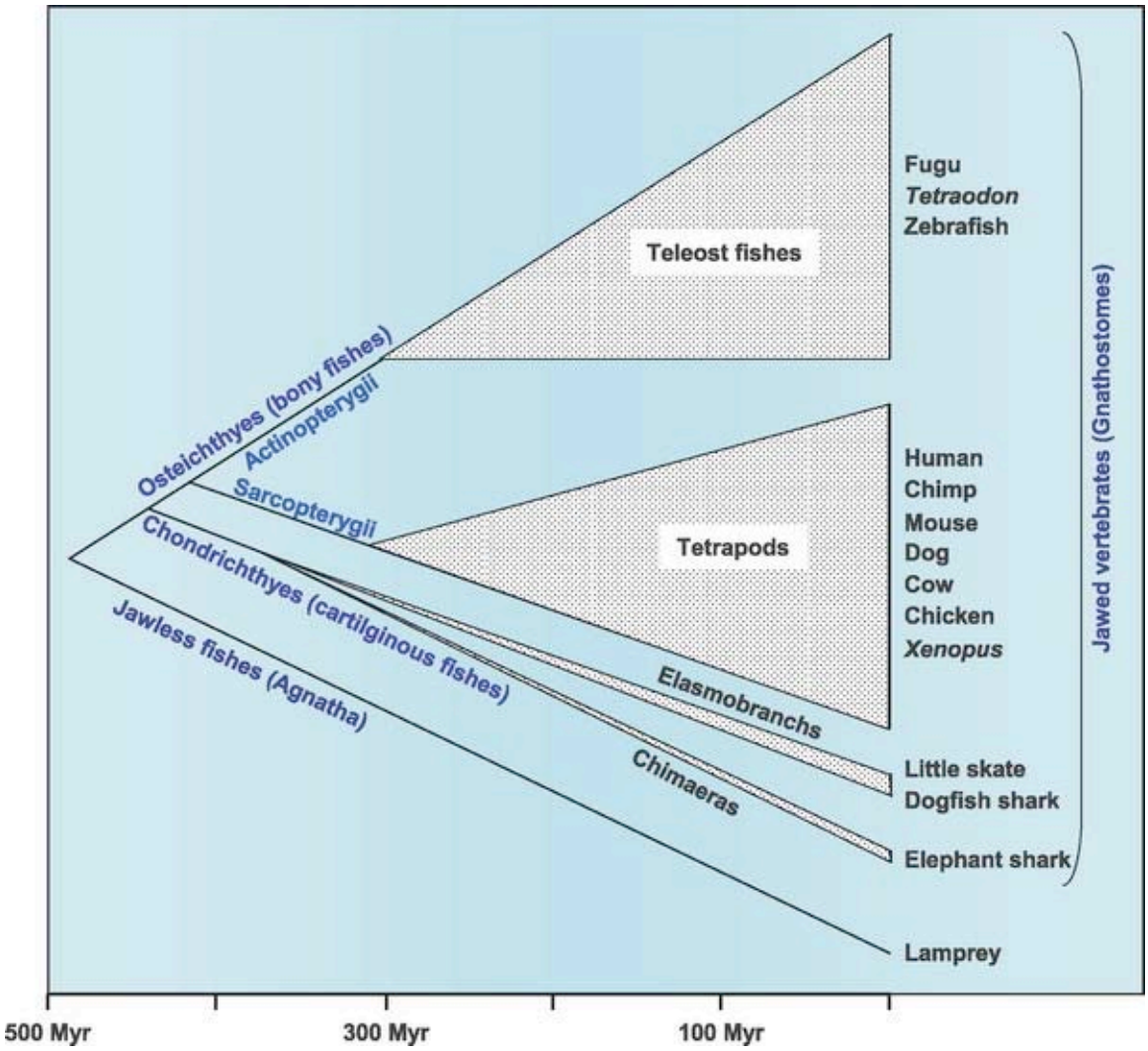

Figure 35. Phylogenetic tree of vertebrates. The vertical axis represents the abundance of extant species in each of the groups. Names of representative members of each lineage are shown. The extant Actinopterygii (ray-finned fishes) include fish such as fugu and zebrafish. Sarcopterygii (lobe-finned fishes) include coelacanths, lungfish, and the tetrapods (amphibians, birds, reptiles and mammals). Among these, only the teleost and tetrapod branches are shown. The divergence times shown are the minimum divergence times based on fossil records (Venkatesh et al., 2007).

The following five paragraphs contain a brief overview of the results as an introduction to the discussion.

Results from Western blotting experiments suggest that the AQP3 protein may be expressed in the gill, kidney, stomach, and brain, although these experiments need to be

expanded to confirm this result. To improve the results, more protein could be used, i.e., 300 μg, additionally new higher titre antibodies could be made with higher affinity for AQP3. Future testing could use a sucrose density gradient to further purify the crude membrane fractions from tissues so that purer membrane protein samples can be used which would also reduce the background.

The immunohistochemistry revealed localization of the *Squalus acanthias* AQP3 protein in the basolateral membranes of kidney tubule cells and in big and round cells, not typical of the pavement cells on the surface of the gill. But, it is not surprising to see AQP3 in the gill as it has been shown to be present in teleost fish, including zebrafish (*Danio rerio*), rainbow trout (*Oncorhynchus mykiss*), as well as the European eel (*Anguilla anguilla*) (Cutler et al., 2006; Lignot et al., 2002) even though the localization of AQP3 expression is different from that of teleost fish.

The Northern blotting results demonstrated AQP3 mRNA expression in the intestine, gill, esophagus, stomach, eye, kidney, brain, liver, muscle, and rectal gland although PCR results did not show any bands for muscle and liver. The Northern blotting experiments could be repeated to confirm the findings and determine the source of the discrepancy in those results. Repeat experiments could give better results if the filters were hybridized for a longer period of time to block out the nucleic acid on them.

The results of the quantitative real-time PCR suggest a trend toward a difference in the level of mRNA expression in the esophagus when salinities change between 75% SW and 120% SW fish. This trend could also be improved by repeating experiments using more experimental animals that might allow a significant difference between these groups and the 100% SW control fish. The kidney results were little different between the

100% and 120% SW samples, but the 75% SW results were lower than both of these groups, although this difference proved not to be statistically significant. Because of these differences and the fact that we know aquaporins transport water, these data suggest that AQP3 may be functionally involved in water homeostasis in these animals, as was first hypothesized in this project, but the results themselves are inconclusive.

The study of the differences in strategies of elasmobranchs in marine and freshwater environments to maintain their osmotic homeostasis can provide insight into the evolutionary history of these control mechanisms (Lacy and Reale, 1999). Because some marine species are able to move into and out of freshwater suggests they have sophisticated regulatory mechanisms for their salt and water balance. Although *Squalus acanthias* is not known to move into and out of freshwater, the elaborate morphology of its kidney suggests that it also has a complex highly-controlled system.

Urea plays a central role in osmoregulation in marine elasmobranchs, the coelocanth, some amphibians, and the mammalian kidney (Smith and Wright, 1999). Some can dramatically alter tissue urea levels and excretion rates in response to changes in external salinity or water availability (Lacy and Reale, 1985). It is not clear whether or not facilitative transporter proteins are responsible for urea reabsorption in the elasmobranch kidney. At least one urea transporter has been characterized in *Squalus acanthias* (ShUT) by Smith and Wright (1999). But there is also a model for a passive model of urea absorption in the elasmobranch kidney proposed by Friedman and Hebert in their 1990 study. Their model demonstrates the presence of a countercurrent multiplication system, and differential permeabilities of tubular segments to urea, water, and sodium. It was hypothesized that the distal tubule permeability for water and urea

would permit diffusion of urea from tubular fluid to the intrabundle space (Friedman and Hebert, 1990). The question is raised, now that AQP3 has been localized in *Squalus acanthias* kidney tubules, does this aquaglyceroporin also provide a channel for urea and water in the bundle zone.

In the immunostaining of *Squalus acanthias* kidney, the localization of AQP3 appeared basolaterally in the tubule cells which had not been established in elasmobranchs before this study. It had only been demonstrated in teleost fish and mammalian (including human) kidney (Cutler and Cramb, 2002; Agre et al., 2002; Echevarria et al., 1994). Electron micrographs from the Lacy and Reale study show similarities to the morphology seen in the immunostaining in the Results Section. The tubules shown in Figure 27 could be the same as shown in the bundle zone in Figure 36.

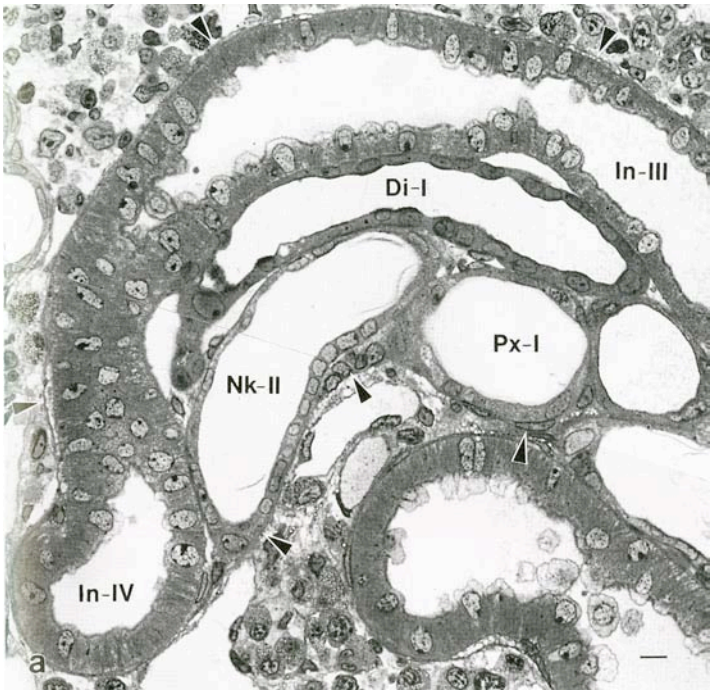

Figure 36. Bundle zone in *Squalus acanthias*, showing longitudinal to oblique sections of the nephron tubules. The arrowheads indicate the peritubular sheath (from Lacy and Reale, 1995).

The fluorescence shown basolaterally in long thin-walled tubules in Figure 27 would make sense as Lacy and Reale describe the thinnest walled tubules as part of the neck segment (Nk) closest to the glomerulus (proximal tubule: again see Figure 36). Here one would expect the most urea reabsorption and highest osmotic water permeability (Friedman and Hebert, 1990). Thus, one possibility is that Aquaporin 3 is involved in these processes in this segment, as it is an aquaglyceroporin which can allow the passage of urea molecules as well as water. However, additionally, it should be noted that the distal tubule is also a similar thin-walled tubule segment (Figure 36).

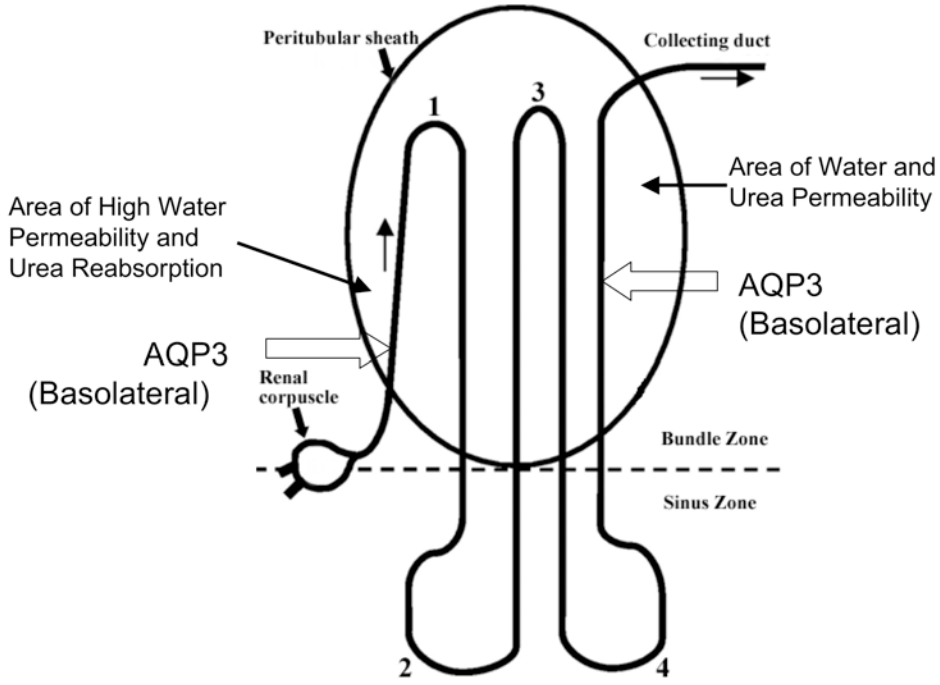

Figure 37. Proposed model of localization of AQP3 in a shark kidney nephron.

Consequently, another possible location for Aquaporin 3 expression in the kidney nephron is in the large basolateral membrane infolds of distal tubule cells in the bundle zone, as shown in the electron micrograph of the distal tubules of the little skate (Figure 38). The triangular shape of the immunostaining, as seen in Figure 30 of *Squalus acanthias,* may correspond to the triangular lateral cell borders that are elaborated into interdigitating folds, which are far more elaborate in the basolateral corners of these cells than elsewhere (from Lacy and Reale, 1999). Figure 37 diagrams the possible location of AQP3 in the bundle zone where there is high water and urea permeability in the proximal and distal areas.

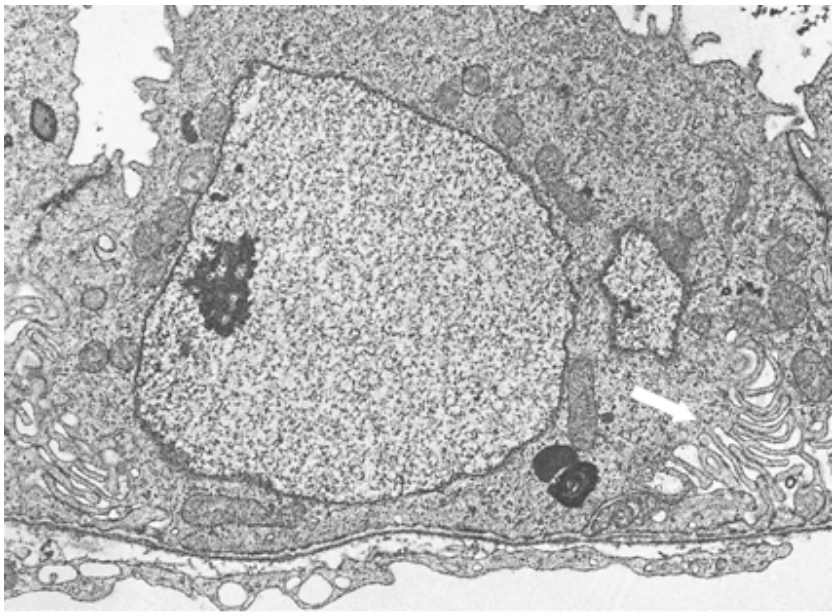

Figure 38. Distal tubules of little skate showing large basolateral membrane infolds within the bundle zone. Interdigitating folds seen on lower right indicated with arrow (from Lacy and Reale, 1999).

As can be seen in Figure 39, the sinus zone of the shark kidney, has large spaces (blood sinus) through which the blood flows. As can be seen in Figure 27 of the results, sections showing AQP3 staining showed no such sinus spaces suggesting AQP3 is expressed in tubule segments present in the bundle zone.

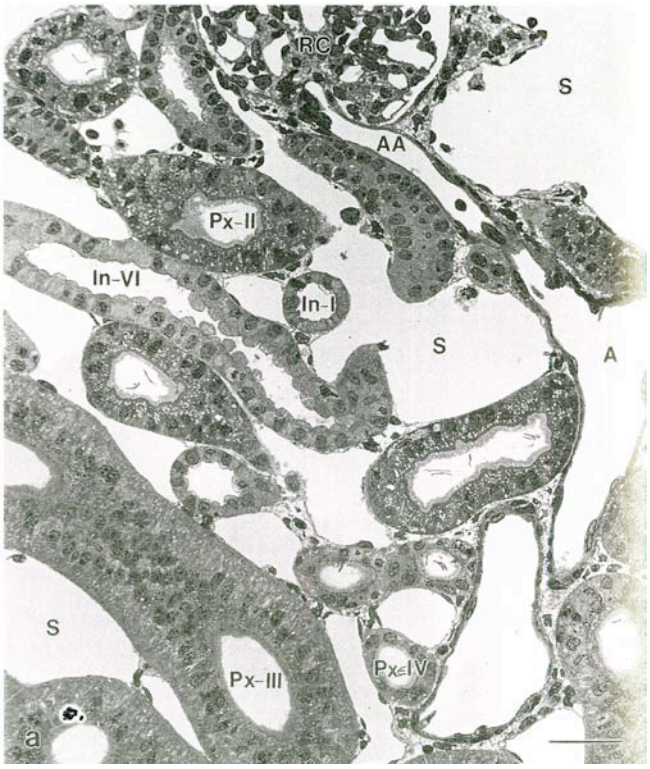

Figure 39. Sinus zone of kidney, *Squalus acanthias*. The renal corpuscle (RC) and its afferent arteriole (AA) originating from a small artery (A) as well as profiles of the proximal tubules can be seen among the larger blood sinuses (S) (Lacy and Reale, 1999)

In teleost fish, AQP3 has been shown to play a complex role in cells within the major osmoregulatory organs of teleost fish (Cutler et al., 2006). In their study, there was no apparent change in the location or protein abundance of renal AQP3 after eels were moved from freshwater to seawater, which is a similar result to this study where there was no significant difference seen in the quantitative PCR results measuring AQP3 mRNA abundance in shark kidney.

In the human kidney, aquaporins are essential for maintaining body water homeostasis. AQP3 is present in the basolateral membrane of the connecting tubule (a distinct segment that occurs between the distal convoluted tubule and the cortical collecting duct) and the collecting duct principal cells (Figure 40) (Nejsum, 2005).

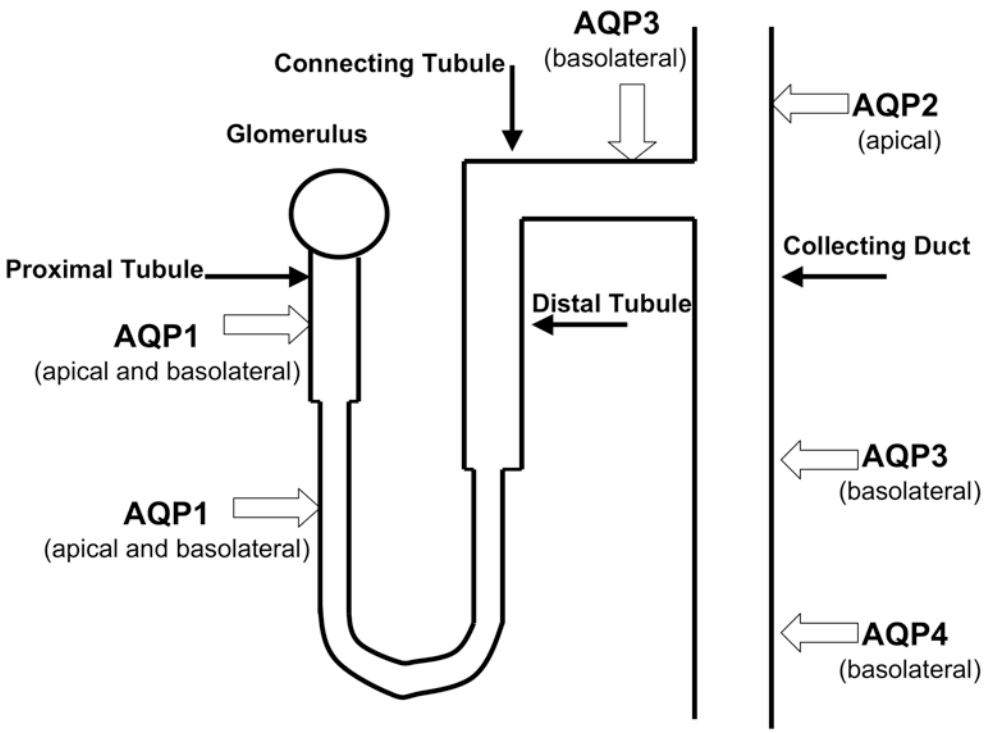

Figure 40. Simplified drawing of a human nephron and collecting duct showing the sites of aquaporin localization (AQP1, AQP2, AQP3 and AQP4). AQP3 is present in the basolateral membrane of the connecting tubule and collecting duct principal cells (Nejsum, 2005).

Because vasopressin (antidiuretic hormone or ADH) is the hormone responsible for recovering water from the collecting duct, it alters water uptake by affecting the number of aquaporins in the apical membrane of the cells of the collecting duct (Moyes and Schulte, 2006) and is, therefore, a subject needing further investigation in elasmobranchs.

Detailed immunolocalization of AQP3 in the epithelial tissues of the medullary collecting ducts of rat kidney has also been demonstrated. It was suggested that AQP3

plays a role in providing water to water-deprived cells to maintain their intracellular osmolality and cell volume (Echevarria et al., 1994).

Although the results were weak for the presence of AQP3 in the rectal gland of *Squalus acanthias*, other aquaporins may play a complex role in salt secretion. The same authors who argued strongly against water flux via aquaporins in the rectal gland, were still puzzled about the lower than expected basolateral urea permeability that they observed in their experiments. They asked how a low urea permeability can be achieved in the face of a relatively high water permeability unless there is the presence of an aquaporin. Although this would suggest the presence of a water-selective aquaporin rather than a (likely - urea permeable) aquaglyceroporin such as AQP3 (Zeidel et al., 2004).

It has been suggested that AQP3 may be functionally involved in water flow into or out of the basolateral tubular network of chloride cells in order to prevent swelling or dehydration in teleost fish. AQP3 may also be involved in urea and/or ammonia excretion across the gills (Cutler and Cramb, 2002; Lignot et al., 2002). However, AQP3 seemed to be expressed in ovoid cells on the secondary lamellae of shark gill and these cells are therefore likely to be pavement cells rather than the generally much larger chloride cells (Claiborne, et al., 2008).

AQP3 is known to be a key water channel in mammals and has been identified in both freshwater and seawater-acclimated eels (Lignot, et al., 2002). It has been expressed within the eel gill epithelium, particularly the chloride cells, and was down-regulated following seawater transfer. This may occur in order to protect the cells from swelling or dehydration which is a similar function to the role of AQP3 that is expressed in rat skin

and urinary bladder epithelia (Matsuzaki et al., 1999, 2000). In teleost fish, AQP3 may also be involved in the branchial chloride cells for he excretion of nitrogenous waste products such as urea and/or ammonia excretion (Cutler and Cramb, 2002; Lignot et al., 2002). The localization in the apical pole of AQP3 in teleost gill epithelium was unexpected, as in mammals AQP3 is mainly expressed in the basolateral membranes of renal collecting duct cells and epithelial cells in the small intestine and colon (Koyama et al., 1999). Similarly, the possible presence of AQP3 in *Squalus acanthias* gill cells was also a surprise but it may have the same physiological role in the processes of water and small solute movement and in nitrogenous waste products.

The mRNA expression demonstrated in the esophagus of *Squalus acanthias* in this study was similar to that shown previously in immunological studies in teleost fish (Cutler et al., 2006) and rats (Matsuzaki et al., 1999). In humans, aquaporins 3 and 5 may participate in gastrointestinal fluid secretion and absorption, as well as possible hepatic glycerol and ketone body transport during fasting (Agre et al., 2002). The physiological significance of glycerol permeation is still not understood, but has been carefully documented (Yang et al., 2001)

In humans, there are functional relationships between the cystic fibrosis transmembrane regulator (CFTR) and both AQP3 and AQP5 that indicate the regulatory defect in cystic fibrosis may involve both proteins as cystic fibrosis is a disease of decreased fluid transport by epithelia (Agre et al., 2002). AQP3 has been shown to be activated by the CFTR in human airway epithelial cells (Schreiber et al., 1999). Also, AQP3 has also been demonstrated in human and rat eye, particularly the bulbar conjunctival epithelium and glands and weakly present in corneal epithelium (Hamann et

al., 1998). A future direction for this study might therefore be to investigate the colocalization of CFTR in the shark tissues and cells that express AQP3.

Most of the roles of AQP3 in this discussion can probably be ascribed to their water-transporting function. But why do the aquaglyceroporins transport glycerol as well as water since glycerol is not generally thought to be a solute of major importance in mammals? From the analysis of AQP3-deficient mice, AQP3 is expressed in the basal layer of keratinocytes and exhibited reduced stratum corneum hydration, reduced skin elasticity and delayed wound healing, probably relating to the water-retaining property of glycerol (Verkman, 2005).

Clearly, more studies of AQP3 will provide insight into its many roles in living organisms. Gene knockout or knockdown studies, along with a wide range of physiological testing such as the infusion of metabolites and hormones, would help to clarify AQP3 functionality. Colocalization studies with other transport proteins (including other aquaporins) and positive identification using immunohistochemistry will also provide important clues into the roles of AQP3.

Further research will improve the understanding of elasmobranch osmoregulation. And because elasmobranchs are ecologically important components in virtually every marine habitat, it is important to understand how salinity changes impact the animals osmoregulatory system, and secondarily affect feeding behavior, migration movements, development and reproduction (Hammerschlag, 2006).

In summary, AQP3 was cloned and characterized from the kidney and rectal gland of the dogfish shark, *Squalus acanthias.* The dogfish shark AQP3 shares a high degree of homology with other vertebrate AQP3 and is expressed in the tissues involved

in body water homeostasis. Immunohistochemistry demonstrated that AQP3 is expressed in the basolateral membranes of the tubule cells of the kidney. Expression levels were measured following acclimation to salinity changes to gain insights into the function of AQP3 expression in the kidney and esophagus during events that would manipulate the osmotic homeostasis of the fish. Because there was a significant difference in the levels of mRNA expression between the 75% and 120% SW, these data suggest that AQP3 expression may not be constitutive in the esophagus but may be regulated by external salinity.

An understanding of the roles of aquaporins and aquaglyceroporins provide new approaches to many complex problems and become therapeutic targets for pathophysiological conditions associated with water balance disorders. It is realistic to conclude that there are many more chapters to be written in the story of aquaporins in all organisms including sharks.

REFERENCES

Agre, P., L.S. King, M. Yasui, W.B. Guggino, O.P. Ottersen, Y. Fujiyoshi, A. Engel, S. Nielsen, 2002. Aquaporin water channels – from atomic structure to clinical medicine. *The Journal of Physiology* 542: 3-16.

Ausubel, F.M., R. Brent, R.E. Kingston, D.D. Moore, J.G. Seidman, J.A. Smith, K. Struhl, 1994. Current Protocols in Molecular Biology. Greene Publishing Associates and Wiley-Interscience, New York, pp. 326-328.

Bradford, M.M., 1976. A rapid and sensitive method for the quantitation of microgram quantities utilizing the principle of protein-dye binding. *Analytical Biochemistry* 72: 248-254.

Campbell, N.A., J. B. Reece, 2005. Biology. Benjamin Cummings Publishers, San Francisco, pp. 922-977.

Carrier, J.C., J.A Musick, M.R. Heithaus, 2004. Biology of Sharks and Their Relatives. CRC Press, Boca Raton, pp. 247-268.

Chomczynski, P., K. Mackey, 1995. Substitution of chloroform by bromochloropropane in the single-step method of RNA isolation. *Analytical Biochemistry* 225: 163-164.

Chomczynski, P., N. Sacchi, 1987. Single-step method of RNA isolation by acid guanidinium thiocyanate-phenol-chloroform extraction. *Analytical Biochemistry* 162: 156-159.

Claiborne, J.B., Choe, K.P., Morrison-Shetlar, A.I., Weakley, J.C., Havird, J., Freiji, A., Evans, D.H., Edwards, S.L., 2008. Molecular detection and immunological localization of gill Na^+/H^+ exchanger in the dogfish (*Squalus acanthias*). *American Journal of Physiology – Regulatory, Integrative and Comparative Physiology* 294: 1092-1102.

Coleman, R.A., D.C. Wu, J. Liu, and J.B. Wade, 2000. Expression of aquaporins in the renal connecting tubule. *American Journal of Physiology – Renal Physiology* 279: F874-F883.

Cutler, C. P, S. Brezillon, S. Bekir, I.L. Sanders, N. Hazon, G. Cramb, 2000. Expression of a duplicate Na,K-ATPase β-isoform in the European eel (*Anguilla anguilla*). *American Journal of Physiology – Regulatory, Integrative and Comparative Physiology* 279: R222-R229.

Cutler, C. P. and G. Cramb, 2002. Branchial expression of an aquaporin 3 (AQP-3) homologue is downregulated in the European eel (*Anguilla anguilla*) following seawater acclimation. *Journal of Experimental Biology* 205: 2643-2651.

Cutler, C. P. and G. Cramb, 2002. Two isoforms of the $Na^+/K^+/2Cl^-$ cotransporter (NKCC1) are expressed in the European eel (*Anguilla anguilla*). *Biochimica et Biophysica Acta* 1566: 92-103.

Cutler, C. P., 2007. Cloning and identification of four aquaporin genes in the dogfish shark (*Squalus acanthias*). *The Bulletin, Mount Desert Island Biological Laboratory* 46: 147-150.

Cutler, C. P., A-S Martinez, G. Cramb, 2007. The role of aquaporin 3 in teleost fish. *Comparative Biochemistry and Physiology* 148: 82-91.

Cutler, C.P., C. Phillips, N. Hazon, G. Cramb, 2007. Cortisol regulates eel (*Anguila anguilla*) aquaporin 3 (AQP3) mRNA expression levels in gill. *General and Comparative Endocrinology* 152: 310-313.

Dunbar, B. S., 1994. Protein Blotting: A Practical Approach, Oxford University Press, New York, pp. 75-83.

Echevarria, M., E. E. Windhager, S. S. Tate, and G. Frindt, 1994. Cloning and expression of AQP3, a water channel from the medullary collecting duct of rat kidney. *Proceedings of the National Academy of Sciences of the United States of America* 91: 10997-11001.

Evans, D.H., 2002. Encyclopedia of Life Sciences. Macmillan Publishers Ltd., New York, pp. 1-4.

Evans, D.H., J.B. Claiborne, 2006. The Physiology of Fishes. CRC Press/Taylor & Francis Group, LLC, Boca Raton, pp. 177-230.

Evans, D.H., P.M. Piermarini, and K.P. Choe, 2004. Homeostasis: Osmoregulation, pH regulation, and nitrogen excretion. In: Carrier, J.C., J.A Musick, and M.R. Heithaus, 2004. Biology of Sharks and Their Relatives. CRC Press, Boca Raton, pp. 247-268.

Evans, D.H., P.M. Piermarini, and K.P. Choe, 2005. Thee multifunctional fish gill: dominant site of gas exchange, osmoregulation, acid-base regulation, and excretion of nitrogenous waste. *Physiological Review* 85: 97-177.

Friedman, P.A. and S.C. Hebert, 1990. Diluting segment in kidney of dogfish shark: Localization and characterization of chloride absorption. *American Journal of Physiology* 258: R398-R408.

Fu, D., A. Libson, L.J. Miercke, C. Weitzman, P. Nollert, and J. Krucinski, 2000. Structure of a glycerol-conducting channel and the basis for its selectivity. Science 290: 481-486.

Fujiyoshi, Y., K. Mitsuoka, B.L. deGroot, A. Philippsen, H. Grubmuller, P. Agre, 2002. Structure and function of water channels. *Current Opinion in Structural Biology* 12: 509-515.

Hamann, S., T. Zeuthen, M. La Cour, E.A. Nagelhus, O.P. Ottersen, P. Agre, S. Nielsen, 1998. Aquaporins in complex tissues: distribution of aquaporins 1-5 in human and rat eye. *American Journal of Physiology* 274: 1332-1345.

Hammerschlag, N., 2006. Osmoregulation in elasmobranchs: a review for fish biologists, behaviourists and ecologists. *Marine and Freshwater Behaviour and Physiology* 39: 209-228.

Hara-Chikuma, M., A.S.Verkman, 2006. Physiological roles of glycerol-transporting aquaporins: the aquaglyceroporins. *Cellular and Molecular Life Sciences* 63: 1386-1392.

Hazon, N., A. Wells, R.D. Pillans, J.P. Good, W.G. Anderson, C.E. Franklin, 2003. Urea based osmoregulation and endocrine control in elasmobranch fish with special reference to euryhalinity. *Comparative Biochemistry and Physiology* 136: 685-700.

Hazon, N., Tierney, M.L., Anderson, W. G., MacKenzie, S., Cutler, C. and Cramb, G., 1997. Ion and water balance in Elasmobranch Fish. In. Ionic regulation in Animals (N. Hazon, F.B. Eddy, and G. Flik Eds.). Springer-Verlag, Berlin, Heidelberg, New York. pp 70-81.

Helling, R.B., H.M. Goodman, H.W. Boyer, 1974. Analysis of endonuclease R-*Eco*RI fragments of DNA from lamboid bacteriophages and other viruses by agarose-gel electrophoresis. *Journal of Virology* 14: 1235-1244.

Koyama, Y., T. Yamamoto, T. Tani, K. Nihei, D. Kondo, H. Funaki, E. Yaoita, K. Kawasaki, N. Sato, K. Hatakeyama, and I. Kihara, 1999. Expression and localization of aquaporins in rat gastrointestinal tract. *American Journal of Physiology –Cell Physiology* 276: C621-C6127.

Lacy, E.R. and E. Reale, 1999. Urinary system, in *Sharks, Skates, and Rays*. W.C. Hamlett, Ed., Johns Hopkins University Press, Baltimore, 353-397.

Lacy, E.R., E. Reak, D. S. Schlusselberg, W.K. Smith, and D.J. Woodward, 1985. A renal countercurrent system in marine elasmobranch fish: a computer-assisted reconstruction. *Science* 227:1351-1354.

Laemmli, U.K., 1970. Cleavage of structural proteins during the assembly of the head of bacteriophage T4. *Nature* 227: 680-685.

Lignot, J-H., C.P. Cutler, N. Hazon, and G. Cramb, 2002. Immunolocalisation of aquaporin 3 in the gill and the gastrointestinal tract of the European eel (*Anguilla anguilla*). *The Journal of Experimental Biology* 205: 2653-2663.

Ma, T., Y. Song, B. Yang, A. Gillespie, E. Carlson, C.J. Epstein, A.S. Verkman, 2000. Nephrogenic diabetes insipidus in mice lacking aquaporin-3 water channels. *Proceedings of the National Academy of Sciences of the USA* 97: 4386-4391.

MacIver, B., Z. S. Karim, M. L. Zeidel, C. P. Cutler, and W. G. Hill, 2007. Partial functional characterization of an aquaporin 3 ortholog from the European eel, *Anguilla anguilla*. *The Bulletin, Mount Desert Island Biological Laboratory* 46: 147-150.

Marshall, W.S. and M. Grosell, 2005. Ion Transport, osmoregulation, and acid-base balance, in *The Physiology of Fishes*. CRC Press/Taylor & Francis Group, LLC, Boca Raton, pp. 177-230.

Matsuzaki, T., T. Suzuki, H. Koyama, S. Tanaka, K. Takata, 1999. Water channel protein AQP3 is present in epithelia exposed to the environment of possible water loss. *The Journal of Histochemistry and Cytochemistry* 47: 1275-1286.

Meischke, L., 2005. Immunohistochemistry Lab Protocol, courtesy of Dr. Cutler, University of St. Andrews, St Andrews in Fife, Scotland.

Morgan, R.L., P.A. Wright, and J.S. Ballantyne, 2003. Urea transport in kidney brush-border membrane vesicles from an elasmobranch, *Raja erinacea*. *Journal of Experimental Biology* 206: 3293-3302.

Moyes, C.D., Schulte, P.M., 2006. Principles of Animal Physiology. Benjamin Cummings Publishers, San Francisco, pp. 452-502.

Nejsum, L.N., 2005. The renal plumbing system: aquaporin water channels. *Cellular and Molecular Life Sciences* 62: 1692-1706.

Nelson, David L., Michael M. Cox, 2005. Principles of Biochemistry. W.H. Freeman And Company, New York, pp. 87-95.

Nozaki, K., D. Ishii, K. Ishibashi, 2008. Intracellular aquaporins: clues for intracellular water transport? *European Journal of Physiology* 456: 701-707.

Olson, Kenneth R., 1999. Sharks, Skates and Rays: The Biology of Elasmobranch Fishes. The Johns Hopkins University Press, Baltimore, MD., pp. 329 – 352.

Piermarini, P.M. and D.H. Evans, 2000. Effects of environmental salinity on Na^+/K^+-ATPase in the gills and rectal gland of a euryhaline elasmobranch (*Dasyatis sabina*). *The Journal of Experimental Biology* 203: 2957-2966.

Polak, J. M. and S. Van Noorden, 2003. Immunocytochemistry. BIOS Scientific Publishers Limited, Oxford, U.K., pp. 134-137.

Preston, G.M., T.P. Carroll, W.B. Guggino, P. Agre, 1992. Appearance of water channels in *Xenopus* oocytes expressing red cell CHIP28 protein. *Science* 256: 385-387.

Promeneur, D., Y. Liu, J. Maciel, P. Agre, L.S. King, N. Kumar, 2007. Aquaglyceroporin PbAQP during intraerythrocytic development of the malaria parasite, *Plasmodium berghei. Proceedings of the National Academy of Sciences of the USA* 104: 2211-2216.

Rai, T., S. Sasaki, S. Uchida, 2006. Polarized trafficking of the aquaporin-3 water channel is mediated by an NH 2-terminal sorting signal. *American Journal of Physiology - Cell Physiology* 290: 298-304.

Sambrook, J., D. Russell, 2001. Molecular Cloning: A Laboratory Manual. CSHL Press, Woodbury, NY, pp. 184-189.

Schreiber, R., R. Nitschke, R. Greger, and K. Kunzelmann, 1999. The cystic fibrosis transmembrane conductance regulator activates aquaporin 3 in airway epithelial cells. *Journal of Biological Chemistry* 274: 11811-11816.

Smith, C. P. and P. A. Wright, 1999. Molecular characterization of an elasmobranch urea transporter. *American Journal of Physiology* 276: 622-R626.

Venkatesh, B., E. F. Kirkness, Y.H. Loh, A.L. Halpern, A.P. Lee, J. Johnson, N. Dandona, L.D. Viswanathan, A. Tay, J.C. Venter, R.L. Strausberg, and S. Brenner, 2007. Survey sequencing and comparative analysis of the elephant shark (*Callorhinchus milii*) genome. *Public Library of Science – Biology* 5: 101.

Verkman, A.S., 2005. More than just water channels: unexpected cellular roles of aquaporins. *Journal of Cell Science* 118: 3225-3232.

Wilson, G., and Meischke, L., 2004. Immunohistochemistry Lab Protocol, coutesy of Dr. Cutler, University of St. Andrews, St Andrews in Fife, Scotland.

APPENDIX A

METHODS RECIPES

Solution D

472.640 g 4M Guanidinium

(An isothiocyante chaotropic salt that disrupts molecular activity.)

7.35 g 25 mM Sodium Citrate

5 ml 0.5% Sarkocyl, a non-ionic detergent, N-Laurosarcosine.

6.94 ml 0.1 β- Mercaptoethanol, a reducing agent that breaks disulfide bonds

RNA Denaturation Master Mix

180 µl 50% formamide

63 µl 17.5% formaldehyde

36 µl 10% 10X MOPS

7.5 µl dye (see DNA agarose electrophoresis)

Reverse Transcriptase Master Mix

1.0 µl Oligonucleotide primer

4.0 µl 5X buffer

2.0 µl dNTP's

1.0 µl DTT (dithiothreitol, a reducing agent)

0.5 µl RNase inhibitor (SUPERASE•IN™ from Ambion)

PCR Master Mix

H_20	14.85 μl
10 mM dNTP's	0.4 μl
10X Buffer	2.0 μl
Taq enzyme	0.25 μl
Total	17.5 μl (multiplied by the number of lots)

PCR Buffer from Manufacturer (1x concentration)

50 mM KCl

1.5 mM $Mg^{2+}Cl_2$ (as Mg^{2+} is an enzyme cofactor)

10 mM TRIS pH 8.3

TOPO Cloning Reaction

PCR product	1.34 μl
Salt Solution	0.33 μl
TOPO vector	0.33 μl

10% Polyacrylamide Resolving Gel

H_20	16.95 ml
40% acrylamide (29:1)	8.75 ml
1.5 M Tris (8.8 pH)	8.75 ml
20% SDS	0.175 ml
10% ammonium persulfate	0.35 ml
TEMED	0.028 ml
Total	35 ml

5% Polyacrylamide Stacking Gel

H_20	5.14 ml
40% acrylamide (29:1)	0.875 ml
1.0 M Tris (6.8 pH)	0.875 ml
20% SDS	0.035 ml
10% ammonium persulfate	0.070 ml
TEMED	0.007 ml
Total	7 ml

Blocking Buffer for Western Blotting

150 mM NaCl	4.38 g
10 mM Tris-Cl (pH 8.0)	0.606 g
0.05% (v/v) Tween-20 (detergent)	0.25 ml

APPENDIX B

METHODS RECIPES

Series of Dehydration Solutions for Immunohistochemistry

50% Ethanol

70% Ethanol

85% Ethanol

95% Ethanol

100% Ethanol, twice

HistoChoice, twice

Series of Rehydration Solutions for Immunohistochemistry

HistoChoice, twice

100% Ethanol

95% Ethanol

85% Ethanol

70% Ethanol

50% Ethanol

PBS

Solution A (permeabilization solution)

200 ml PBS

200 ml H_20

3.5 g NaCl

40 μl Tween 20 (Sigma)

Solution B (aldehyde blocking solution)

400 ml PBS

1.07 g NH_4Cl (Fisher)

Solution C (Blocking Solution)

To begin, 1g of BSA was added to 100 ml PBS and allowed to dissolve without mixing. Then 1 g gelatin was added and dissolved by heating and stirring and decanted into a bottle (Meischke, 2005).

Q-PCR Master Mix

4 μm Sense primer	83.75 μl
4 μm Antisense primer	83.75 μl
2 μm ROX (reference dye)	25.125 μl
H_20	309.875 μl
Brilliant II Q-PCR mix	837.5 μl